STUDIES OF THE *GIARDIA INTESTINALIS* TROPHOZOITE CELL CYCLE

A Thesis Submitted to the Committee of Graduate Studies in Partial Fulfillment of the Requirements for the Degree of Master of Science in the Faculty of Arts and Science

TRENT UNIVERSITY

Peterborough, Ontario, Canada

Environmental and Life Sciences M.Sc. Graduate Program

May 2017

ABSTRACT

Studies of the *Giardia intestinalis* trophozoite cell cycle

Kathleen Horlock-Roberts

To study the *Giardia intestinalis* cell cycle, counterflow centrifugal elutriation (CCE) was used to separate an asynchronous trophozoite culture into fractions enriched for cells at the different stages of the cell cycle. For my first objective, I characterized the appearance of a third peak (Peak iii) in our flow cytometry analysis of the CCE fractions that initially suggested the presence of 16N cells that are either cysts or the result of endoreplication of Giardia trophozoites. I determined that this third peak consists of doublets of the 8N trophozoites at the G2 stage of the cell cycle that were not removed effectively by gating parameters used in the analysis of the flow cytometry data. In the second objective, I tested the use of a spike with RNA from the GS isolate of Giardia as an external normalizer in RT-qPCR on RNA from CCE fractions and encystation cultures of Giardia from the WB isolate. My results showed that the GS RNA spike is as effective as the use of previously characterized internal normalizer genes for these studies. For the third objective, I prepared two sets of elutriation samples for RNA-seq analysis to determine the transcriptome of the Giardia trophozoite cell cycle. I confirmed the results of the cell cycle specific expression of several genes we had previously tested by RT-qPCR. Furthermore, our RNA-seq identified many genes in common with those identified from a microarray analysis of the Giardia cell cycle conducted by a collaborator. Finally, I observed an overall <4 fold change in differentially expressed genes during the G1/S and G2/M phase of the cell cycle. This is a modest change in gene expression compared to 10 - 30 fold changes for orthologous genes in mammalian cell cycles.

Keywords: elutriation, RNA-sequencing, flow cytometry, RT-qPCR, cell cycle

ACKNOWLEDGEMENTS

I would first like to thank my supervisor Dr. Janet Yee for all her support, guidance and patience throughout both my undergraduate degree and my Master's. I greatly appreciate all the opportunities I been given under her supervision and the chance to learn new techniques and to grow as a scientist. I will always remember the first day she brought me into her laboratory to show me 'Giardia' for the first time, which inspired me to pursue a career in research. I would also like to thank Dr. Craig Brunetti and Dr. Barry Saville for agreeing to be members of my supervisory committee and for all their input and support during my thesis.

Secondly, a thank you goes to Dr. Staffan Svard for giving me the opportunity to collaborate and learn from him. A huge thank-you goes to Dr. Mike Donaldson as well for his analysis of the RNA-seq data, his knowledge and expertise was greatly appreciated in order to understand my RNA-sequencing results. I would also like to thank Guillem Dayer, Megan Teghtmeyer and Adam Kemp from Dr. Janet Yee's lab for their advice, help, support and for making the laboratory a great place to work. I would also like to thank Dr. Steven Rafferty for his help during my thesis (and for helping to eat all the baked treats I brought in) as well as all past and present members of the Yee and Rafferty laboratories. A special thank you goes to Chase Reaume for teaching me about CCE and always being willing to listen to my questions.

I would also like to thank my family and friends for their support during my thesis, I could not do it without you. Finally I would like to thank my loving boyfriend Dan Lownsbrough for encouraging me to finish and reminding me why I fell in love with science in the first place. Thank you everyone.

TABLE OF CONTENTS

LIST OF FIGURES

LIST OF TABLES

ABBREVIATIONS

AMP – Adenosine monophosphate

ATP – Adenosine triphosphate

BLASTp – Basic Local Alignment Search Tool (Protein)

CCE – Counterflow centrifugal elutriation

CDK – Cyclin-Dependent Kinase

CWP1 – Cyst wall protein 1

DAPI – 4',6-diamidino-2-phenylindole

DAVID – Database for Annotation, Visualization and Integrated Discovery

DIC – Differential Interference Contrast

F# - Counterflow centrifugal elutriation fraction (F) and fraction number (#)

FT – Flow through

GAPDH – Glyceraldehyde 3-phosphate dehydrogenase

GMP – Guanosine monophosphate

GS SPS – GS sugar proton symporter

I-TASSER – Iterative Threading Assembly Refinement

NIMA – Never in Mitosis A

MAPK – Mitogen activated protein kinase

PLK- Polo-like Kinase

RP L2 – ribosomal protein L2

RT-qPCR – quantitative Reverse Transcription Polymerase Chain Reaction

TK – Thymidine Kinase

TMP – Thymidine monophosphate

INTRODUCTION

1.1: *Giardia intestinalis*

Giardia intestinalis is a waterborne protozoan parasite that causes the diarrheal disease known as giardiasis or 'Beaver Fever" and infects approximately 280 million people worldwide each year (Lane and Lloyd, 2002). The host becomes infected from ingesting food or water contaminated with fecal matter containing Giardia. Clinical symptoms of the disease include diarrhea, flatulence, abdominal cramps, nausea, and weight loss, although many infected hosts are asymptomatic (Halliez and Buret, 2013). The exact mechanism of how the disease causes the symptoms is debated; however, it begins with the parasite attaching tightly to the enterocytes located in the intestine. This binding results in the enterocyte cell's death, shortening of the brush border (causing malabsorption) and activation of the host's lymphocytes (Halliez and Buret, 2013).

Giardia isolates are categorized into eight assemblages (A-H). Certain assemblages infect a variety of hosts, such as assemblage A which infects humans and other mammals, whereas other assemblages appear to be host specific, such as Assemblages C and D which infect dogs (Adam, 2001). Three different isolates of Giardia (WB, GS and P15) from three different assemblages (A, B and E respectively) are capable of being grown in axenic culture and their genomes have been sequenced (Jerlstrom-Hultqvist et al., 2010). The WB and GS isolate are of interest as they both infect humans, although the GS isolate is more pathogenic to human hosts (Adam, 2001; Ankarklev et al., 2010). The WB and GS genomes share a 77% nucleotide identity and a 78% amino acid identity in the regions encoding for proteins. A small subset of genes unique to each isolate has been identified (Franzen et al., 2009).

1.2: Giardia life cycle

Giardia intestinalis has two developmental forms, the infectious cyst and the motile trophozoite (Fig. 1). Cysts are environmentally resistant and are the dormant form of the parasite (Adam, 2001). Infection in the host is caused by the ingestion of the cyst. As the cyst travels to the stomach of the host, the acidic environment triggers the cyst to undergo excystation, a process that results in the emergence of the pathogenic trophozoites (Adam, 2001). These trophozoites attach to the host's upper intestinal wall by means of a ventral adhesive disk, where they divide by binary fission, thereby proliferating and colonizing the intestine. As they move lower in the intestine, trophozoites are triggered to encyst, a process in which they differentiate back into the cyst form. These cysts are then excreted in the host's feces to become sources of future infections (Adam, 2001).

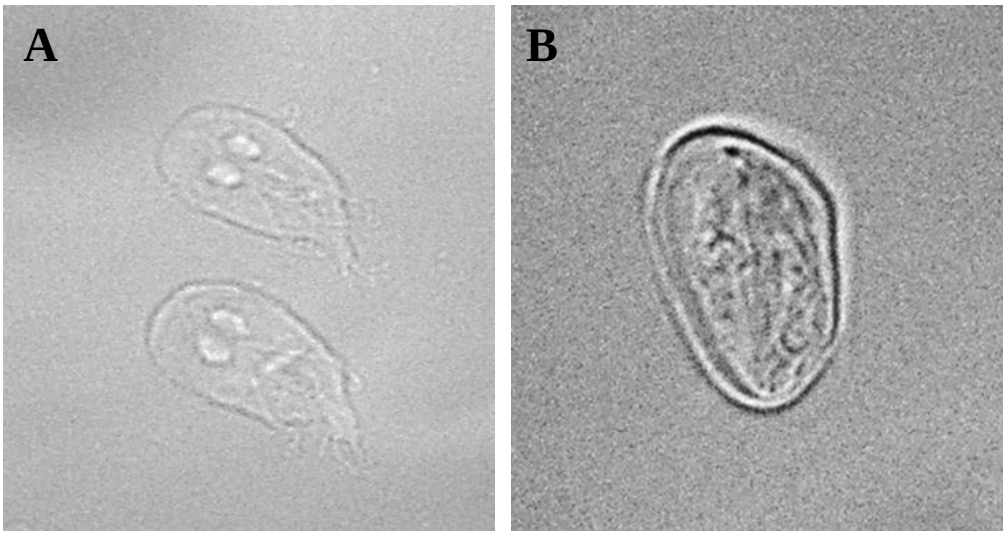

Figure 1: Life forms of *Giardia intestinalis*. A) DIC image of the motile trophozoite form **B)** DIC image of the infectious cyst form.

1.2.1: Giardia encystation

Giardia trophozoites differentiate into infectious cysts when they are exposed to an increased concentration of bile and higher pH environment in the lower small intestine (Gillin et al., 1988). Encystation can be split into two phases, early and late (Einarsson and Svard, 2015). During early encystation, encystation specific vesicles (ESV) form to transport cyst wall proteins (CWPs) to the membrane of the cell to build a cyst wall. During the late phase, the nuclei divide and replicate the DNA again, resulting in a cell with a total DNA content of 16N (4X 4N per nuclei). The final step of differentiation occurs into the mature cyst is when the cyst wall filaments are cross-linked together, which forms creates the environmentally resistant oval-shaped cyst wall (Fig. 2) (Einarsson and Svard, 2015). Excreted cysts are then able to survive in freshwater for up to 3 months (deRegnier et al., 1989).

Giardia encystation can be studied in laboratory cultures by several different *in vitro* encystation protocols. The first method was developed by the Gillin laboratory and uses two steps (Gillin et al., 1988). In the first step, Giardia trophozoites are grown in pre-encystation medium that lacks bile. In the second step, cells are transferred into the encystation medium containing porcine bile (0.25 mg/mL), lactic acid, at a basic pH to 7.8. A second *in vitro* encystation protocol involves growing the Giardia trophozoites in medium that lacks cholesterol, which mimics the nutrient deprivation of the host's lower intestine (Lujan et al., 1996). The last method involves culturing the Giardia trophozoites in a medium with a high bovine bile concentration (10 mg/mL) and at pH 7.8 (Kane et al., 1991). Recently, the Kane method was modified by Svard's laboratory at Uppsala University by using a lower concentration of bile (2.5-5 mg/mL) to induce encystation. In

our laboratory, we have found the Uppsala method to be the most efficient in inducing encystation of our trophozoite cultures.

1.2.2: Giardia cell cycle

The cell cycle is the process by which a cell grows and divides to give rise to two daughter cells. The stages of the cell cycle are denoted as G1, S, G2 and M. A G1 (Gap 1) stage cell replicates its DNA at the synthesis or S-phase, and the resultant cell with twice the DNA content will be at G2 (Gap 2). The G2 cell then divides during mitosis (M-phase) to give two daughter cells. Each Giardia trophozoite contains two nuclei with an equivalent DNA content (Adam, 2001). At the G1 stage of the trophozoite cell cycle, the DNA content of the cell is tetraploid since each nucleus contains 2N of DNA (2X 2N per nuclei). After DNA replication in S-phase, the Giardia trophozoite becomes octaploid (2X 4N per nuclei) at the G2 stage (Fig. 2) (Bernander et al., 2001). The G2 stage is also the point where the trophozoite can enter the encystation pathway to become infectious cysts. Consequently, the G2 stage is a restriction point for differentiation into the cyst form of the parasite (Bernander et al., 2001). Since the cell cycle regulates the proliferation of the trophozoites and the initiation of encystation, studies on the cell cycle could offer potential insights on the treatment and spread of the disease.

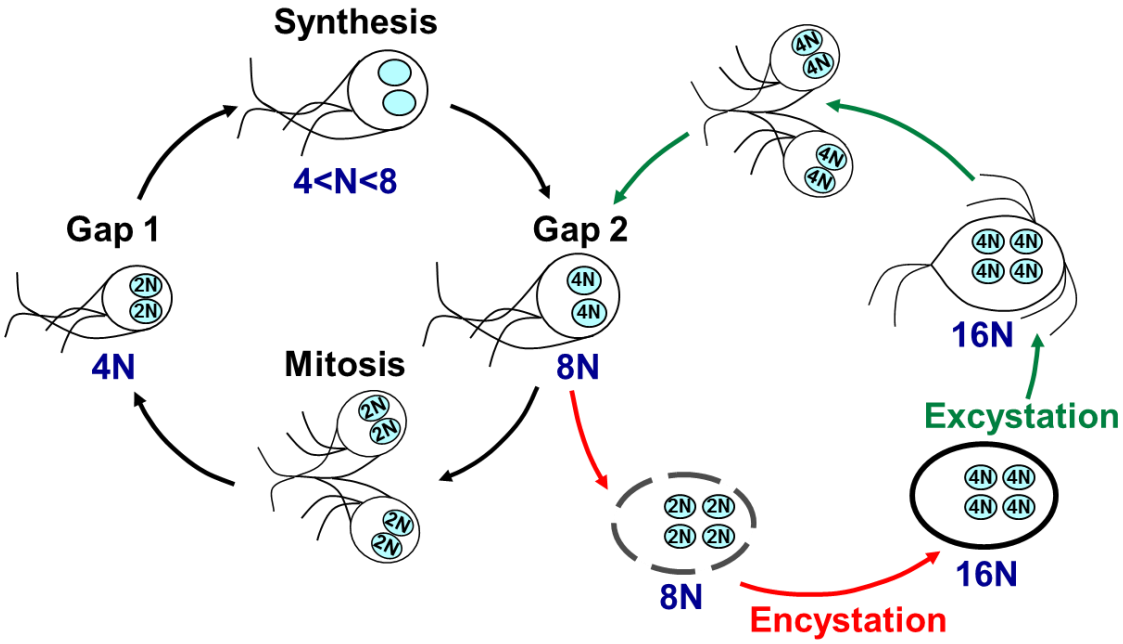

Figure 2: DNA content of cell in the Giardia cell cycle. The growth and division of Giardia trophozoites during the cell cycle are shown on the left in black. The stages in the encystation pathway are indicated by the red arrows and steps in the excystation pathway are indicated by the green arrows.

1.3: Flow cytometry

Flow cytometry measures the DNA content of individual cells and is a useful technique in determining the percentage of cells at the different stages of the cell cycle in a given sample. To determine the DNA content, an intercalating fluorescent dye is used to bind the DNA (Thakur et al., 2015). The sample is then loaded into the flow cytometer instrument where the stream of cells is focused by hydrodynamic streaming so that the cells pass in a single file in front of a laser (Rieseberg et al., 2001). The laser excites the dye bound to the DNA to emit a fluorescent signal. The intensity of the signal is directly proportional to the amount of DNA in the given cell (Brown and Wittwer, 2000). Consequently, the G2 (8N) cells will emit twice the fluorescent signal as the G1 cells since the G2 cells have twice the DNA content of G1 cells. This signal is relayed to a computer in order to create a histogram with the amount of fluorescence per cell plotted on the x-axis and the number of cells at that given fluorescence is on the y-axis (Figure 3). In this histogram analysis of Giardia cells, the fluorescently-labelled G1 cells appear as a peak at approximately 200 fluorescence/cell (Peak i) , the labelled G2 cells are at approximately 400 (Peak ii) and the valley between these two peaks represents the S phase cells (Fig. 3). The location of a third Peak (iii) at approximately 800 on the x-axis suggests that it contains cells that have twice of the DNA content of G2 cells (Peak ii). Since Giardia cysts are 16N, it is possible that Peak iii cells represent Giardia cysts.

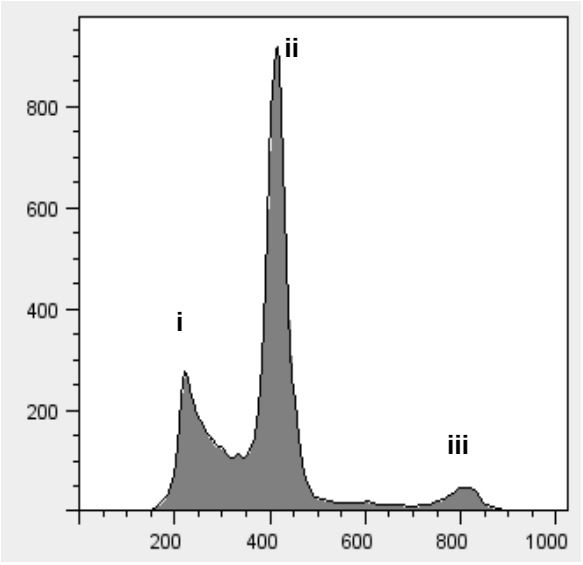

Figure 3: Flow cytometry histogram of an asynchronous culture of Giardia trophozoites. Peak **i** represents the G1 phase (4N) cells, **ii** the G2 phase (8N) cells and Peak **iii** represents possible 16N cells that may be cysts. The valley between Peaks i and ii represent cells undergoing DNA synthesis (S phase).

One consideration in analyzing flow cytometry data is the formation of cellular aggregates. The hydrodynamic streaming in the flow cytometry instrument is used to force the cells into a narrow stream so that they pass by the laser one by one as single cells. If cells clump and pass in front of the laser, the fluorescence will be recorded for the clump rather than the individual cells. Large clumps of cells (containing aggregates of many cells) can be easily detected since they will appear as "cells" that have a much higher fluorescence than the expected single cells. Signals from these large aggregates can be eliminated from the analysis by applying gating parameters. However, small aggregates, especially clumps of just two cells (doublets) are more difficult to detect and remove from flow cytometry analysis (Rieseberg et al., 2001).

1.4: Cell Cycle Synchronization in Giardia

To study gene expression during the cell cycle, samples containing pure populations of cells from each stage of the cell cycle should ideally be obtained. One way to obtain these samples is to use a "block and release" method in which a drug is added to stop the growth of an asynchronous population of cells at a specific stage of the cell cycle (Banfalvi, 2008; Davis et al., 2001). Once all cells are blocked, the drug is removed and the released cells should progress through the rest of the cell cycle in synchrony. For Giardia trophozoites several drugs have been tested in this block and release method, although only two have been shown to arrest cells in specific stages of the cell cycle: aphidicolin, which arrests cells in the G1/S stage; and nocodazole which arrests cells in the G2/M stage of the cell cycle (Poxleitner et al., 2008; Reaume et al., 2013; Reiner et al., 2008). However, using a drug to induce a block in the cell cycle may have deleterious effects on the cells (Davis et al., 2001). For example, aphidicolin was shown to induce

DNA damage in treated Giardia trophozoites, and nocodazole changed the cell shape and increased the percentage of 16N cells (Reaume, 2013; Reaume et al., 2013). Such changes can also influence gene expression, which could give a biased or inaccurate expression profiles of genes during the synchronized cell cycle (Davis et al., 2001).

1.5: Counterflow Centrifugal Elutriation (CCE)

An alternative method to using drugs to synchronize a culture for cell cycle analysis is to use a physical method that separates cells in an asynchronous culture into the different stages of the cell cycle. This method, called counterflow centrifugal elutriation (CCE) does not cause cell perturbations, and has been used in several cell types (Banfalvi, 2008, 2011; Davis et al., 2001; Reaume, 2013), including in our laboratory for Giardia trophozoites. CCE separates cells based on their size, shape and density (Banfalvi, 2011) by subjecting the cells to two opposing forces in the separation chamber. The centrifugal force arises from spinning the sample in a centrifuge and the counterflow force results from a peristaltic pump pushing liquid through the system (Fig. 4). When the centrifugal force is greater than the counterflow force, the cells remain in the bottom of the chamber (Fig. 4A). When the two forces are equal, cells are suspended within the chamber based on their size due to their sedimentation properties (Fig. 4B) (Banfalvi, 2011). Smaller sized cells would be less affected by the centrifugal force and are therefore located near the exit or top of the chamber. Larger sized cells are more affected by the centrifugal force and are therefore located at the bottom of the chamber. An increase in the counterflow force at this point will cause the smallest sized cells to be eluted first out of the chamber (Fig. 4C). As the counterflow force is gradually increased,

cells of increasing sizes are eluted from the chamber. In this way, CCE is able to elute the smaller G1 cells first, followed by the S phase cells and the G2/Mitotic cells.

1.6: Gene Expression Analysis of the cell cycle by RT-qPCR

A technique that has a significant impact on the study of gene expression is reverse transcriptase quantitative polymerase chain reaction (RT-qPCR) (Bustin et al., 2005). In one application of this technique, a fluorescent dye (SYBR Green) is incorporated into the reaction mix. This dye binds to the minor groove of double stranded DNA during every extension step in the PCR reaction (Navarro et al., 2015). Since the amount of double-stranded DNA increased with every PCR amplification cycle, the fluorescence intensity in the sample would also increase. During the PCR reaction, the number of cycles and the amount of fluorescence emitted from each sample is continuously measured (Wong and Medrano, 2005). The number of PCR cycles that is required for a sample to accumulate sufficient fluorescence to reach a set threshold fluorescence level is called the Ct value for threshold cycle or Cq value for quantification cycle.

A sample with more starting template will reach the threshold level with fewer PCR cycles than a sample with less starting temple (Wong and Medrano, 2005). Therefore, a sample with a low Cq indicates a high amount of starting material whereas a high Cq suggests a low amount of starting template. The template used in such gene expression analysis would be the cDNA synthesized from the RNA in the samples that are under study. Since a reverse transcription step (RT) is required to convert the RNA into cDNA, this type of quantitative PCR analysis is referred to as RT-qPCR.

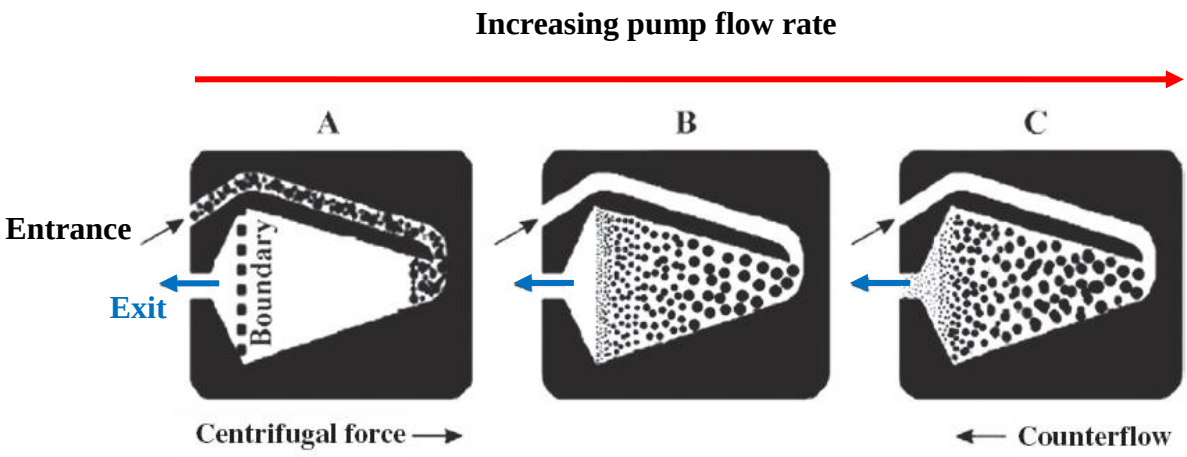

Figure 4: Counterflow Centrifugal Elutriation chamber at different stages of the elution. A) Chamber where centrifugal force is greater than the counterflow force **B)** centrifugal force is equal to counterflow force. Cells suspended in the chamber based on size, smaller sized cells are located near the boundary but have not exited the chamber yet **C)** Counterflow force greater than centrifugal force, cells are starting to be eluted from the chamber. Modified from Banfalvi, 2011.

1.7: Normalization of RT-qPCR Data

In order to give meaning to Cq values obtained from RT-qPCR, the data must first be normalized to control for differences in the amount of starting RNA, the efficiency of cDNA synthesis, the efficiency of PCR amplification for each primer pair, and other non-biological differences among the samples tested (Bustin et al., 2005; Huggett et al., 2005; Ling and Salvaterra, 2011). The most common practice is to use an internal reference gene to normalize the data between different samples (Bustin et al., 2005; Huggett et al., 2005). An internal reference gene is commonly referred to as a housekeeping gene because these genes are continuously expressed at a constant level as they are essential for the function of the cell (Huggett et al., 2005). A good normalizer will not be affected by experimental conditions and thus will have constant mRNA levels in all samples being investigated. Some common housekeeping genes include those that encode structural proteins (actin, tubulin), ribosomal proteins (18S, 28S rRNA), and proteins involved in central metabolism (glyceraldehyde-3-phosphate dehydrogenase, GAPDH) (Huggett et al., 2005; Suzuki et al., 2000). However, the expression of these genes may vary greatly in some cases. For example the expression level of GAPDH changes in different tissues while β-actin levels change in leukemia patients (Huggett et al., 2005; Kozera and Rapacz, 2013). For this reason, the stable expression of internal normalizers used in RT-qPCR should always be confirmed for each experiment, as what may work well as a normalizer under one experimental or biological condition may not be appropriate under another (Huggett et al., 2005). While only one reference gene is commonly reported in published papers, it is recommended to use two or more reference genes for RT-qPCR, as

expression profiles that are consistent with multiple normalizers would give more confidence in the results obtained (Bustin et al., 2005; Vandesompele et al., 2002).

An alternative normalization strategy is to use an external normalizer that 'spikes' or adds a foreign RNA template into the samples in the RT-qPCR experiment (Huggett et al., 2005). Instead of using the endogenous gene to normalize the gene(s) of interest, an exogenous gene that is only found in the spiked RNA is measured in its place. This method has been used on *Trypanosoma brucei* cells, as well in Sprague-Dawley rat nodose ganglia RNA (Bucerius et al., 2011; Johnston et al., 2012). The spiked exogenous RNA is not subject to changes in RNA expression due to the biological conditions, and as the same amount is added in each sample, the relative level of the exogenous normalizer measured by RT-qPCR should be consistent in all the samples (Huggett et al., 2005).

1.8: Previous results from RT-qPCR studies on CCE of Giardia cultures

Previous work in our laboratory has experimentally determined the conditions for the CCE fractionation technique that results in the enrichment of G1, S and G2/M phase trophozoites from asynchronous Giardia cultures (Reaume, 2013). We studied several genes of interest that were believed to be regulated in the trophozoite cell cycle by using the fractions enriched in the different stages of the cell cycle from the CCE experiments. From the RT-qPCR analysis, the core histones genes (H2A, H2B, H3 and H4) were found to be upregulated in G1/S phase fractions, and Cyclin A, Cyclin B and Cyclin B-like genes were upregulated in G2/M enriched fractions (Reaume, 2013). However, all of the 11 genes tested, displayed very modest changes (<5 fold) in expression levels (Reaume, 2013).

1.9: RNA-sequencing for transcriptome analysis

While RT-qPCR is a useful technique for measuring gene expression, only a relatively small number of genes can be studied at a single time. However, advances in high throughput DNA sequencing has led to the development of the technique called RNA-sequencing (RNA-seq) (Wang et al., 2009). This technique measures the entire transcriptome of a cell under a specific condition. Furthermore, the transcript levels between samples or conditions can be compared to show changes in gene expression (Wang et al., 2009). RNA-sequencing is a highly sensitive technique with a single base pair resolution (Wang et al., 2009). In addition, RNA-seq has very low background signal in comparison to other methods such as DNA microarray, is highly accurate at quantifying the expression of genes, and it achieves high levels of reproducibility (Wang et al., 2009).

To begin an RNA-seq experiment, mRNA is enriched from a sample of total RNA and is then reverse transcribed into cDNA (Wang et al., 2009). An adaptor sequence is added to one end of the cDNA molecule for single end sequencing, while adaptors are added to both ends for paired end sequencing (Wang et al., 2009; Wolf, 2013). Paired end sequencing has the benefit of giving more information about the transcriptome, such as insertions and deletions and is commonly used in *de novo* transcriptome determination (Sengupta et al., 2011). The sequence reads are aligned directly to the reference genome if known, or assembled *de novo* to create the genome transcription map for the organism (Wang et al., 2009). The number of sequencing reads per gene are then counted to give quantitative data about the transcriptome (Wolf, 2013). The higher the number of reads, the more a gene is expressed, depending on the total mappable reads and length of the

transcript (Wolf, 2013). In addition, strand-specific RNA-sequencing allows the researcher to retain the information on which strand of the DNA is transcribed (Zhao et al., 2015). Strand specific sequencing is advantageous to determine gene expression from overlapping genes and in cases where there is significant anti-sense transcription (Zhao et al., 2015).

Several RNA-seq experiments have been performed recently with Giardia, to study the transcriptome of different trophozoite isolates in response to oxidative stress, and to investigate the transcriptome of trophozoites, pre-cysts and cysts exposed to UV radiation (Einarsson et al., 2015; Ma'ayeh et al., 2015). Furthermore, RNA-seq has been used to study gene expression changes in Giardia during encystation (Einarsson et al., 2016). RNA-seq analysis of the trophozoite cell cycle could help to determine which genes are regulated during the cell cycle, thereby providing a better understanding of the growth of the parasitic form that is found within the host. In addition, during the RT-qPCR analysis performed previously in the Yee laboratory, the genes tested displayed modest changes in expression levels (<5 fold changes) during the trophozoite cell cycle (Reaume, 2013; Reiner et al., 2008). Further RNA-seq analysis would determine whether the small changes in expression observed for the small number of genes initially tested are exceptional examples or if many other genes also show low variation in their expression level during the cell cycle.

1.10: Research goals

The aims of my research can be separated into three different objectives:

1) A third peak of cells that appear to have a DNA content that is twice the amount of DNA in G2 cells was observed in flow cytometry analysis of asynchronous cultures of Giardia trophozoites (Fig. 3). The cells in this peak (referred to as Peak iii) are also differentially enriched in latter CCE fractions of Giardia trophozoite cultures. My hypothesis is that these Peak iii cells are cysts that form spontaneously in normal Giardia cultures. Therefore, I will first examine the Peak iii cells for markers that are characteristic of Giardia cysts. I will also determine the relative DNA content of the CCE fractions that are enriched for the Peak iii cells to verify that cells with double the DNA content of G2 cells are present in these samples.

2) My second objective is to investigate the use of an external normalizer for RT-qPCR analysis of gene expression during the Giardia cell cycle. This involves spiking RNA samples extracted from CCE fractionation of a WB isolate Giardia culture with a small amount of RNA from a Giardia GS isolate. RT-qPCR will be performed to assay the expression of a gene found only in the GS isolate in the spiked sample. The effect of using the GS-specific gene as the external normalizer will be compared to the use of the actin gene, found in both GS and WB isolates, as the internal normalizer.

3) My third objective is to prepare two sets of CCE fractionations for RNA-seq analysis. I will analyze the sets of differentially expressed genes in the different stages of the cell cycle as represented by the CCE fractions. This will provide a comprehensive transcription profile of the Giardia cell cycle.

MATERIALS AND METHODS

2.1: *Giardia intestinalis* Cultures

Cultures of *Giardia intestinalis* trophozoites from the WB isolate (ATCC # 50803) or the GS isolate (ATCC # 50580) were grown to logarithmic phase (10^5 to 10^6 cells/mL) at 37^{o}C in 16 mL glass cultures tubes in TYI-S-33 media with the addition of an antibiotic/antimycotic solution (Keister, 1983) (Tables A1 – A4 in Appendix I). Cells were pelleted by centrifugation at 1200 x *g* for 15 minutes at 4^{o}C (Beckman Coulter Allegra X14R centrifuge). The yield of collected cells was determined on a ViCell instrument (Beckman-Coulter).

2.2: Counterflow Centrifugal Elutriation

The following CCE protocol for the fractionation of Giardia trophozoites was optimized by a previous Master's student in the Yee laboratory and the summary can be found in Table A5 in Appendix II (Reaume, 2013). In brief, trophozoites were cultured until a total number of cells between 10^7 – 10^9 was obtained (approximately 640 mL of culture from 40 16 mL culture tubes). Cells were collected by centrifugation and re-suspended in 2 mL of 1x PBS (pH 7.2). An aliquot of 20 µL was removed and placed in 480 µL of 1x PBS (pH 7.2) for analysis on an automated cell counter to determine the concentration. An additional 200 µL of cells were removed and kept aside to be used as the unsorted (control) fraction for future analysis. 100 µL of diluted food colouring (2 drops into 2 mL 1x PBS (pH 7.2)) was then added to the resuspended cell pellet to help visualize cells injected into the elutriation system and the prepared cells were kept on ice until injection. Preparation of cells and the elutriation were completed on the same day.

Elutriation parameters were established by previous work in Dr. Yee's laboratory to fractionate Giardia trophozoites (Reaume, 2013). Elutriations were conducted in a Beckman Coulter Avanti J- 26 XPI series centrifuge with a JE 5.0 rotor and a 4 mL elutriation chamber. Centrifugation speed was kept constant at 2,400 RPM (1,100 x *g*) and at a temperature between 20-22^{o}C. Cells were injected into the system at a peristaltic pump rate of 1 mL/min and 50 mL of the flow through was collected into a 50 mL Falcon tube. The flow rate was then incrementally increased with 50 mL collected in each fraction (1-12) as well as a final blow out of the system where the flow rate was 50 mL/min and centrifuge speed 0 RPM to collect any cells left in the chamber (Table A6 in Appendix II).

Each fraction of cells collected in a 50 ml Falcon tube was centrifuged and all the supernatant was removed except for 3 mL. The samples were centrifuged again and all the supernatant was removed except for 1 mL. The cell pellets were then resuspended in the remaining supernatant and transferred to 1.5 mL microcentrifuge tubes. The cells in the microcentrifuge tubes were collected by centrifugation and resuspended in 1 mL of 1x PBS (pH 7.2). A small volume (20 - 50 µL) of cells was removed from each sample and added to a volume of 1x PBS to make a total volume of 500 µL to determine the cell count on a ViCell instrument (Beckman-Coulter). Remaining cells were then used for flow cytometry, immunofluorescent assays, and RT-qPCR. All centrifugation steps in this procedure were performed at 1,100 x g for 15 min at 4°C.

2.3: RNA extraction and cDNA synthesis

RNA was extracted from Giardia WB or GS trophozoites by the use of Trizol reagent as per the manufacture's instructions (Thermo Fisher Scientific) (Appendix III).

The extracted RNA was measured on a Nanodrop (ND 1000 Spectrophotometer) to determine the concentration of the RNA as well as the purity.

In the set up for cDNA synthesis for the trophozoite cell cycle, 20 ng of GS RNA was added to 980 ng of WB RNA from each elutriation fraction. This represents a 2% spike of the GS RNA into each WB RNA sample. A mixture containing a poly$(T)_{21}$ primer, dNTPs and reverse transcriptase was added to initiate cDNA synthesis (Appendix IV). The concentrated cDNA was then diluted to 0.5 ng/µL in RNase-free water (DEPC H_2O) and stored at -80^oC.

2.4: Giardia Encystation

Giardia WB trophozoites were grown to confluence in TYDK media (Table A6 in Appendix V) and induced to encyst by replacing the media with modified encystation media (Table A7 in Appendix V). Cultures were allowed to encyst at 37°C for 0, 7, 12 and 24 hours, and RNA was extracted from cells collected at each time point. This experiment was performed by Julianne Hoekstra from the Yee laboratory (Hoekstra, 2016). For cDNA synthesis, 490 ng of WB RNA from each encystation time point was used along with the addition of 10 ng of GS RNA representing 2% spike.

2.5: Quantitative PCR analysis (RT-qPCR)

In the RT-qPCR analysis for the trophozoite cell cycle, three different primer sets were used (Table A8 in Appendix VI); four primers were used for the encystation experiment (Table A9 in Appendix VI). The RT-qPCR reactions were performed in 96-well plates with SYBR Green as the detection dye on a Mx3000p instrument (Stratagene/Agilent) (Tables A10 and A11 in Appendix VI). The following reaction

conditions were used: an initial 4 minutes denaturation at 95^{o}C, followed by 40 cycles of the following: 30 seconds at 95^{o}C, 1 minute at primer specific annealing temperature and 30 seconds at 72^{o}C. Finally, a melting curve is performed by incrementally increasing the temperature from 55^{o}C to 95^{o}C.

For each sample, three cDNA samples, one No Reverse Transcriptase (NoRT) and one No Template Control (NTC) were measured by RT-qPCR. The NoRT sample contained 0.5 ng/µL of RNA that had not undergone reverse transcription and is used to detect genomic DNA contamination. The NTC contained RNase-free water to check for contamination in the reagents. The fluorescent threshold for each RT-qPCR run was set at 0.1 to limit variability between reactions.

2.6: Flow Cytometry Analysis

Giardia cells from the elutriations were fixed and stained by the method described by Troell and Svard, 2011 (Troell and Svard, 2011). Cells were centrifuged at 1,100 x *g* for 15 minutes at 4^{o}C (Beckman Coulter Microfuge 22R) and all but approximately 100 µL of the supernatant was removed. Cells were re-suspended in the remaining supernatant and 150 µL of citric acid fixative (40 mM citric acid [monohydrate], 20 mM sodium phosphate [dibasic], 0.2 M sucrose, and 1% Triton X-100, pH 3.0) by pipetting up and down twice. Samples were left at room temperate for 5 minutes followed by the addition of 350 µL of Diluent Buffer (125 mM $MgCl_2$ in 1x PBS). Samples were inverted to mix then left at 4^{o}C for no longer than 7 days.

On the day of flow cytometry cells were pelleted by centrifugation at 900 x *g* for 10 minutes at 4^{o}C and re-suspended in 500 µL of 1x PBS. 50 µL was removed and placed

into 450 µL of 1x PBS to determine the cell concentration by an automated cell counter. 1.25 µL of 20 mg/mL RNase A was added to the remaining cells and the samples were incubated at 37^{o}C in a water bath for 30 minutes. Cells were then pelleted by centrifugation at 900 x *g* for 10 minutes at 4^{o}C. The supernatant was removed and the cell pellet was re-suspended in a volume of 1x PBS that would bring the cell density to 5 x 10^6 cells/mL. A volume of 50 µM SYTOX Green (diluted in DMSO), a DNA stain, sufficient to bring the concentration of 1 µM was added to the fixed cells. Samples from this point on were protected from light and were placed on ice for 20 minutes prior to analysis.

Stained cells were analyzed on a Beckman Coulter Cytomics FC 500 flow cytometer. The unsorted control was used to calibrate each run before running the elutriation samples. Data generated by the flow cytometry results was analyzed using FlowJo Analysis Software v.7.2.2. Manual gating was used on histograms that represent the number of cells verses the amount of fluorescence (DNA content) per cell to calculate the percentages of G1, S, G2/M, and Peak iii cells present in each fraction.

2.7: Fluorescence microscopy

Glass coverslips (#1.5) were pre-treated with 0.1% polyethyenimine (prepared in 1 x PBS) for 10 minutes then rinsed with dH_2O and allowed to dry, PEI treated side up. Coverslips were then placed (PEI side up) in a Tupperware container that was lined with damp paper towel and pre-warmed in a 37^{o}C incubator. 50-75 µL of cells from each fraction (with an approximate total number of cells of 6 x 10^6 cells) were pipetted onto the PEI side of the coverslips; the container was closed and placed back into the 37^{o}C incubator for 10 minutes to allow the cells to attach to each coverslip. Coverslips were

then removed and placed in a coverslip rack, which was placed in a beaker of pre-chilled methanol to -20^{o}C. The beaker containing the coverslips was placed into the -20^{o}C freezer for 10 minutes to fix the cells. Coverslips were removed and allowed to air dry for 5 minutes before being stored in a sealed container overnight.

The following steps were all performed in metal staining trays covered in parafilm. Solutions were added to the parafilm as droplets and the coverslips were placed on top of the drops, cell side down. Cells were permeabilized by floating the coverslip on 100 µL of 0.5% Triton X for 10 minutes. The cells were then blocked with blocking buffer for 1 hour, followed by incubation with a Cyst Wall Protein 1 antibody conjugated to the Alexa647 fluorophore for 2 hours at 37^{o}C. Aluminum foil was the added over the trays and left on for the remaining steps. The coverslips were washed 4 in 1x PBS, 5 minutes per wash, followed by incubation in 100 µL of 3.7% paraformaldehyde for 10 minutes. Coverslips were washed twice with 1x PBS, 5 minutes per wash and then incubated with 100 µL of 0.25 µg/mL of DAPI (diluted in Millipore water) for 10 minutes. Coverslips were washed a final 2 times in 1x PBS, 5 minutes each and a final wash in Millipore water for 5 minutes.

For the determination of DNA content in the nuclei of cells, coverslips were mounted onto slides using Vectorshield mounting medium without DAPI (Vectorlabs). Slides were stored at room temperature protected from light and were visualized the next day or stored at 4^{o}C until visualized. Images were visualized with a Leica DM6000 B epifluorescent microscope with a 100X objective (1600X total magnification) under oil immersion. The brightness, gain, intensity and exposure time were the same for all images taken (Table A12, in Appendix VII).

2.8: CellProfiler

To measure the relative fluorescence intensity of each nuclei, the program CellProfiler (ver. 2.1.1) was used. Image files of the DAPI stained cells were uploaded to the software and modules to identify primary objects (nuclei) and intensity (fluorescence) were selected to measure the objects. For each nuclei, the average intensity was recorded and grouped based on the intensity values. The average intensity was determined and reported with a standard deviation.

2.9: RNA-sequencing

The RNA extracted from each elutriation fraction was treated with DNase I (Thermo Fisher Scientific) followed by cleanup of the RNA with the RNeasy Mini kit (Qiagen, product # 74104) and the quality of the RNA was measured using a 2100 Bioanalyzer (Agilent). One microgram of total RNA from each sample was converted into a cDNA library by polyadenylate selection by the TruSeq stranded mRNA library preparation kit (Cat # RS-122-2101/2102, Illumina Inc.) according to the manufacturer's protocol (#15031047). The libraries were then sequenced as 125 bp paired ends using a HiSeq2500 Instrument (Illumina) at the SNP/SEQ facility of the SciLifeLab National Genomics Infrastructure (Uppsala, Sweden). The analysis of the raw data was performed by Dr. Michael Donaldson at Trent University as follows. The fastq sequences generated from the sequencing was assessed for quality by using FastQC v0.11.5. The reads were trimmed in order to remove the adapter sequences and any low-quality bases by using the Trimmomatic v0.36 software (Bolger et al., 2014). The trimmed fastq files were aligned to the *Giardia intestinalis* genome sequence assembly (Giardiaintestinalis_AssemblageA, from http://giardiadb.org/giardiadb/, v28) using TopHat v2.1.1 (Kim et al., 2013). Reads

mapped to the Giardia genes were counted using featureCounts (Liao et al., 2014). Differentially expressed genes between the samples were identified by using the recommended settings in SARTools (Varet et al., 2016) and analyzed by DESeq2. Transcripts with a false discovery rate (FDR) – corrected p-values <0.05 were reported as differentially expressed (Reiner et al., 2003).

2.10: DAVID Analysis of RNA-seq data

To determine if there were any clusters of genes with similar features or functions present in the results from the RNA-seq analysis, DAVID (Database for Annotation, Visualization and Integrated Discovery) was used. The upregulated gene ID lists were inputted into the Functional Annotation tool. The default settings for the analysis were chosen, except that the PFAM and SUPFAM databases were also selected under the protein domains menu heading. After the functional annotation clustering button was pressed, the following options were changed: Similarity threshold was set to 0.85, the EASE score was changed to 0.05 and the classification stringency was set medium. Clusters with an enrichment score greater than 1.3 were kept.

RESULTS AND DISCUSSION

3.1: Objective 1: Characterization of Peak iii cells identified in the flow cytometry analysis of Giardia trophozoite cultures

3.1.1: Flow cytometry

During the Giardia trophozoite cell cycle, cells have a total DNA content of 4N at G1 or 8N at G2 (Fig. 2, Introduction); these cells are represented in Peaks i and ii, respectively, when asynchronous cultures are analyzed by flow cytometry (Fig. 5). However, we also observed a small percentage (3 - 10%) of cells that appear to have a DNA content that is twice the content of the G2 cells (Fig. 5A and B, Peak iii).

This third peak is also observed in the latter fractions of a counterflow centrifugal elutriation (CCE) experiment that is used to enrich cells from different stages of the cell cycle (Fig. 6). Furthermore, the proportion of cells in Peak iii gradually increases as the CCE fractionation increases (Fig. 6, F6 - F12).

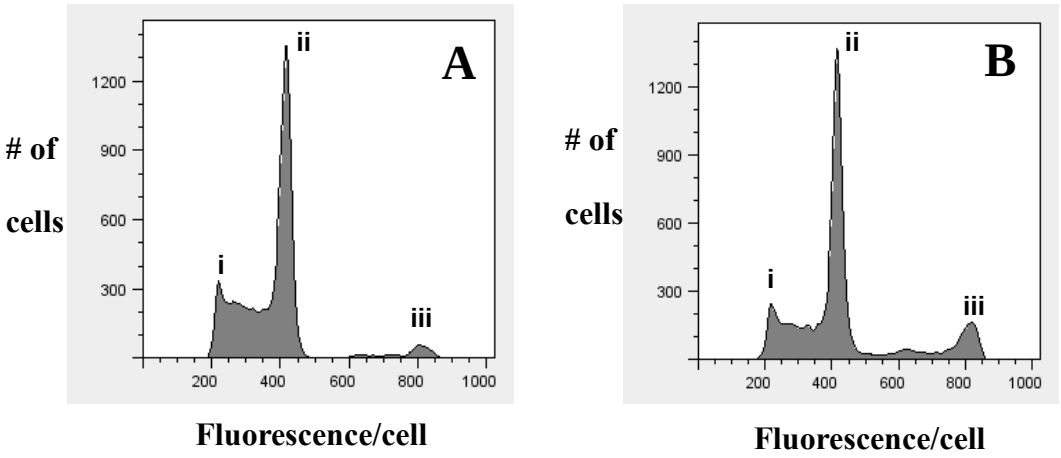

Figure 5: Flow cytometry analysis of two asynchronous Giardia trophozoite cultures. The x-axis represents the fluorescence per cell while the y-axis represents the number of cells at a given fluorescence. Peak **i)** represents 4N cells, Peak **ii)** represents 8N cells and Peak **iii)** are cells with double the DNA content of ii. **A)** Histogram of cell distribution of an asynchronous culture with a small (3%) population of cells at Peak iii. **B)** Histogram of cell distribution of an asynchronous culture with a larger (10%) population of cells at Peak iii.

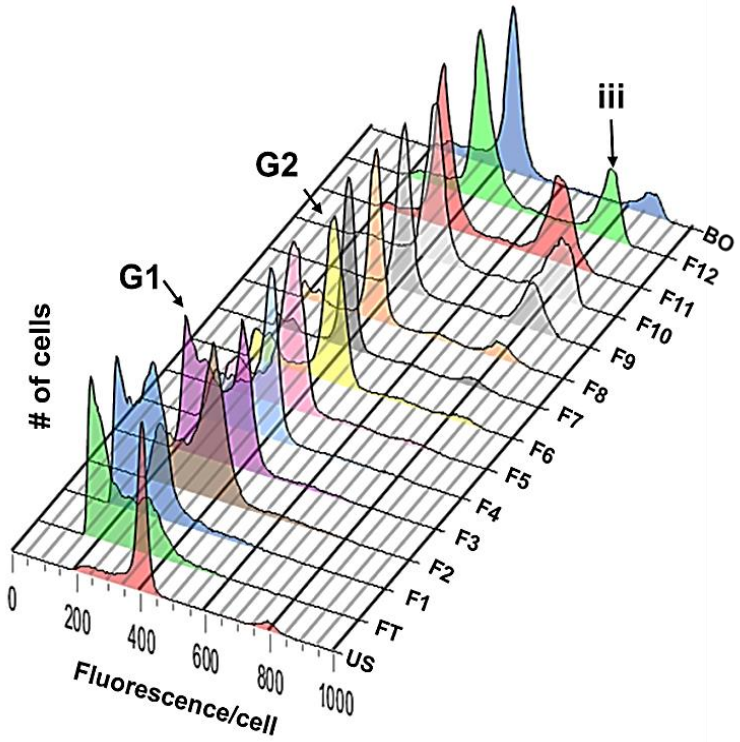

	% of Total Cells			
	G1	**S**	**G2**	**iii**
Unsorted	2	22	60	5
FT	24	54	8	0.2
F1	17	76	2	0.1
F2	9	30	44	0.5
F3	17	45	30	0.4
F4	9	37	43	0.8
F5	9	22	59	1.5
F6	6	21	60	2
F7	3	11	69	5
F8	3	11	61	8
F9	0.4	5	53	19
F10	1	8	50	29
F11	1	9	39	33
F12	1	12	46	23
BO	2.5	17	56	11

Figure 6: Flow cytometry results of a CCE experiment testing for cysts. The relative percentages of each stage of the cell cycle (G1, S, G2) and the percentage of Peak iii cells in the unsorted asynchronous control and fractions collected by CCE are shown in the table on the right. The x-axis of the histogram on the left represents the relative SYTOX Green fluorescence (DNA content) per cell, while the y-axis represents the number of cells at the given fluorescence.

Since cysts are the only form of Giardia cells known to have a DNA content that is double that of G2 cells (Fig. 2, introduction), I sought to determine if the cells in the third peak shown in the flow cytometry histograms represent 16N cysts. Therefore, the CCE fractions were analyzed by RT-qPCR and immunofluorescent microscopy for characteristics of cysts or encysting trophozoites.

3.1.2: RT-qPCR analysis

First, I determined the mRNA level of the cyst wall protein 1 (CWP1) gene in the CCE fractions. This gene encodes a major protein component of the Giardia cyst wall, and the expression of this gene is induced in Giardia trophozoites during encystation (Castillo-Romero et al., 2010; Einarsson et al., 2016; Hehl et al., 2000; Morf et al., 2010). Based on the literature, the mRNA expression of CWP1 is increased by 20 – 100 fold at the 24 hours encystation time-point in both RT-qPCR experiments and recent RNA-seq analysis (Einarsson et al., 2016; Hehl et al., 2000; Morf et al., 2010; Su et al., 2011). There should be a corresponding increase in the level of CWP1 mRNA in the latter CCE fractions if they are enriched for Giardia cysts.

In my experiment, the expression profile from the average of three independent RT-qPCR runs from the RNA extracted from an elutriation experiment is shown in Figure 7. The data for CWP1 was normalized to the RNA levels of the actin gene, and the normalized data in each fraction is calibrated to the data for Fraction 5. Fraction 5 was chosen as the calibrator sample since it consistently contains the highest percentage of G2 cells among the CCE fractions.

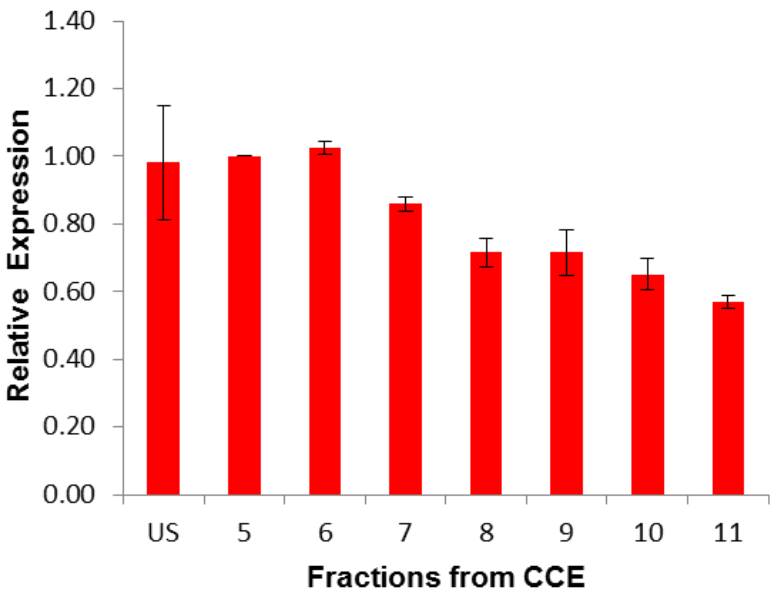

Figure 7: Relative mRNA expression of the CWP1 gene from late CCE fractions. The relative mRNA expression of CWP1 from the unsorted (US) and Fractions 5-11 from a CCE experiment. Error bars represent the standard deviation of three independent RT-qPCR runs. Expression levels are normalized to the actin gene and relative to the calibrator fraction (Fraction 5).

In my RT-qPCR analysis of the CCE fractions, I observed a slight decrease in CWP1 mRNA in CCE Fractions 7 – 11, which are the same fractions that showed an increasing percentage of Peak iii cells in the flow cytometry analysis (Fig. 6). As the expression of the CWP1 in the CCE fractions did not increase, it is unlikely that a high percentage of cysts were present in these fractions.

3.1.3: Immunofluorescence microscopy

Giardia cysts can also be visualized by differential interference contrast (DIC) and fluorescent microscopy. A Giardia cyst has a round shape (see DIC panel in Fig. 8A) compared to the teardrop shape of Giardia trophozoites. Furthermore, a Giardia cyst contains four nuclei (see DAPI panel in Fig. 8A) compared to the two nuclei in a Giardia trophozoite. Most importantly, Giardia cysts are recognized by a monoclonal antibody against the cyst wall protein 1 (CWP1). When this antibody is conjugated to a fluorophore and used in an immunofluorescent microscopy assay (IFA), the reactive Giardia cysts fluoresce when viewed under the appropriate filter (see CWP1 panel in Fig. 8A).

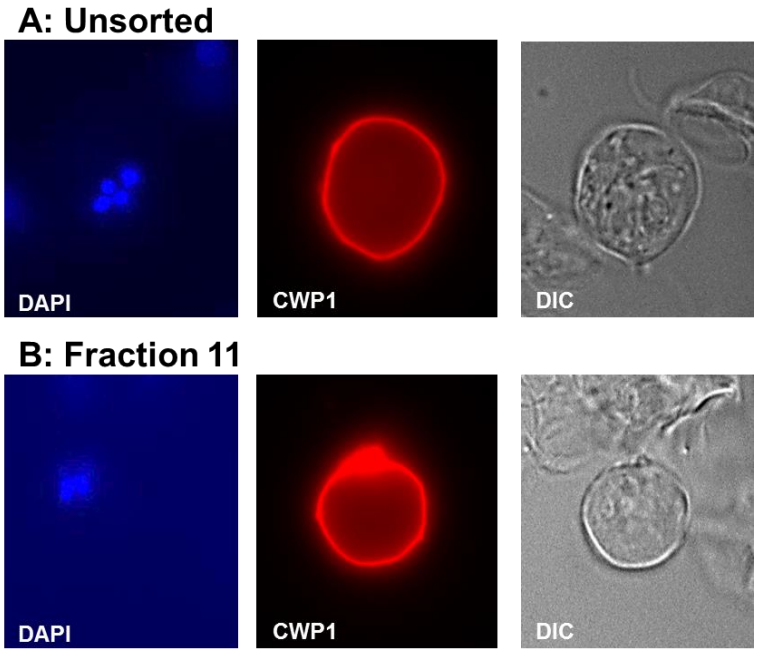

Figure 8: Immunofluorescence microscopy of cysts in a CCE experiment. Shown here are the unsorted asynchronous control (A) and Fraction 11 (B) from a CCE experiment. Cells were stained with DAPI to visualize the nuclei, an antibody specific to CWP1 protein to detect cysts and the corresponding DIC image of the same field of view.

CCE fractions (F9 - 11) that were determined by flow cytometry analysis to contain a high percentage of Peak iii cells (Fig. 6) were subjected to immunofluorescent microscopy assay with the CWP1 monoclonal antibody. The percentage of CWP1 positive cells in the CCE fractions and an unsorted Giardia trophozoite sample were determined and compared with the percentages of Peak iii cells in the same samples as measured by flow cytometry (Table 1).

Table 1: Percentage of cysts in late CCE fractions. The percentage of cysts from the immunofluorescent assay (IFA) was calculated by counting the number of cysts and dividing it by the total number of cells (cysts and trophozoites) viewed over several fields of view on a microscope slide. The total number of cells counted range from 100 - 200. The percentage of Peak iii cells by flow cytometry (FC) was determined by analyzing the results with FlowJo Analysis Software v.7.2.2.

	% Cysts from IFA	**% Peak iii cells from FC**
Unsorted	2.6	5
F9	0.4	19
F10	0.9	29
F11	2.4	33

In Table 1, the percentages of cysts in the three CCE fractions detected by IFA with the CWP1 monoclonal antibody are much lower than the percentages of Peak iii cells measured by flow cytometry (Fig. 6). Typically to induce encystation *in vitro*, the trophozoites are exposed to a different medium in order to mimic the conditions of encystation that occurs in the host. However, a small percentage of cysts can arise spontaneously in standard Giardia trophozoite cultures (Morf et al., 2010). I also observe the presence of cysts in my trophozoites cultures but this percentage (<3%) is much lower

than the total percentage of cells in the third peak (19 - 33%) within the latter CCE fractions (Table 1).

3.1.4: Quantification of the amount of DNA per nuclei by fluorescent intensity

Since the IFA results show that the third peak (Peak iii) has only a small percentage of cysts, we investigated the possibility that the Peak iii cells are endoreplicated Giardia trophozoites. Endoreplication is a process where a cell replicates or synthesizes its genome again, without continuing to mitosis (Lee et al., 2009). Endoreplication has a variety of roles and functions in different cell types, for example it is used in the development of *D. melanogaster* embryos, is used for nutrient uptake, and is used in tissue regeneration after being exposed to stress (Lee et al., 2009). In fact, stress-induced endoreplication has been observed in tumor tissues, damaged cardiomyoctes and in aging mouse hepatocytes (Lee et al., 2009). In Giardia, endoreplication has also been observed as a stress response to external stimuli. When trophozoite cells are exposed to the G2/M cell cycle blocking drug nocodazole, there is an increase of 16N cells in the flow cytometry histograms (Reaume et al., 2013).

If an 8N/G2 trophozoite cell replicates its DNA without cell division, it would result in a 16N trophozoite. To determine if this occurred, I stained the CCE fractions with DAPI, a DNA binding dye, and looked for trophozoites with more than two nuclei per cell. As I did not detect any trophozoites with more than two nuclei per cell, any 16N cell would need to have 8N of DNA in each of its two nuclei. Therefore, I measured the fluorescent intensity of the nuclei in the DAPI-stained Giardia trophozoites within the CCE fractions. This was performed by analyzing the images from the epifluorescent microscope with the CellProfiler program (Table 2).

Table 2: Average intensity per nuclei of cells in different CCE fractions. The average intensity of each nucleus after DAPI staining was measured using the CellProfiler program. The expected stage of the cell cycle for each CCE fraction is given as either G1 or G2. Over 100 cells for each fraction (except for Fraction 10 where 20 cells were used) were analysed with the standard deviation for each average calculated. The average fluorescent intensity/nucleus for F2 was assigned a value of 2 for the DNA content/nucleus, and used as a calibrator for the remaining samples for this parameter.

				DNA content/nucleus	
CCE Fraction	**Expected stage of cell cycle**	**# nuclei per cell**	**Avg. Intensity/nucleus ± SD**	**Expected**	**Calculated**
US	Mostly G2	2	0.079 ± 0.012	4N	4.5
F2	G1	2	0.035 ± 0.002	2N	2.0
F5	G2	2	0.065 ± 0.010	4N	3.7
F7	G2	2	0.078 ± 0.019	4N	4.5
F10	G1	2	0.032 ± 0.007	2N	1.8
	G2	2	0.059 ± 0.018	4N	3.4

Since flow cytometry of the CCE fractions showed that Fraction 2 is enriched in G1 cells (Fig. 6), the average fluorescent intensity/nucleus for Fraction 2 is likely representative of the DNA content of 2N per nucleus of a G1 cell (see Fig. 2 in Introduction). A value of 2.0 is assigned to represent the calculated DNA content/nucleus of the cells in the F2 sample, and the DNA content/nucleus for the other samples were determined relative to this reference based on their fluorescent intensity. The results showed that the estimated DNA content/nucleus in the cells in CCE Fractions 5 and 7 are approximately double the value of the cells in Fraction 2 (Table 2). This is consistent with the flow cytometry analysis indicating that Fractions 5 and 7 are enriched in G2 cells (Fig. 6). Although flow cytometry showed that Fraction 10 contains 26% of Peak iii cells (Fig. 6), the CellProfiler analysis did not identify cells with a DNA content/nucleus that is greater than the 4N/nucleus expected for G2 cells. Therefore, the third peak seen in the

flow cytometry results likely does not represent cells that have undergone endoreplication. Indeed, Fraction 10 has two distinct populations of cells: one that has the DNA fluorescent intensity corresponding to a G1 cell and the other that corresponds to a G2 cell. This indicates that the this CCE fraction is not enriched in a particular stage of the trophozoite cell cycle and has a cell population that is similar to an unsorted and asynchronous Giardia sample.

The fluorescent signal that is emitted by each cell is measured for the height of the pulse, the time of flight (width) and the pulse integral (area) (Fig. 9A) (Kang et al., 2010). However, the ratio between the height of the peak and the area is used to discriminate singlet cells from doublet cells. A singlet G1 cell will have a 200:200 (1:1) ratio of height to area, whereas a G1 doublet cell will have the same height as a singlet cell (200), however the area will be twice as large (400) leading to a ratio of 1:2 (Fig. 9B). As such, we can exclude some doublet cells by selecting only for the cells that fall on the 1:1 ratio of pulse height to pulse area during our flow cytometry analysis.

As the majority of cells in an asynchronous Giardia culture are predominately in the G2 stage of the cell cycle, there is a higher chance to form a G2/G2 doublet, which could correspond to the appearance of the third peak in the flow cytometry histograms. While gating the height verses the area removes large cell aggregates, doublet Giardia cells seem to be falling on the 1:1 ratio of height to area. Thus, the Peak iii would represent the G2/G2 doublets. As well, in Figure 4B, there is a small population of cells that appear to be at 600 on the x-axis. This might be a small population of a G1/G2 doublet cells forming. These doublets are present in the latter CCE fractions (Fig. 6), suggesting that the method is separating the larger cell aggregates. It is probable that the

third peak seen in our flow cytometry analysis represents an aggregation of two G2 cells. Therefore, Peak iii cells will be excluded from the remainder of flow cytometry analysis described in this thesis.

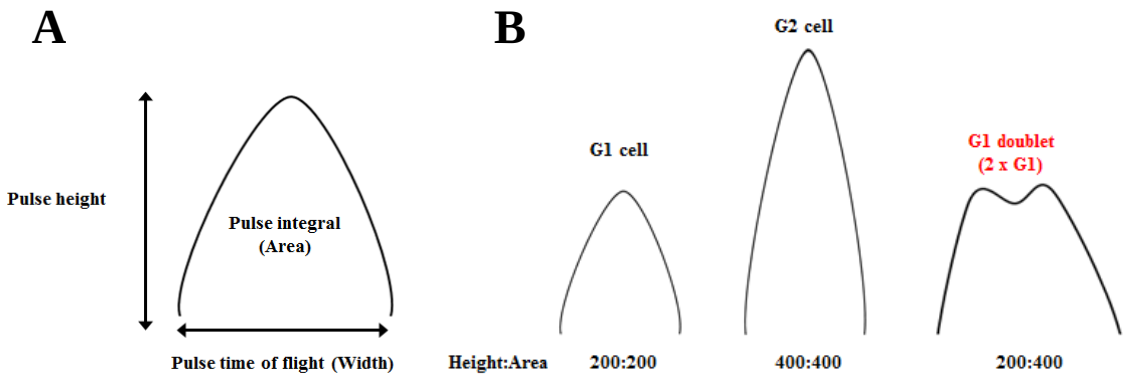

Figure 9: Pulse parameters in cell determination. A) The three fluorescent parameters measured after emission of the excited fluorescent dye by a laser. **B)** Representation of the pulses generated from a G1 trophozoite, G2 trophozoite and a G1 doublet, as they would pass in front of the laser.

3.2: Objective 2: Investigation of the addition of the GS isolate of Giardia trophozoite cells as an external normalizer for RT-qPCR analysis.

3.2.1: Comparison of an internal to external normalizer in a Counterflow Centrifugal Elutriation Experiment

In RT-qPCR, the use of a normalizer gene is essential for determining the accurate expression level for the gene of interest. In the second objective of my research, I compared the use of an external normalizer to an internal normalizer gene in the Giardia cell cycle analysis with our CCE fractions. In order to test the normalizers during the trophozoite cell cycle we first obtained fractions enriched with the different stages of the trophozoite cell cycle by CCE (Fig. 10).

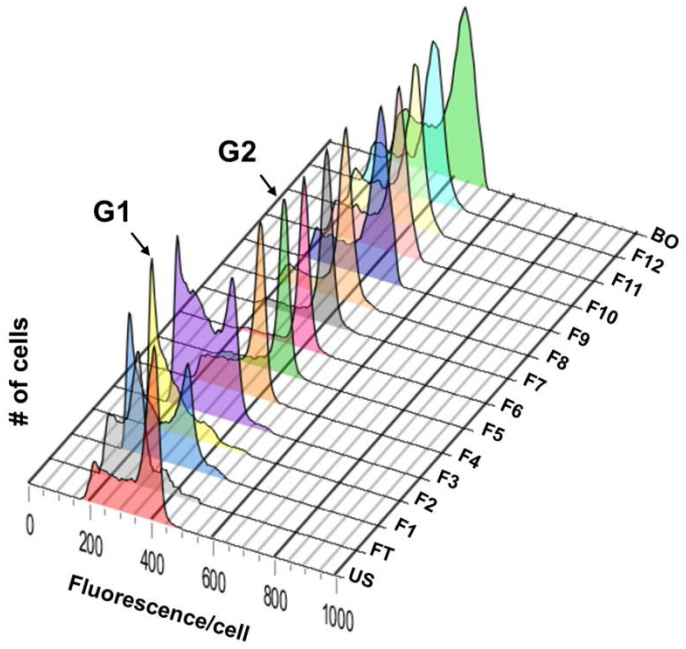

	% of Total Cells		
	G1	**S**	**G2**
Unsorted	9	30	61
FT	18	69	13
F1	31	34	35
F2	43	49	8
F3	20	48	32
F4	7	31	62
F5	2	8	90
F6	2	7	91
F7	3	11	86
F8	6	15	79
F9	8	21	71
F10	7	24	69
F11	10	23	67
F12	14	18	68
BO	13	21	66

Figure 10: Flow cytometry results of a CCE experiment for external normalizer assessment. The relative percentages of each stage of the cell cycle (G1, S, G2) cells in the unsorted asynchronous control and fractions collected by CCE are shown in the table on the right. The x-axis of the histogram on the left represents the relative SYTOX Green fluorescence (DNA content) per cell, while the y-axis represents the number of cells at the given fluorescence.

In RT-qPCR analysis, the expression level of a gene of interest is usually compared to the level of a reference or normalizer gene. This normalizer is ideally a gene that has consistent expression across samples being compared within an experiment. For my experiments, the ideal normalizer gene should have a constant mRNA level throughout the trophozoite cell cycle, or among all the fractions collected from the CCE experiment. The actin gene, which encodes a structural protein, was previously used as an internal normalizer for our cell cycle studies with the CCE fractions (Reaume, 2013). I investigated the addition of a spiked-in RNA sample as an external normalizer. A small but constant proportion of RNA (2%) from the GS isolate was added to the RNA extracted from CCE fractions of a WB isolate of Giardia. In the RT-qPCR analysis of the spiked RNA sample, I measured the mRNA expression of a gene encoding a sugar proton symporter (SPS) that is present only in the GS isolate. Since 2% of GS RNA was added relative to the WB RNA in each sample, it is expected that the mRNA level of the GS sugar proton symporter gene will be similar among the spiked CCE samples.

Previous research has shown that the mRNA expression level of the histone H4 gene is higher in G1 and S phase trophozoite cells (Reaume, 2013; Reiner et al., 2008). Therefore, I compared the use of the external spike and the use of an internal reference gene to normalize the expression of the histone H4 gene. When the actin gene was used as the internal normalizer, the histone H4 mRNA level increases by an average of 2-fold in Fractions 3 and 4, which are fractions with a high percentage of G1 and S phase cells (Fig. 11A). When the GS SPS gene was used as the external normalizer, the histone H4 mRNA showed a similar increase of H4 mRNA in Fractions 3 and 4. However, there were larger standard deviations associated with the use of the GS SPS normalizer (see

error bars), which suggested that there was variation in the amount of spiked GS RNA relative to the amount of WB RNA in each CCE fraction. Since RT-qPCR is a sensitive technique, small pipetting errors in adding the RNA spike can be magnified during analysis. Despite this, the expression profiles for histone H4 obtained by RT-qPCR using the actin gene as the internal normalizer and the GS SPS gene as the external normalizer are the same. This shows that the actin gene is an appropriate internal normalizer for gene expression studies of the Giardia cell cycle, and it is also possible to use an external spike of GS RNA as an alterative normalizer in these studies.

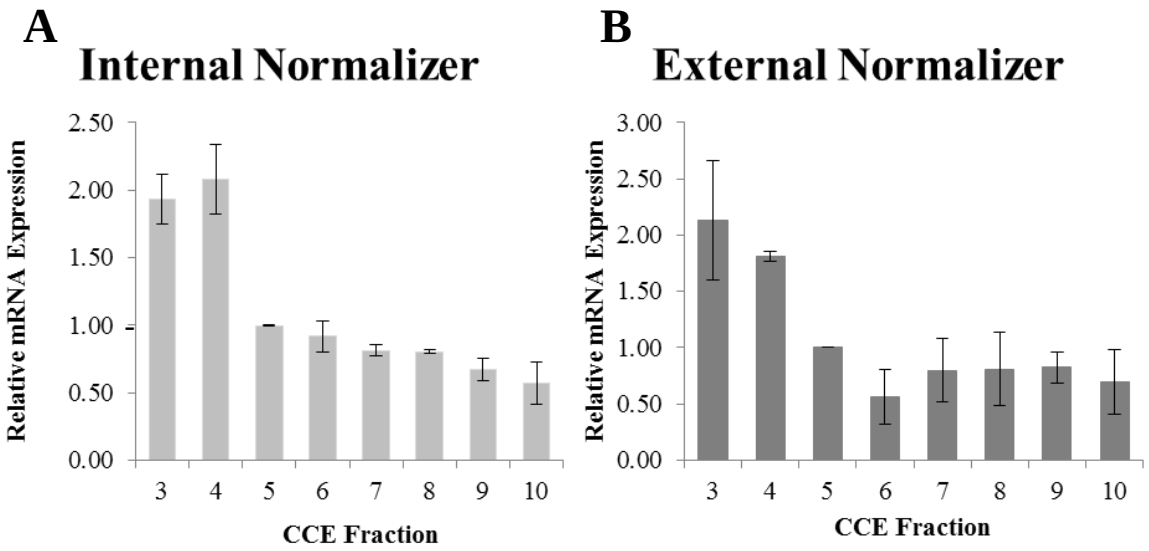

Figure 11: Comparison of Histone H4 mRNA expression profile in CCE fractions using the internal normalizer (Actin) to external normalizer (GS SPS). The mRNA expression profile for the histone H4 gene in CCE fractions was compared using actin as an internal normalizer (A) or GS SPS as an external normalizer (B). Shown is the average relative mRNA expression based on three qPCR runs with the same cDNA preparation. In both cases, highest expression of Histone H4 is in both Fraction 3 and 4.

3.2.2: Comparison of an internal to external normalizer in an Encystation Experiment

To determine if external spiking could successfully be used in other RT-qPCR analyses in Giardia, RNA was extracted from WB trophozoites induced to undergo encystation *in vitro* for 0, 7, 12, and 24 hours. The RNA from the encysting WB Giardia samples was spiked with 2% GS trophozoite RNA and the mRNA levels of the GS SPS gene was used as the external normalizer. For the internal normalizer, I used the gene for ribosomal protein L2 (RP L2) that was tested previously for RT-qPCR studies in Giardia encystation in our laboratory (Walden, 2014).

I first compared the expression of the CWP1, a gene that is highly expressed during encystation, using either the RP L2 gene or the GS SPS gene as the normalizer. A similar mRNA expression profile of the CWP1 gene was observed with both the internal (RP L2) and external (SPS) normalizer, (Fig. 12A). I next analyzed the Myb1 gene that is expected to have a smaller fold change in expression during encystation (Einarsson et al., 2016; Morf et al., 2010). Based on recent RNA-seq data, Myb1 RNA increases 2.5 fold by 7 hours and 3.4 fold by 22 hours (Einarsson et al., 2016). Myb1 is a transcription factor that induces the transcription of a small subset of genes during early encystation (Sun et al., 2002). With both the internal and external normalizers, the expression profile of the Myb1 gene was upregulated by at least 2 fold in the 7 hour-time point, with slightly higher expression in the 12 and 24 hour time points compared to the 0 hour control (Fig. 12B). These results show that the RP L2 gene is an appropriate internal normalizer for gene expression studies of Giardia encystation and it is also possible to use an external spike of GS RNA as an alterative normalizer for these experiments. However, the greatest

utility of the external spike with the GS RNA would be in other Giardia gene expression studies where an appropriate internal normalizer gene is either not possible or had not been identified.

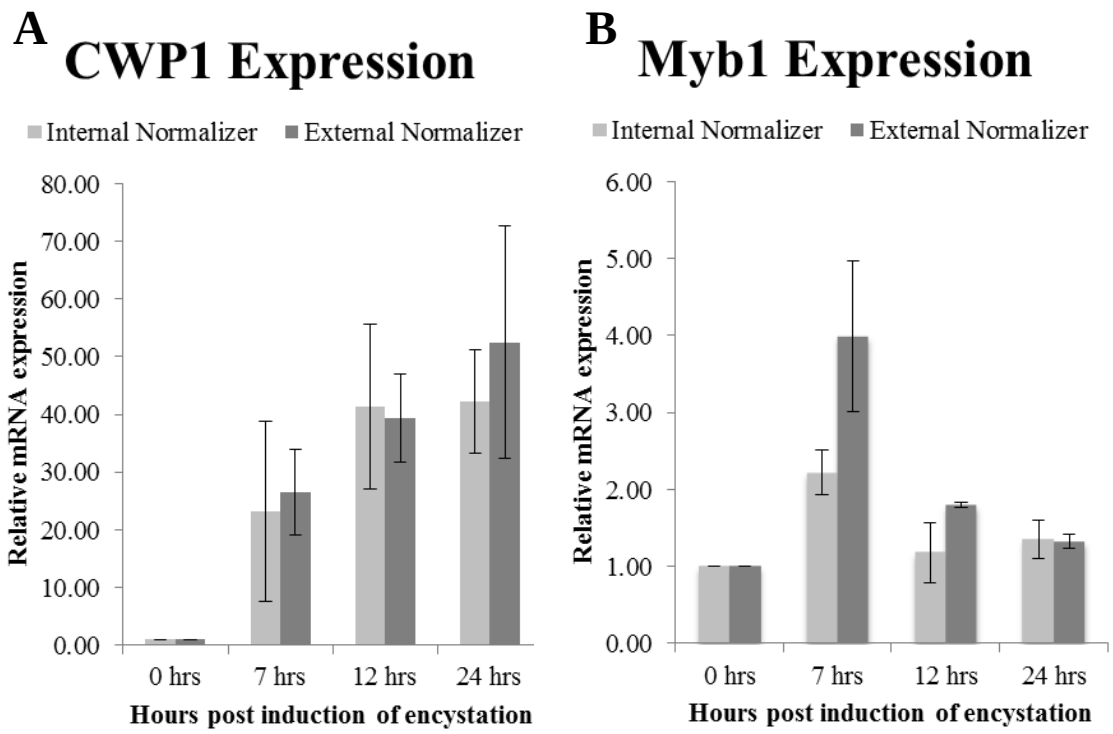

Figure 12: CWP1 and Myb1 expression profiles from an encystation experiment after using internal and external normalizers. **A)** CWP1 expression profile is similar to when using either the internal (Ribosomal protein L2) or external (GS SPS) gene as a normalizer. **B)** The expression profile of the Myb1 gene is also similar when using the internal normalizer Ribosomal protein L2 or the external gene GS SPS as a normalizer. Shown is the average relative mRNA expression based on three qPCR runs with the same cDNA preparation for both the CWP1 and Myb1 expression profiles.

3.3: Objective 3: Transcriptome analysis of the Giardia trophozoite cell cycle by RNA-Seq

3.3.1: Conditions for RNA-seq experiment and analysis

For my last objective I prepared two sets of elutriations (shown as E2 in Fig. 13 and E3 in Fig. 14) for RNA-sequencing at the facility of our collaborator at Uppsala, Sweden. These two elutriations have similar percentages of G1, S and G2 cells in corresponding fractions, which suggested they are good choices as biological replicates (Tables 3 and 4). Some of the Fractions (FT/F1 and F2 in E2; FT and F1 in E3) did not yield sufficient amount of high-quality RNA for RNA-seq analysis. To reduce costs, our collaborator decided to submit only Fractions 3, 5, 7, 9 and 11 from the two-elutriation sets for RNA-seq.

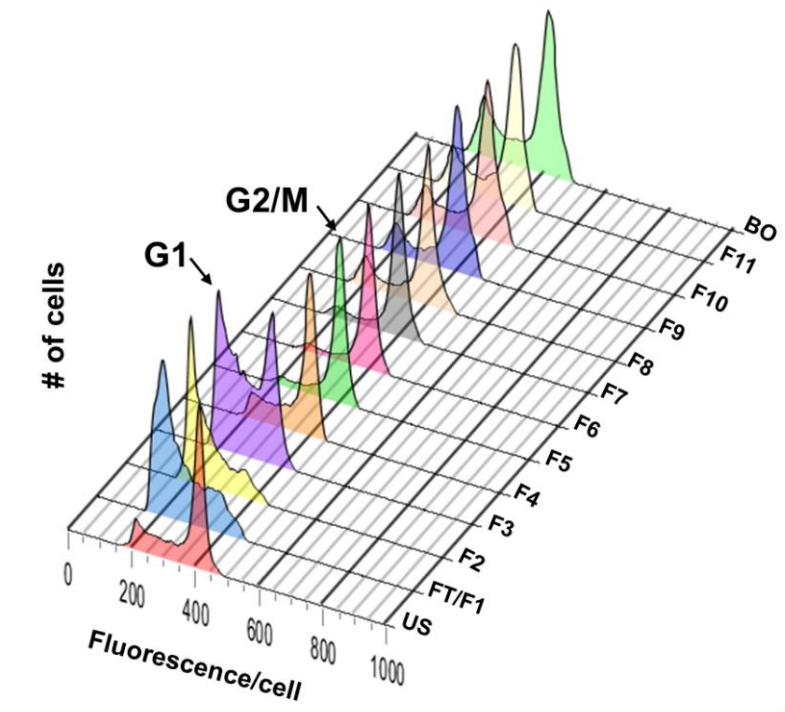

Figure 13: Flow cytometry results of the CCE experiment for 1st replicate (E2) for RNA-seq analysis. The x-axis of the histogram on the left represents the relative SYTOX Green fluorescence (DNA content) per cell, while the y-axis represents the number of cells at the given fluorescence.

Table 3: Percentages of each stage of the cell cycle form CCE experiment E2 for RNA-seq analysis. The relative percentages of each stage of the cell cycle (G1, S, G2/M) cells in the unsorted asynchronous control and fractions collected by CCE are shown below. The amount of RNA before and after DNase I treatment is shown in the two columns on the right. Only Fractions 3, 5, 7, 9 and 11 (highlighted in grey) were submitted for RNA-seq.

	% of Total Cells			RNA recovery	
	G1	**S**	**G2/M**	**Before DNase I treatment (µg)**	**After DNase I and column clean up (µg)**
Unsorted	10	25	65	21.11	4.73
FT/F1	50	30	20	NA	NA
F2	40	43	17	1.48	0.55
F3	26	36	38	7.88	3.98
F4	8	21	71	17.28	10.48
F5	3	13	84	15.81	5.18
F6	4	9	87	16.30	4.91
F7	7	9	84	15.83	4.90
F8	13	12	75	10.99	2.53
F9	9	15	76	12.88	2.08
F10	13	15	72	7.72	1.73
F11	13	16	71	7.42	2.99
F12	17	16	67	NA	NA
BO	18	19	63	21.84	2.64

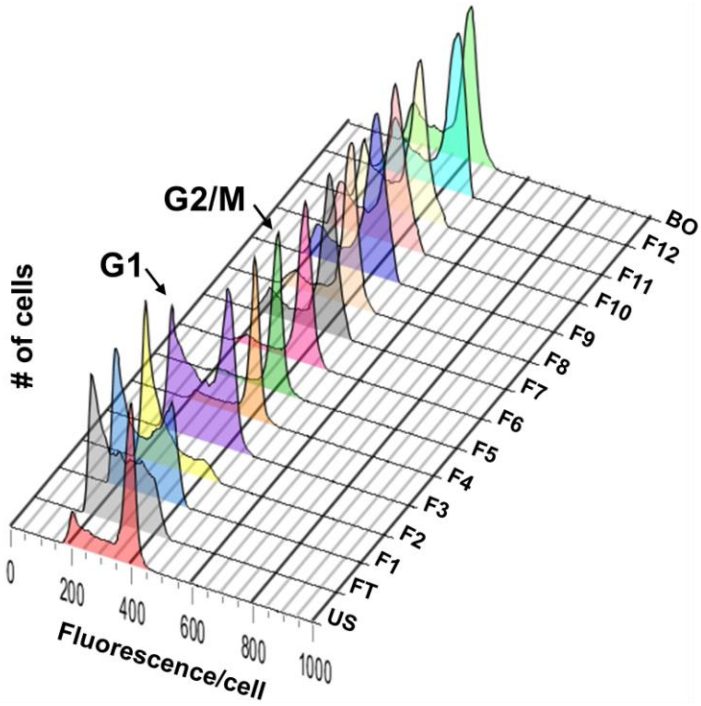

Figure 14: Flow cytometry results of the CCE experiment for 2nd replicate (E3) for RNA-seq analysis. The x-axis of the histogram on the left represents the relative SYTOX Green fluorescence (DNA content) per cell, while the y-axis represents the number of cells at the given fluorescence.

Table 4: Percentages of each stage of the cell cycle form CCE experiment E3 for RNA-seq analysis. The relative percentages of each stage of the cell cycle (G1, S, G2/M) cells in the unsorted asynchronous control and fractions collected by CCE are shown below. The amount of RNA before and after DNase I treatment is shown in the two columns on the right. Only Fractions 3, 5, 7, 9 and 11 (highlighted in grey) were submitted for RNA-seq.

	% of Total Cells			RNA recovery	
	G1	S	G2/M	Before DNase I treatment (µg)	After DNase I and column clean up (µg)
Unsorted	10	21	69	31.47	7.83
FT	41	34	25	2.25	NA
F1	34	34	32	2.70	NA
F2	58	33	9	3.82	NA
F3	25	26	49	22.30	17.38
F4	4	13	83	29.85	26.25
F5	2	6	92	27.37	8.75
F6	3	8	91	20.09	14.38
F7	8	9	83	13.36	5.58
F8	9	12	79	17.04	15.80
F9	11	13	76	9.52	1.74
F10	13	18	69	9.48	2.16
F11	15	18	67	6.52	0.97
F12	17	16	67	5.79	1.39
BO	12	19	69	10.68	1.94

3.3.2: Number of differentially expressed genes in all comparisons

The two elutriation sets (E2 and E3) representing two independent biological replicates and corresponding fractions from each set were analyzed together (i.e. Fraction 3 in E2 was analyzed together with Fraction 3 in E3). To identify differentially expressed (DE) genes, a pairwise comparison of the data from Fractions 3, 7, 9 and 11 relative to Fraction 5 was performed (Appendix VIII). Fraction 5 was chosen to be the reference or calibrator sample because it had the highest enrichment of G2 cells among all the samples that were analyzed by RNA-seq (Table 5). Fraction 3 is the sample enriched in G1 cells

for this analysis and the comparison of Fraction 3 to Fraction 5 yielded the highest number of DE genes (Table 5).

Table 5: Number of differentially expressed genes from the DESeq2 analysis. These genes have a FDR p-value <0.05 for significance.

Comparison	# of up regulated genes	# of down regulated genes	Total # of differentially expressed genes
F3 to F5	393	631	1024
F7 to F5	3	0	3
F9 to F5	73	66	140
F11 to F5	64	2	66

Our collaborators at the University of Uppsala in Sweden also performed a microarray experiment on Giardia trophozoites to study the transcriptome during the trophozoite cell cycle. In their experiment, they used aphidicolin to synchronize the cell cycle in a Giardia WB trophozoite culture. This drug binds DNA polymerase and blocks the Giardia trophozoites during DNA synthesis, or the S phase of the cell cycle. Once released from the drug, cells then progress in synchrony from the S phase. Cells were collected at 0, 1, 2, 3, 4, 5, 6, 6.5 and 8 hours post release from the drug representing the following stages of the cell cycle: S phase, early G2/M phase, early to middle G2/M phase, and middle to late G2/M and G1 phase cells. The microarray results can be found in Table A26 in Appendix XI, and represent genes that had a fold change of 1.4 or greater in the microarray results. I determined which genes identified in the microarray experiment are also identified in my RNA-seq data, since genes that are found in both data sets are likely to be the most robust.

3.3.3: Genes up-regulated in G1/S (Fraction 3):

Among the elutriation fractions that were analyzed by RNA-seq (F3, 5, 7, 9 and 11), Fraction 3 contains the highest percentage of cells in G1 and S stages (Fig. 13 and 14). Twenty-seven genes identified as G1 and S-phase genes from Svard's microarray studies are also found to be up-regulated in Fraction 3 from our RNA-seq data (Table 6). Thymidine kinase (GL50803_8364) is one of the genes identified in the microarray and the RNA-seq data as a S-phase gene. Thymidine kinase is a part of the salvage pathway of pyrimidine deoxynucleotides that phosphorylates thymidine to produce TMP (Kauffman and Kelly, 1991). As TMP is used during the DNA synthesis stage of cell cycles, it was expected to have the highest expression during late G1/ S phase (Kauffman and Kelly, 1991). Previous RT-qPCR analysis performed in our laboratory showed that the mRNA level of the thymidine kinase gene increases in the elutriation fractions that are enriched in S-phase cells (Reaume et al., 2017, submitted). In addition, the deoxyguanosine kinase/deoxyadenosine kinase (GL50803_4558) was identified in Fraction 3 of the RNA-seq results. Deoxypurine kinases produce dGMP and dAMP, and similar to thymidine kinase, generate deoxyribonucleotides required for DNA synthesis. These genes are shown to be regulated during S-phase in mammalian cells (Fyrberg et al., 2006).

As well, one gene encoding a putative Cyclin (GL50803_15094) was upregulated by 1.77 fold in the G1/S enriched fraction from the RNA-seq data. Cyclins are one of the main classes of regulators of the eukaryotic cell cycle with the highest transcript levels found where they exert their function. Cyclin proteins interact with their corresponding cyclin dependent kinase (CDK) to phosphorylate their target proteins during specific

points in the cell cycle (Harper and Adams, 2001). Initial BLASTp searches of the amino acid sequence of the protein encoded by this gene did not show extensive matches to other cyclins. However, analysis of the predicted 3D structure of the protein by I-TASSER (Iterative Threading Assembly Refinement) showed that it has similarity to the structure of the Pho85 Cyclin-10 in *S. cerevisiae*. The match has a score of 0.7769 out of a maximum score of 1.000. The I-TASSER program gives a predicted protein structure of the query sequence and compares it with known proteins structures in the protein structure database (Zhang, 2008).

Genes encoding hypothetical proteins is the most abundant category (34%) of up-regulated genes in G1/S in both the RNA-seq and microarray data (Table 6), and the most abundant category found in the G1/S RNA-seq data (Appendix VIII, Table A13). The function of the proteins encoded by these genes have not been characterized although the RNA corresponding to some of these genes have the highest fold increase in Fraction 3, which suggests they play a role during G1/S phase in the trophozoite cell cycle.

However, several genes identified as G2/M in the microarray data were also present in Fraction 3's RNA-seq data (Table 6). These genes are likely due to the population of G2 cells present in Fraction 3 (38% and 49% for the two experiments respectively). Nevertheless, the genes identified in the middle – late G2/M in the microarray data set might represent early G1 phase genes. Giardia spends a very short time (~0.7 h) in G1 phase compared to G2 (~4 h) (Reiner et al., 2008). After aphidicolin treatment, the G1 phase is even shorter and the S phase begins shortly after finishing mitosis (unpublished work from Dr. Svard's laboratory). Therefore, it is possible that the

expression of the early G1 and S genes are occurring in the late G2 time point in the microarray experiment.

Table 6: Genes upregulated in Fraction 3 from both RNA-seq analysis and microarray data. Cell cycle stages from the microarray experiment is shown in the left column. Fold changes are from the RNA-seq experiment and all genes have a FDR p-value < 0.05.

Cell Cycle Stage	Gene Description	Gene ID	Fold change from RNA-seq
G1	Adaptin, Beta	GL50803_21423	1.28
G1	Axoneme-associated protein GASP-180	GL50803_16745	1.60
G1	Deoxyguanosine kinase/deoxyadenosine kinase subunit, putative	GL50803_4558	2.89
G1	Giardin, Beta	GL50803_4812	1.78
G1	Giardin, Delta	GL50803_86676	2.03
G1	H-SHIPPO 1	GL50803_9148	1.48
G1	hypothetical protein	GL50803_6185	2.36
G1	hypothetical protein	GL50803_10524	2.35
G1	hypothetical protein	GL50803_10808	2.04
G1	hypothetical protein	GL50803_23017	2.01
G1	Kinase, NEK	GL50803_11390	1.90
G1	Kinase, NEK	GL50803_24321	1.43
G1	Kinase, NEK	GL50803_17231	1.43
G1	P115, putative	GL50803_8855	2.00
G1	Protein 21.1	GL50803_16532	2.24
G1	Protein 21.1	GL50803_23492	2.24
G1	Protein 21.1	GL50803_40390	2.00
G1	Protein 21.1	GL50803_27925	1.74
G1	Protein 21.1	GL50803_8174	1.74
G1	Protein 21.1	GL50803_11165	1.70
G1	SALP-1	GL50803_4410	2.21
G1	Spindle pole protein, putative	GL50803_24537	1.57
G1	Thymidine kinase	GL50803_8364	2.82
S	ATP-dependent RNA helicase-like protein	GL50803_15048	1.71
S	hypothetical protein	GL50803_16602	1.62
S	hypothetical protein	GL50803_10675	1.45
S	hypothetical protein	GL50803_90434	1.27
G2/M - early	ATP-dependent RNA helicase HAS1, putative	GL50803_16887	1.82
G2/M - early	Glutamate-rich WD-repeat protein	GL50803_14174	1.54
G2/M - early	hypothetical protein	GL50803_15062	1.50
G2/M - early	hypothetical protein	GL50803_10675	1.45
G2/M - early	Phosphatase	GL50803_15215	1.27

Cell Cycle Stage	Gene Description	Gene ID	Fold change from RNA-seq
G2/M - early	Spindle pole protein, putative	GL50803_17055	1.33
G2/M - early/mid	Heat shock protein HSP 90-alpha	GL50803_13864	1.30
G2/M - mid/late	ATP/GTP binding protein, putative	GL50803_10370	1.65
G2/M - mid/late	hypothetical protein	GL50803_16581	2.54
G2/M - mid/late	hypothetical protein	GL50803_29796	2.31
G2/M - mid/late	hypothetical protein	GL50803_16648	1.64
G2/M - mid/late	hypothetical protein	GL50803_16543	1.59
G2/M - mid/late	hypothetical protein	GL50803_14921	1.28
G2/M - mid/late	Spindle pole protein, putative	GL50803_24537	1.57

I used DAVID (Database for Annotation, Visualization and Integrated Discovery) to analyze the genes upregulated in G1/S (Fraction 3) in the RNA-seq data and determined that there are three clusters of encoded proteins with similar features and functions (Table 7). The first cluster contains proteins with an ankyrin domain, which are used in protein – protein interactions (Table A15 in Appendix IX). Ankyrin domain proteins have a variety of roles in eukaryotes including transcription, cell differentiation and cell cycle control (Hryniewicz-Jankowska et al., 2002). For example, the human p16 protein, which contains an ankyrin domain, is responsible for inhibiting phosphorylation of the kinases Cdk4 and Cdk6 that regulate the cell cycle (Donjerkovic and Scott, 2000). Among the 63 ankyrin domain genes identified in the RNA-seq analysis, 44 encode members of the protein 21.1 family. Although there are 243 genes encoding protein 21.1 in the Giardia genome, they have no known role to date. However, 40 genes for 21.1 proteins identified as upregulated in G1/S from my RNA-seq data (Appendix IX, Table A15) are also differentially expressed during Giardia encystation (Einarsson et al., 2016). Of those 40 proteins, 33 have the highest expression in trophozoites and the remaining 7 have the highest expression in cysts. Thus these specific 21.1 proteins, especially the

seven proteins that have a higher expression in cysts, might also have a role in the linking of the trophozoite cell cycle to encystation.

Table 7: Gene clusters identified by DAVID functional annotation tool in G1/S enriched genes identified by RNA-seq. Clusters identified had an enrichment score above 1.3 and the fold change range is given.

Cluster identified by DAVID	Number of genes identified	Fold change range (max – min)
Ankyrin domain	63	2.32 – 1.27
Cellular protein localization/transport	7	1.52 – 1.26
Phosphoinositide (PX) binding	3	1.79 – 1.27

The second cluster contains transport proteins including adaptins (Table A16 in Appendix IX). These are involved in endocytosis and vesicle transport (Boehm and Bonifacino, 2001; Touz et al., 2012). These genes also show a change in expression during the encystation process (Einarsson et al., 2016), and as such, these genes may play a role during differentiation in Giardia. Since encystation is linked to the cell cycle (Reiner et al., 2008), the adaptins are also likely to have a role in the trophozoite cell cycle.

The final cluster contains proteins with a phosphoinositide binding domain (PX, Phox) (Table A17 in Appendix IX). Proteins with this domain are involved in signal transduction, in particular targeting proteins to membranes by binding various phosphoinositide containing proteins or by targeting specific lipids (Cullen et al., 2001). This PX domain has also been shown to be involved in cell proliferation, differentiation

and membrane trafficking, and the genes identified might be involved in a signaling pathway during G1 or S phase in Giardia (Xu et al., 2001).

3.3.4: Genes up-regulated in G2/M (Fraction 5):

Fraction 5 contains the highest percentage of G2/M cells among the elutriation fractions that were analyzed by RNA-seq (Fig. 13 and 14). One hundred and sixteen genes that were identified as upregulated in G2/M from Svard's microarray studies were also upregulated in fraction 5 of the RNA-seq data (Table 8). In particular, Cyclin B (GL50803_3977) and a hypothetical protein containing a cyclin domain were identified in both the microarray and the RNA-seq results. Five additional cyclin genes were identified only in the RNA-seq data (Appendix VIII, Table A13). The mRNA for Cyclin B-like protein (GL50803_17505) and Cyclin A (GL50803_14488) were shown in previous RT-qPCR experiments in our laboratory to have increased levels in elutriation fractions that are enriched in the G2/M cells (Reaume et al., 2017, submitted). The GL50803_16445 gene encodes a putative cyclin domain based on BLASTp analysis, and its mRNA increased 1.75 fold in the G2/M enriched fraction. My I-TASSER analysis showed that GL50803_13874 is structurally similar to Cyclin-10 from *S. cerevisiae* (TM score of 0.862 out of 1.000) and GL50803_8359 is structurally similar to the PHO80 Cyclin in *S. cerevisiae* (TM score of 0.799 out of 1.000). The mRNA for GL50803_13874 is upregulated 1.60 fold and the RNA for GL50803_8359 is upregulated 1.33 fold in the G2/M enriched fraction.

Interestingly, seven potential cyclins were identified in the G2/M fraction while only one potential cyclin was identified in the G1/S fraction. A possible reason why the majority of cyclins have been identified in the G2/M phase in Giardia is that its cell cycle

has a long G2 compared to a very short G1 (Reiner et al., 2008). This is in contrast to other eukaryotes, especially mammalian cells, where the time in G2 is very short and G1 is long. Giardia may require greater regulation of G2/M compared to the G1/S stage of the cell cycle. One possible reason why Giardia spends a longer time in G2 is that this stage contains the transition point to encystation. A G2 Giardia trophozoite is able to response more quickly to changes in the environment by entering the encystation pathway than cells in G1 phase.

Table 8: Genes upregulated in Fraction 5 from the RNA-seq analysis and also identified in the microarray data. Cell cycle stages from the microarray experiment are indicated in the left column. Fold changes are from the RNA-seq experiment and all genes have a FDR p-value < 0.05.

Cell Cycle Stage	Gene Description	Gene ID	Fold change in RNA-seq
G1	Intraflagellar transport particle protein IFT88	GL50803_16660	1.40
G1	Nucleoside diphosphate kinase	GL50803_14135	1.86
G1	Protein 21.1	GL50803_13766	1.88
G2/M - early	AAA family ATPase	GL50803_16867	2.93
G2/M - early	Coiled-coil protein	GL50803_11867	1.38
G2/M - early	Hypothetical protein	GL50803_11955	1.97
G2/M - early	Hypothetical protein	GL50803_14850	1.70
G2/M - early	Hypothetical protein	GL50803_10423	1.46
G2/M - early	Spindle pole protein, putative	GL50803_16013	1.91
G2/M - early	Spindle pole protein, putative	GL50803_13372	1.60
G2/M - early	Syntaxin-like protein 1	GL50803_7309	1.62
G2/M - early	Ubiquitin-conjugating enzyme E2-17 kDa 3	GL50803_15252	1.81
G2/M - early	Unspecified product	GL50803_11954	1.67
G2/M - early/mid	Caltractin	GL50803_104685	1.85
G2/M - early/mid	Centrin	GL50803_6744	1.76
G2/M - early/mid	GTL3 aka MD0260	GL50803_104866	1.60
G2/M - early/mid	Hypothetical protein	GL50803_13851	2.39
G2/M - early/mid	Hypothetical protein	GL50803_16267	2.20
G2/M - early/mid	Hypothetical protein	GL50803_7328	2.09
G2/M - early/mid	Hypothetical protein	GL50803_114546	2.00
G2/M - early/mid	Hypothetical protein	GL50803_9636	1.92
G2/M - early/mid	Hypothetical protein	GL50803_41834	1.48

Cell Cycle Stage	Gene Description	Gene ID	Fold change in RNA-seq
G2/M - early/mid	Hypothetical protein	GL50803_15039	1.30
G2/M - early/mid	Kinase	GL50803_5643	1.41
G2/M - early/mid	Kinase, CAMK CAMKL	GL50803_17566	1.42
G2/M - early/mid	Kinase, CMGC GSK	GL50803_17625	1.78
G2/M - early/mid	Kinase, CMGC SRPK	GL50803_17335	1.60
G2/M - early/mid	Kinesin-6	GL50803_102455	2.70
G2/M - early/mid	Phosphatase, Dual specificity protein phosphatase CDC14A	GL50803_9270	1.66
G2/M - early/mid	Phosphatase, Protein phosphatase 2A regulatory subunit, putative	GL50803_9894	1.34
G2/M - early/mid	Protein 21.1	GL50803_5188	2.15
G2/M - early/mid	Protein 21.1	GL50803_9720	2.05
G2/M - early/mid	Pyruvate kinase	GL50803_3206	2.40
G2/M - early/mid	Unspecified product	GL50803_20253	1.73
G2/M - mid/late	Actin related protein	GL50803_8726	2.00
G2/M - mid/late	Adenylate kinase	GL50803_28234	1.47
G2/M - mid/late	Axoneme central apparatus protein	GL50803_16202	1.69
G2/M - mid/late	Coiled-coil protein	GL50803_95653	1.90
G2/M - mid/late	Cyclin B, G2/mitotic-specific	GL50803_3977	2.28
G2/M - mid/late	Cyclin domain, hypothetical protein	GL50803_17400	2.85
G2/M - mid/late	Dynein regulatory complex	GL50803_16540	2.60
G2/M - mid/late	Fructose-bisphosphate aldolase	GL50803_11043	2.42
G2/M - mid/late	GiTax, an ortholog of the T. brucei axonemal protein TAX-2 that is important for flagella function	GL50803_17116	1.56
G2/M - mid/late	GTP-binding protein ARD-1, putative	GL50803_8140	1.38
G2/M - mid/late	Guanylate kinase	GL50803_7203	1.75
G2/M - mid/late	High cysteine protein	GL50803_94003	1.57
G2/M - mid/late	Hypothetical protein	GL50803_12105	3.47
G2/M - mid/late	Hypothetical protein	GL50803_3538	3.18
G2/M - mid/late	Hypothetical protein	GL50803_11342	2.91
G2/M - mid/late	Hypothetical protein	GL50803_17255	2.84
G2/M - mid/late	Hypothetical protein	GL50803_7242	2.75
G2/M - mid/late	Hypothetical protein	GL50803_6542	2.63
G2/M - mid/late	Hypothetical protein	GL50803_9219	2.59
G2/M - mid/late	Hypothetical protein	GL50803_5883	2.25
G2/M - mid/late	Hypothetical protein	GL50803_8865	2.09
G2/M - mid/late	Hypothetical protein	GL50803_23874	2.07

Cell Cycle Stage	Gene Description	Gene ID	Fold change in RNA-seq
G2/M - mid/late	Hypothetical protein	GL50803_5167	2.03
G2/M - mid/late	Hypothetical protein	GL50803_4149	2.01
G2/M - mid/late	Hypothetical protein	GL50803_16720	2.00
G2/M - mid/late	Hypothetical protein	GL50803_9305	1.94
G2/M - mid/late	Hypothetical protein	GL50803_32489	1.90
G2/M - mid/late	Hypothetical protein	GL50803_8979	1.87
G2/M - mid/late	Hypothetical protein	GL50803_14796	1.86
G2/M - mid/late	Hypothetical protein	GL50803_4624	1.86
G2/M - mid/late	Hypothetical protein	GL50803_17312	1.85
G2/M - mid/late	Hypothetical protein	GL50803_37381	1.85
G2/M - mid/late	Hypothetical protein	GL50803_8460	1.77
G2/M - mid/late	Hypothetical protein	GL50803_88556	1.69
G2/M - mid/late	Hypothetical protein	GL50803_6725	1.69
G2/M - mid/late	Hypothetical protein	GL50803_14198	1.62
G2/M - mid/late	Hypothetical protein	GL50803_103202	1.61
G2/M - mid/late	Hypothetical protein	GL50803_10422	1.60
G2/M - mid/late	Hypothetical protein	GL50803_7207	1.57
G2/M - mid/late	Hypothetical protein	GL50803_16663	1.55
G2/M - mid/late	Hypothetical protein	GL50803_112112	1.55
G2/M - mid/late	Hypothetical protein	GL50803_10527	1.47
G2/M - mid/late	Hypothetical protein	GL50803_14947	1.47
G2/M - mid/late	Hypothetical protein	GL50803_27141	1.45
G2/M - mid/late	Hypothetical protein	GL50803_13467	1.42
G2/M - mid/late	Hypothetical protein	GL50803_10881	1.42
G2/M - mid/late	Hypothetical protein	GL50803_12230	1.39
G2/M - mid/late	Hypothetical protein	GL50803_21527	1.37
G2/M - mid/late	Hypothetical protein	GL50803_8770	1.36
G2/M - mid/late	Hypothetical protein	GL50803_8426	1.36
G2/M - mid/late	Hypothetical protein	GL50803_13288	1.34
G2/M - mid/late	Kinase, AGC AKT	GL50803_11364	2.52
G2/M - mid/late	Kinase, CMGC CDK	GL50803_16802	3.64
G2/M - mid/late	Kinase, CMGC CDK	GL50803_8037	2.41
G2/M - mid/late	Kinase, CMGC MAPK	GL50803_22850	1.80
G2/M - mid/late	Kinase, CMGC RCK	GL50803_6700	1.87
G2/M - mid/late	Kinase, NEK	GL50803_95593	2.59
G2/M - mid/late	Kinase, NEK	GL50803_8445	1.82
G2/M - mid/late	Kinase, NEK	GL50803_11311	1.73
G2/M - mid/late	Kinase, NEK	GL50803_17069	1.72
G2/M - mid/late	Kinase, NEK	GL50803_12148	1.44
G2/M - mid/late	Kinesin like protein	GL50803_17264	1.38
G2/M - mid/late	Kinesin-13	GL50803_16945	3.09
G2/M - mid/late	Malate dehydrogenase	GL50803_3331	3.64
G2/M - mid/late	Median body protein	GL50803_16343	2.23

Cell Cycle Stage	Gene Description	Gene ID	Fold change in RNA-seq
G2/M - mid/late	Mitotic spindle checkpoint protein MAD2	GL50803_100955	2.71
G2/M - mid/late	NOD3 protein, putative	GL50803_4165	1.61
G2/M - mid/late	Nuclear LIM interactor-interacting factor 1	GL50803_4063	1.52
G2/M - mid/late	Nucleoside diphosphate kinase	GL50803_14135	1.86
G2/M - mid/late	Phosphatidylinositol transfer protein alpha isoform	GL50803_4197	1.45
G2/M - mid/late	Protein 21.1	GL50803_10911	2.19
G2/M - mid/late	Protein 21.1	GL50803_14158	1.80
G2/M - mid/late	Protein 21.1	GL50803_6007	1.51
G2/M - mid/late	Protein 21.1	GL50803_8850	1.51
G2/M - mid/late	Protein 21.1	GL50803_7679	1.46
G2/M - mid/late	Ser/Thr protein phosphatase PP1-alpha 2 catalytic subunit	GL50803_14568	2.27
G2/M - mid/late	Serine-pyruvate aminotransferase	GL50803_3313	1.59
G2/M - mid/late	Tubulin tyrosine ligase	GL50803_14498	1.45
G2/M - mid/late	Unspecified product	GL50803_9637	1.83
G2/M - mid/late	Unspecified product	GL50803_23497	1.68
G2/M - mid/late	Unspecified product	GL50803_37431	1.45
G2/M - mid/late	Unspecified product	GL50803_8769	1.37
G2/M - mid/late	WD-40 repeat protein	GL50803_15218	1.77
G2/M - mid/late	WD-40 repeat protein	GL50803_15956	1.54
G2/M - mid/late	Zinc transporter domain protein	GL50803_13204	1.51

Two Cyclin-dependent kinase (CDK) genes (GL50803_16802, GL50803_8037) were identified in both the microarray and the RNA-seq experiments (Table 8). A third CDK (GL50803_15397) was found only in the RNA seq data. The two CDK genes from both the RNA-seq and microarray data (GL50803_16802, GL50803_8037) were upregulated by 2-fold, which is among the highest changes observed for genes in Fraction 5. This is unexpected as the mRNA and protein levels of CDKs are constant during the cell cycle in model eukaryotic organisms where the activities of the CDKs are regulated by their interaction with their cognate cyclin partner (Sorrell et al., 2001). However, in

plants the transcripts corresponding to a specific CDK type (type b) increases during G1, S and G2/M stages of the cell cycles (Sorrell et al., 2001). The RNA-seq and microarray results suggest that the Giardia CDKs, similar to their orthologs in plants, are regulated at their transcript levels during the cell cycle.

I also used DAVID on the G2/M enriched Fraction 5 from the RNA-seq data to identify 8 clusters of genes encoding proteins of related functions/features (Table 9, Tables A18-25 in Appendix X). However, several genes belong to two or more clusters and some of the clusters (i.e. ATP-binding proteins) are not informative about the specific roles of the proteins in the cell cycle. Therefore, I will focus my discussion on the genes identified in the DAVID analysis that are also known to be involved in the cell cycle in other eukaryotes. Several mitotic kinase genes were found to be upregulated in G2/M (Fraction 5) of the RNA-seq data (Appendix X, Tables A18 and A19): polo like kinase (PLK, GL50803_104150), MAPK (GL50803_22850), STE20 (GL50803_14436), NEK and SRPK kinase (GL50803_17335) genes. PLK is involved with the dephosphorylation of Cdk1/Cyclin-B to promote entry into mitosis (Glover et al., 1998). Previous RT-qPCR results in our laboratory also showed that the Giardia PLK gene is upregulated in G2/M enriched elutriation fractions.

Table 9: Gene clusters identified by DAVID functional annotation tool for G2/M genes. Clusters identified had an enrichment score above 1.3 and the fold change range is given.

Cluster identified by DAVID	**Number of genes identified**	**Fold change range (max – min)**
Serine/threonine kinases	26	3.64 – 1.25
Protein phosphorylation	52	3.64 – 1.25
Ankyrin domain	67	2.93 – 1.25
Glucose catabolic process	9	3.64 – 1.48
ATP binding	70	3.64 – 1.25
Microtubule cytoskeleton	11	3.09 – 1.31
Calcium/EF hand	6	2.47 – 1.34
Metal ion binding	35	2.47 – 1.32

Mitogen activated protein kinases (MAPK) are involved in differentiation in the parasite Leishmania (Morales et al., 2010), and are needed for mitosis progression in *Xenopus* egg extracts (Liu et al., 2004). STE20 kinases are known to phosphorylate and activate the MAPK family of kinases, in particular MAPKKK (Dan et al., 2001). Thus, the STE20 kinase might be involved in regulating the activation of the MAPK.

The NEK kinases that contain a Never in Mitosis A (NIMA) domain are involved in cell cycle regulation in mitosis, as well as in cell proliferation and signaling (Fry et al., 2012). Thus in Giardia, the 23 NEK kinase genes identified are likely to be involved in mitosis. The SRPK is a serine-arginine kinase that phosphorylates serine residues in serine-arginine motifs and is suggested to be involved in mitosis (Giannakouros et al., 2011). In particular, it is hypothesized that SRPK proteins might be involved in chromosome condensation, and the regulation of Cyclin A1 transcription (Giannakouros et al., 2011).

Other proteins with known roles in mitosis identified in the DAVID clusters are kinesin and dynein (Appendix X, Table A23), which are components of cytoskeletal motors and are involved in the assembly of microtubules (Vicente and Wordeman, 2015). The kinesins have roles in all stages of mitosis, from prophase to cytokinesis, with different functions at each stage (Vicente and Wordeman, 2015). Briefly, kinesins interact with the microtubules and other structures to assist with their movement within the cell, such as with the condensation and movement of chromosomes (Vicente and Wordeman, 2015). In particular, Giardia kinesin-5 (GL50803_16425) is up-regulated in G2/M from my RNA-seq data. Kinesin-5 is involved in the formation of bipolar spindles which form during centrosome separation during prophase in mammalian cells (Vicente and Wordeman, 2015). Kinesin-5 proteins are also involved in spindle elongation during anaphase in yeast (Vicente and Wordeman, 2015).

The Giardia kinesin-13 (GL50803_16945) is the most up-regulated (3-fold) among the motor proteins in G2/M in my RNA-seq data (Appendix X, Table A23). Kinesin-13 is used to align chromosomes to the metaphase plate and modulate the length of the microtubules (Vicente and Wordeman, 2015). In Drosophila, kinesin-13 proteins interact to assist with chromosome segregation (Vicente and Wordeman, 2015). In Giardia the kinesin-13 protein is localized to the median body and flagella, and is involved in regulating the mitotic microtubule dynamics (Dawson et al., 2007).

Dynein is a microtubule motor complex protein involved in moving the chromosomes and organizing the spindle location (Raaijmakers et al., 2013). As well, dynein proteins localize to the nuclear envelope, centrosomes and the spindle microtubules during the G2/M phase of mammalian cells (Raaijmakers et al., 2013). This

family of proteins is also involved in flagella movement and with cellular division (Raaijmakers et al., 2013). The up-regulation of dyneins and kinesins in G2/M in my RNA-seq data is consistent with the roles of these proteins in mitotic division.

Lastly, it was interesting that one of the DAVID clusters represents proteins involved in glycolysis (Table A21 in Appendix X). Energy regulation is linked to cell cycle as the metabolic needs during replication are increased (Kaplon et al., 2015). Yeast cells also show an increase in glycolysis-related genes during its cell cycle (Kaplon et al., 2015). In addition, the expression for glycolysis genes also increases during Giardia encystation (Einarsson et al., 2016). Thus it is possible that these genes, involved in the glycolysis pathway are regulated in the Giardia trophozoite cell cycle in order to provide the metabolic demands during cell proliferation.

The overall fold changes for genes in our RNA-seq analysis were relatively low, with the highest fold change at 3.67 (Table A13 in Appendix VIII). These are relatively small changes compared to those of cell cycle regulated genes in mammalian cells (upwards of 35 fold) (Cho et al., 1998; Harris et al., 1991; Penelova et al., 2005; Whitfield et al., 2002). However, *Trypanosoma brucei*, another protozoan parasite, also showed a <4 fold difference in gene expression during its cell cycle (Archer et al., 2011). Other eukaryotes such as *Candida albicans* and *S. pombe* (Cote et al., 2009; Rustici et al., 2004) also have small changes in gene expression associated with the cell cycle. This suggests that a large change in an organism's gene expression is not always required for cell cycle progression. Another possible explanation for the modest change in gene expression during the Giardia cell cycle is that it is not necessary for this parasite to

highly regulate this process as its proliferative stage (trophozoites) occurs inside the host where there is a constant nutrient-rich environment.

3.3.5: Genes up-regulated in the latter fractions (Fraction 7, 9 and 11):

Lastly we also analyzed the RNA-seq results from the latter CCE fractions (F7, 9 and 11) to determine if there was an enrichment in genes differentially expressed (DE) in any specific stage of the cell cycle that were identified in the microarray data. Fraction 7 contained only 3 DE genes and none of these were identified in the microarray data. There are 140 DE genes in Fraction 9, but only 24 of these genes are also found in the microarray. Furthermore, similar numbers of these DE genes are assigned to either G1/S or G2/M stages. Fraction 11 contained 66 DE genes but only 6 were also identified in the microarray. Since Fractions 7, 9 and 11 did not contain an enrichment of DE genes associated with a specific stage of the cell cycle based on the microarray data, these elutriation fractions likely contain increasing aggregations of cells from all stages of the cell cycle. Therefore, the RNA-seq data from these fractions were not further analyzed.

CONCLUSIONS AND FUTURE WORK

For my first objective I characterized the third peak (Peak iii) observed in my flow cytometry histograms. This third peak represents a small percentage of the total cells in unsorted asynchronous Giardia trophozoite cultures, but it gradually increases in latter fractions collected from the application of counterflow elutriation to these cultures. I hypothesized that this peak represented Giardia cysts but RT-qPCR analysis showed no increase in the mRNA corresponding to a cyst wall protein (CWP1) in the Peak iii enriched elutriation fractions. Immunofluorescence analysis showed a small percentage of cysts forming spontaneously in my Giardia trophozoite cultures, but cysts were not enriched in elutriation fractions containing high percentages of Peak iii cells. Furthermore, DNA quantification of the nuclei in the cells within these elutriation fractions showed no evidence that the cells that have undergone endoreplication. These results led me to conclude that the cells in Peak iii are doublet G2 cells that were not removed during the gating steps of the flow cytometry analysis. Potential modifications in order to reduce the amount of cell aggregates include increasing the vortexing time prior to sample injection and the inclusion of 1 % bovine serum albumin (BSA) in the elutriation medium. The addition of BSA helps prevent cells from aggregating together or with cellular debris, as well as from adhering to the walls of the elutriation chamber (Banfalvi, 2011).

For my second objective I compared the use of an external and internal normalizer in RT-qPCR experiments. I determined that the external normalizer showed similar results to internal normalizer for the analysis of elutriation fractions and samples from an encysting Giardia culture. These results showed that the actin gene is a suitable internal

normalizer for gene expression studies in the cell cycle, and the gene encoding ribosomal protein L2 is a suitable internal normalizer for gene expression studies during encystation. Furthermore, this study demonstrated the utility of spiking WB RNA with GS RNA as an external normalizer for future gene expression studies in Giardia − especially in biological conditions when an appropriate internal normalizer gene is unknown or could not be identified.

For my last objective I identified 1024 genes differentially expressed between G1/S (elutriation Fraction 3) and G2/M (elutriation Fraction 5). Several genes of interest including Cyclins, CDKs, thymidine kinase, and a polo-like kinase were found to be up regulated in specific stages of the trophozoite cell cycle. As well, 160 genes were identified in both the RNA-seq fractions and the microarray experiment from our collaborators. However, the most numerous genes identified in both the G1/S enriched Fraction 3 and the G2/M enriched Fraction 5 are those encoding hypothetical proteins that have not been functionally characterized. Future work would be needed to determine how these hypothetical proteins are involved in the cell cycle. Furthermore, Western blot analysis could be used to determine if the differential expression of genes identified in our RNA-seq data also have altered protein levels during the cell cycle.

REFERENCES

Adam, R.D. (2001). Biology of Giardia lamblia. Clinical microbiology reviews *14*, 447-475.

Ankarklev, J., Jerlstrom-Hultqvist, J., Ringqvist, E., Troell, K., and Svard, S.G. (2010). Behind the smile: cell biology and disease mechanisms of Giardia species. Nature reviews Microbiology *8*, 413-422.

Archer, S.K., Inchaustegui, D., Queiroz, R., and Clayton, C. (2011). The cell cycle regulated transcriptome of Trypanosoma brucei. PloS one *6*, e18425.

Banfalvi, G. (2008). Cell cycle synchronization of animal cells and nuclei by centrifugal elutriation. Nature protocols *3*, 663-673.

Banfalvi, G. (2011). Synchronization of mammalian cells and nuclei by centrifugal elutriation. Methods in molecular biology *761*, 25-45.

Bernander, R., Palm, J.E., and Svard, S.G. (2001). Genome ploidy in different stages of the Giardia lamblia life cycle. Cellular microbiology *3*, 55-62.

Boehm, M., and Bonifacino, J.S. (2001). Adaptins: the final recount. Molecular biology of the cell *12*, 2907-2920.

Bolger, A.M., Lohse, M., and Usadel, B. (2014). Trimmomatic: a flexible trimmer for Illumina sequence data. Bioinformatics *30*, 2114-2120.

Brown, M., and Wittwer, C. (2000). Flow cytometry: principles and clinical applications in hematology. Clinical chemistry *46*, 1221-1229.

Bucerius, F., Kador, M., Boshart, M., and Janzen, C.J. (2011). Reliable quantification of cell cycle-dependent mRNA abundance using fluorescence-activated cell sorting in Trypanosoma brucei. Molecular and biochemical parasitology *175*, 205-208.

Bustin, S.A., Benes, V., Nolan, T., and Pfaffl, M.W. (2005). Quantitative real-time RT-PCR--a perspective. Journal of molecular endocrinology *34*, 597-601.

Castillo-Romero, A., Leon-Avila, G., Wang, C.C., Perez Rangel, A., Camacho Nuez, M., Garcia Tovar, C., Ayala-Sumuano, J.T., Luna-Arias, J.P., and Hernandez, J.M. (2010). Rab11 and actin cytoskeleton participate in Giardia lamblia encystation, guiding the specific vesicles to the cyst wall. PLoS neglected tropical diseases *4*, e697.

Cho, R.J., Campbell, M.J., Winzeler, E.A., Steinmetz, L., Conway, A., Wodicka, L., Wolfsberg, T.G., Gabrielian, A.E., Landsman, D., Lockhart, D.J., *et al.* (1998). A genome-wide transcriptional analysis of the mitotic cell cycle. Molecular cell *2*, 65-73.

Cote, P., Hogues, H., and Whiteway, M. (2009). Transcriptional analysis of the Candida albicans cell cycle. Molecular biology of the cell *20*, 3363-3373.

Cullen, P.J., Cozier, G.E., Banting, G., and Mellor, H. (2001). Modular phosphoinositide-binding domains--their role in signalling and membrane trafficking. Current biology : CB *11*, R882-893.

Dan, I., Watanabe, N.M., and Kusumi, A. (2001). The Ste20 group kinases as regulators of MAP kinase cascades. Trends in cell biology *11*, 220-230.

Davis, P.K., Ho, A., and Dowdy, S.F. (2001). Biological methods for cell-cycle synchronization of mammalian cells. BioTechniques *30*, 1322-1326, 1328, 1330-1321.

Dawson, S.C., Sagolla, M.S., Mancuso, J.J., Woessner, D.J., House, S.A., Fritz-Laylin, L., and Cande, W.Z. (2007). Kinesin-13 regulates flagellar, interphase, and mitotic microtubule dynamics in Giardia intestinalis. Eukaryotic cell *6*, 2354-2364.

deRegnier, D.P., Cole, L., Schupp, D.G., and Erlandsen, S.L. (1989). Viability of Giardia cysts suspended in lake, river, and tap water. Applied and environmental microbiology *55*, 1223-1229.

Donjerkovic, D., and Scott, D.W. (2000). Regulation of the G1 phase of the mammalian cell cycle. Cell research *10*, 1-16.

Einarsson, E., and Svard, S.G. (2015). Encystation of Giardia intestinalis—a Journey from the Duodenum to the Colon. Current Tropical Medicine Reports *2*, 101-109.

Einarsson, E., Svard, S.G., and Troell, K. (2015). UV irradiation responses in Giardia intestinalis. Experimental parasitology *154*, 25-32.

Einarsson, E., Troell, K., Hoeppner, M.P., Grabherr, M., Ribacke, U., and Svard, S.G. (2016). Coordinated Changes in Gene Expression Throughout Encystation of Giardia intestinalis. PLoS neglected tropical diseases *10*, e0004571.

Franzen, O., Jerlstrom-Hultqvist, J., Castro, E., Sherwood, E., Ankarklev, J., Reiner, D.S., Palm, D., Andersson, J.O., Andersson, B., and Svard, S.G. (2009). Draft genome sequencing of giardia intestinalis assemblage B isolate GS: is human giardiasis caused by two different species? PLoS pathogens *5*, e1000560.

Fry, A.M., O'Regan, L., Sabir, S.R., and Bayliss, R. (2012). Cell cycle regulation by the NEK family of protein kinases. Journal of cell science *125*, 4423-4433.

Fyrberg, A., Mirzaee, S., and Lotfi, K. (2006). Cell cycle dependent regulation of deoxycytidine kinase, deoxyguanosine kinase, and cytosolic 5'-nucleotidase I activity in MOLT-4 cells. Nucleosides, nucleotides & nucleic acids *25*, 1201-1204.

Giannakouros, T., Nikolakaki, E., Mylonis, I., and Georgatsou, E. (2011). Serine-arginine protein kinases: a small protein kinase family with a large cellular presence. The FEBS journal *278*, 570-586.

Gillin, F.D., Reiner, D.S., and Boucher, S.E. (1988). Small-intestinal factors promote encystation of Giardia lamblia in vitro. Infection and immunity *56*, 705-707.

Glover, D.M., Hagan, I.M., and Tavares, A.A. (1998). Polo-like kinases: a team that plays throughout mitosis. Genes & development *12*, 3777-3787.

Halliez, M.C., and Buret, A.G. (2013). Extra-intestinal and long term consequences of Giardia duodenalis infections. World journal of gastroenterology *19*, 8974-8985.

Harper, J.W., and Adams, P.D. (2001). Cyclin-dependent kinases. Chemical reviews *101*, 2511-2526.

Harris, M.E., Bohni, R., Schneiderman, M.H., Ramamurthy, L., Schumperli, D., and Marzluff, W.F. (1991). Regulation of histone mRNA in the unperturbed cell cycle: evidence suggesting control at two posttranscriptional steps. Molecular and cellular biology *11*, 2416-2424.

Hehl, A.B., Marti, M., and Kohler, P. (2000). Stage-specific expression and targeting of cyst wall protein-green fluorescent protein chimeras in Giardia. Molecular biology of the cell *11*, 1789-1800.

Hoekstra, J. (2016). The Study of Protein Expression During Encystation of Giardia intestinalis. In Biology (Peterborough ON: Trent University).

Hryniewicz-Jankowska, A., Czogalla, A., Bok, E., and Sikorsk, A.F. (2002). Ankyrins, multifunctional proteins involved in many cellular pathways. Folia histochemica et cytobiologica *40*, 239-249.

Huggett, J., Dheda, K., Bustin, S., and Zumla, A. (2005). Real-time RT-PCR normalisation; strategies and considerations. Genes and immunity *6*, 279-284.

Jerlstrom-Hultqvist, J., Ankarklev, J., and Svard, S.G. (2010). Is human giardiasis caused by two different Giardia species? Gut microbes *1*, 379-382.

Johnston, S., Gallaher, Z., and Czaja, K. (2012). Exogenous reference gene normalization for real-time reverse transcription-polymerase chain reaction analysis under dynamic endogenous transcription. Neural regeneration research *7*, 1064-1072.

Kane, A.V., Ward, H.D., Keusch, G.T., and Pereira, M.E. (1991). In vitro encystation of Giardia lamblia: large-scale production of in vitro cysts and strain and clone differences in encystation efficiency. The Journal of parasitology *77*, 974-981.

Kang, K., Lee, S.B., Yoo, J.H., and Nho, C.W. (2010). Flow cytometric fluorescence pulse width analysis of etoposide-induced nuclear enlargement in HCT116 cells. Biotechnology letters *32*, 1045-1052.

Kaplon, J., van Dam, L., and Peeper, D. (2015). Two-way communication between the metabolic and cell cycle machineries: the molecular basis. Cell cycle *14*, 2022-2032.

Kauffman, M.G., and Kelly, T.J. (1991). Cell cycle regulation of thymidine kinase: residues near the carboxyl terminus are essential for the specific degradation of the enzyme at mitosis. Molecular and cellular biology *11*, 2538-2546.

Keister, D.B. (1983). Axenic culture of Giardia lamblia in TYI-S-33 medium supplemented with bile. Transactions of the Royal Society of Tropical Medicine and Hygiene *77*, 487-488.

Kim, D., Pertea, G., Trapnell, C., Pimentel, H., Kelley, R., and Salzberg, S.L. (2013). TopHat2: accurate alignment of transcriptomes in the presence of insertions, deletions and gene fusions. Genome biology *14*, R36.

Kozera, B., and Rapacz, M. (2013). Reference genes in real-time PCR. Journal of applied genetics *54*, 391-406.

Lane, S., and Lloyd, D. (2002). Current trends in research into the waterborne parasite Giardia. Critical reviews in microbiology *28*, 123-147.

Lasek-Nesselquist, E., Welch, D.M., and Sogin, M.L. (2010). The identification of a new Giardia duodenalis assemblage in marine vertebrates and a preliminary analysis of G. duodenalis population biology in marine systems. International journal for parasitology *40*, 1063-1074.

Lee, H.O., Davidson, J.M., and Duronio, R.J. (2009). Endoreplication: polyploidy with purpose. Genes & development *23*, 2461-2477.

Liao, Y., Smyth, G.K., and Shi, W. (2014). featureCounts: an efficient general purpose program for assigning sequence reads to genomic features. Bioinformatics *30*, 923-930.

Ling, D., and Salvaterra, P.M. (2011). Robust RT-qPCR data normalization: validation and selection of internal reference genes during post-experimental data analysis. PloS one *6*, e17762.

Liu, X., Yan, S., Zhou, T., Terada, Y., and Erikson, R.L. (2004). The MAP kinase pathway is required for entry into mitosis and cell survival. Oncogene *23*, 763-776.

Lujan, H.D., Mowatt, M.R., Byrd, L.G., and Nash, T.E. (1996). Cholesterol starvation induces differentiation of the intestinal parasite Giardia lamblia. Proceedings of the National Academy of Sciences of the United States of America *93*, 7628-7633.

Ma'ayeh, S.Y., Knorr, L., and Svard, S.G. (2015). Transcriptional profiling of Giardia intestinalis in response to oxidative stress. International journal for parasitology *45*, 925-938.

Morales, M.A., Pescher, P., and Spath, G.F. (2010). Leishmania major MPK7 protein kinase activity inhibits intracellular growth of the pathogenic amastigote stage. Eukaryotic cell *9*, 22-30.

Morf, L., Spycher, C., Rehrauer, H., Fournier, C.A., Morrison, H.G., and Hehl, A.B. (2010). The transcriptional response to encystation stimuli in Giardia lamblia is restricted to a small set of genes. Eukaryotic cell *9*, 1566-1576.

Navarro, E., Serrano-Heras, G., Castano, M.J., and Solera, J. (2015). Real-time PCR detection chemistry. Clinica chimica acta; international journal of clinical chemistry *439*, 231-250.

Penelova, A., Richman, L., Neupert, B., Simanis, V., and Kuhn, L.C. (2005). Analysis of the contribution of changes in mRNA stability to the changes in steady-state levels of cyclin mRNA in the mammalian cell cycle. The FEBS journal *272*, 5217-5229.

Poxleitner, M.K., Dawson, S.C., and Cande, W.Z. (2008). Cell cycle synchrony in Giardia intestinalis cultures achieved by using nocodazole and aphidicolin. Eukaryotic cell *7*, 569-574.

Raaijmakers, J.A., Tanenbaum, M.E., and Medema, R.H. (2013). Systematic dissection of dynein regulators in mitosis. The Journal of cell biology *201*, 201-215.

Reaume, C. (2013). The application of counterflow centrifugal elutriation and RT-qPCR in the analysis of the Giardia lamblia cell cycle. In ENLS (Peterborough, Ontario: Trent University).

Reaume, C., Horlock-Roberts, K., Ouellette, C., Cook, N., and Yee, J. (2017). Study of the Giardia intestinalis cell cycle by the application of counterflow centrifugal elutriation (Peterborough, Ontario, Canada: Trent University).

Reaume, C., Moore, B., Hernandez, P., Ruzzini, A., Chlebus, M., Wasserman, M., and Yee, J. (2013). Evaluation of drugs and stationary growth on the cell cycle of Giardia intestinalis. Molecular and biochemical parasitology *187*, 72-76.

Reiner, A., Yekutieli, D., and Benjamini, Y. (2003). Identifying differentially expressed genes using false discovery rate controlling procedures. Bioinformatics *19*, 368-375.

Reiner, D.S., Ankarklev, J., Troell, K., Palm, D., Bernander, R., Gillin, F.D., Andersson, J.O., and Svard, S.G. (2008). Synchronisation of Giardia lamblia: identification of cell cycle stage-specific genes and a differentiation restriction point. International journal for parasitology *38*, 935-944.

Rieseberg, M., Kasper, C., Reardon, K.F., and Scheper, T. (2001). Flow cytometry in biotechnology. Applied microbiology and biotechnology *56*, 350-360.

Rustici, G., Mata, J., Kivinen, K., Lio, P., Penkett, C.J., Burns, G., Hayles, J., Brazma, A., Nurse, P., and Bahler, J. (2004). Periodic gene expression program of the fission yeast cell cycle. Nature genetics *36*, 809-817.

Sengupta, S., Bolin, J.M., Ruotti, V., Nguyen, B.K., Thomson, J.A., Elwell, A.L., and Stewart, R. (2011). Single read and paired end mRNA-Seq Illumina libraries from 10 nanograms total RNA. Journal of visualized experiments : JoVE, e3340.

Sorrell, D.A., Menges, M., Healy, J.M., Deveaux, Y., Amano, C., Su, Y., Nakagami, H., Shinmyo, A., Doonan, J.H., Sekine, M., *et al.* (2001). Cell cycle regulation of cyclin-dependent kinases in tobacco cultivar Bright Yellow-2 cells. Plant physiology *126*, 1214-1223.

Su, L.H., Pan, Y.J., Huang, Y.C., Cho, C.C., Chen, C.W., Huang, S.W., Chuang, S.F., and Sun, C.H. (2011). A novel E2F-like protein involved in transcriptional activation of cyst wall protein genes in Giardia lamblia. The Journal of biological chemistry *286*, 34101-34120.

Sun, C.H., Palm, D., McArthur, A.G., Svard, S.G., and Gillin, F.D. (2002). A novel Myb-related protein involved in transcriptional activation of encystation genes in Giardia lamblia. Molecular microbiology *46*, 971-984.

Suzuki, T., Higgins, P.J., and Crawford, D.R. (2000). Control selection for RNA quantitation. BioTechniques *29*, 332-337.

Thakur, S., Cattoni, D.I., and Nollmann, M. (2015). The fluorescence properties and binding mechanism of SYTOX green, a bright, low photo-damage DNA intercalating agent. European biophysics journal : EBJ *44*, 337-348.

Touz, M.C., Rivero, M.R., Miras, S.L., and Bonifacino, J.S. (2012). Lysosomal protein trafficking in Giardia lamblia: common and distinct features. Frontiers in bioscience *4*, 1898-1909.

Troell, K., and Svard, S. (2011). Giardia A Model Organism (Austria: SpringerWienNewYork).

Vandesompele, J., De Preter, K., Pattyn, F., Poppe, B., Van Roy, N., De Paepe, A., and Speleman, F. (2002). Accurate normalization of real-time quantitative RT-PCR data by geometric averaging of multiple internal control genes. Genome biology *3*, RESEARCH0034.

Varet, H., Brillet-Gueguen, L., Coppee, J.Y., and Dillies, M.A. (2016). SARTools: A DESeq2- and EdgeR-Based R Pipeline for Comprehensive Differential Analysis of RNA-Seq Data. PloS one *11*, e0157022.

Vicente, J.J., and Wordeman, L. (2015). Mitosis, microtubule dynamics and the evolution of kinesins. Experimental cell research *334*, 61-69.

Walden, E. (2014). Counterflow centrifugal elutriation as a technique for separating stages of the encystation of Giardia lamblia. In Biochemistry (Peterborough, Ontario: Trent University).

Wang, Z., Gerstein, M., and Snyder, M. (2009). RNA-Seq: a revolutionary tool for transcriptomics. Nature reviews Genetics *10*, 57-63.

Whitfield, M.L., Sherlock, G., Saldanha, A.J., Murray, J.I., Ball, C.A., Alexander, K.E., Matese, J.C., Perou, C.M., Hurt, M.M., Brown, P.O., *et al.* (2002). Identification of genes periodically expressed in the human cell cycle and their expression in tumors. Molecular biology of the cell *13*, 1977-2000.

Wolf, J.B. (2013). Principles of transcriptome analysis and gene expression quantification: an RNA-seq tutorial. Molecular ecology resources *13*, 559-572.

Wong, M.L., and Medrano, J.F. (2005). Real-time PCR for mRNA quantitation. BioTechniques *39*, 75-85.

Xu, Y., Seet, L.F., Hanson, B., and Hong, W. (2001). The Phox homology (PX) domain, a new player in phosphoinositide signalling. The Biochemical journal *360*, 513-530.

Zhang, Y. (2008). I-TASSER server for protein 3D structure prediction. BMC bioinformatics *9*, 40.

Zhao, S., Zhang, Y., Gordon, W., Quan, J., Xi, H., Du, S., von Schack, D., and Zhang, B. (2015). Comparison of stranded and non-stranded RNA-seq transcriptome profiling and investigation of gene overlap. BMC genomics *16*, 675.

APPENDIX

Appendix I: Modified TYI-S-33 Media for *Giardia intestinalis* Cultures

Table A1: Basic Media recipe. Components used to make basic media, a component of modified TYI-S-33 media. Solution was sterilized by vacuum filtration through a Thermo Scientific Nalgene rapid-flow bottle top filter; 50 mL aliquots were stored at -20^{o}C.

Component	**500 ml**	**1000 ml**
Casein Peptone Digest (N-Z Case Plus)	50 g	100 g
Glucose	25 g	50 g
Yeast Extract (DIFCO)	25 g	50 g
NaCl	5 g	10 g
0.5 M Phosphate Buffer Solution pH 7.2	50 ml	100 ml
Millipore H_2O	350 ml	700 ml

Table A2: Components of Giardia complete media. The pH was adjusted to 7.2 and the media was filtered with a through a Thermo Scientific Nalgene rapid-flow bottle top filter. The bottle of sterilized media was kept at 4^{o}C for up to 4 weeks.

Component	**500 ml**	**1000 ml**
Giardia Basic Media	100 ml	200 ml
Bovine Serum	50 ml	100 ml
2.28 mg/mL $FeNH_4$ Citrate	5 ml	10 ml
6.5% Bovine Bile	4 ml	8 ml
Millipore H_2O	350 ml	700 ml

Supplemental components added to complete media. **320 µL of 50X cysteine ascorbic acid and 80µL of 100X antibiotic/antimycotic were added to each 16 mL culture tube.**

Table A3: Components of 50X Cysteine and Ascorbic Acid (pH 7.2). 320 µL of filter sterilized cysteine ascorbic acid was added per 16 mL of Giardia media per tube.

Component	**Mass/volume used in 20 mL**
L-cysteine	2 g
Ascorbic acid	0.1 g
Millipore H_2O	18 mL

Table A4: Components of 100X antibiotic/antimycotic. (ABAM) in 0.85% saline. 80 µL is added per 16 mL of Giardia media per tube.

Component	**Concentration**	**Units per 16 mL Culture Tube**
Penicillin	10,000 units/mL	160,000 units
Streptomycin	10,000 µg/mL	160,000 µg
Amphotericin B	25 g/mL	400 g

Appendix II: Counterflow Centrifugal Elutriation Experimental Parameters

Table A5: Centrifuge conditions for counterflow centrifugal elutriation.

Parameter	Setting
Total # culture tubes of Giardia	**40 (x 16 ml/tube = 640 mL media)**
Rotor:	**Beckman Coulter JE 5.0 series**
Rotor Speed:	**2,400 RPM (constant)**
Temperature:	**21°C**
Acceleration/Deceleration	**Maximum**
Injection Flow Rate:	**1 mL/min**
Flow Rate Increments:	**3-5 mL/min**
Flow Rate Range:	**1 mL/min to 50 mL/min**
Fraction Volume:	**50 mL**
Total # Fractions	**14**

Table A6: Flow rates of the fractions collected from the counterflow centrifugal elutriation

Fraction	**Flow Rate (mL/minute)**
Flow Through	1
F1	5
F2	8
F3	11
F4	14
F5	17
F6	20
F7	25
F8	30
F9	35
F10	40
F11	45
F12	50
Blow Out	50 & stop centrifuge

Appendix III: RNA Extraction Protocol

1. Add 200 – 500 µL of Trizol reagent to cell suspension and pipette mixture to homogenize
2. Incubate at room temperature for 5 minutes
3. Add 40 – 100 µL of chloroform and shake vigorously by hand for 15 seconds followed by incubation at room temperature for 3 minutes
4. Centrifuge at 12,000 x g for 15 minutes at 4 ^{o}C
5. Transfer the top (clear) RNA layer to a new tube
    a. Add 0.8 mL per 1 mL of supernatant of isopropyl alcohol and invert to precipitate out RNA
6. Incubate samples at room temp for 10 minutes
7. Centrifuge at 12,000 x g for 10-20 minutes
8. Remove the supernatant
9. Wash the RNA pellet with 200 - 500 µL of 75% ethanol
    a. Mix by vortexing and centrifuge at 7,500 x g for 5 minutes
10. Remove the ethanol layer and dry pellet for 5 minutes (don't dry out the pellet)
11. Dissolve RNA in 20 µL RNase free water and incubate for 10 minutes at 55-60^{o}C
12. Take 1µL and do a NanoDrop measurement
    a. Want A260/280 to be 2, and the A260/230 to be over 2 and take concentration
13. Store RNA at -80^{o}C

Appendix IV: cDNA synthesis protocol

Developed and used in Dr. Yee's Laboratory, Trent University.

The following is the protocol used to construct complimentary DNA from extract RNA for each cell fraction collected using counterflow centrifugal elutriation.

Reverse transcription of RNA — cDNA synthesis (with SuperScript III RT)

1. Assemble the components of Annealing Reaction in the following order in a thin-wall 0.5 mL PCR microfuge tube:

   x µL RNase-free H_2O (Add up to a total volume of 10 µL)
   2 µL 5x First-strand buffer (Invitrogen)
   1 µL Poly$(dT)_{21}$ primer (100 ng/mL)
   x µL (equivalent to adding *0.5 or 1 µg total RNA)
   10 µl total volume

Use Program 24 on Techne thermocycler for automated temperature incubation steps below:

2. Incubate sample at 65ºC for 5 min to disrupt any secondary structures in the RNA.

3. Incubate at 40ºC for 15 min to allow Poly$(dT)_{21}$ to anneal to RNA (Primer T_m = 41ºC).

During the annealing step, assemble the components of the Extension Mix in the following order in a microfuge tube:

   1 µL RNase-free H_2O
   1 µL 5x First-strand buffer (Invitrogen)
   2 µL dNTP mix (5 mM each)
   0.75 µL 0.1 M DTT
   0.25 µL of SuperScript III RT enzyme (200 U/mL)
   5 µl total volume

4. At the end of the annealing step, add 5 ml of Extension Mix (pre-warm at 50°C for 5 min) to each Annealing Reaction.

5. Incubate at 50°C for 40 min and then at 55°C for 20 min to allow cDNA synthesis to extend from the annealed Poly$(dT)_{21}$ primer.

6. Incubate at 70°C for 15 min to inactivate the SuperScript III RT.

7. When the cDNA reaction is completed in the thermocycler, remove the tube and give it a quick spin on the microcentrifuge (USE ADAPTERS) to collect all liquid to bottom of tube.

8. The final cDNA sample should be 15 mL containing a total of 1000 ng of RNA. Therefore, its [RNA] = 67 ng/mL. If used 0.5 μg RNA (if using elutriation samples), then [RNA] = 33 ng/μL

9. Prep a diluted 0.5 ng/mL cDNA stock as follow: add 1 ml of 67 ng/μL cDNA sample from above (equivalent to 67 ng of original RNA) to a new microfuge tube containing 133 mL of RNase-free H_2O. OR add 1 μL of 33 ng/μL of cDNA + 65 μL of RNase-free H_2O if using elutriation samples.

10. Store the concentrated and diluted cDNA samples at -80°C. Use 5 μL (5 ng cDNA) of the diluted cDNA stock for each qPCR reaction.

Appendix V: Uppsala method for Trophozoite Growth Media and Encystation Media

Table A6: Components of Uppsala method Trophozoite Growth Media (TYDK medium pH 6.8).

Component	**Mass/volume used in 500 mL**
Peptone (BD ref 21186)	15 g
Glucose	5 g
NaCl (Sigma)	1 g
K_2HPO_4 (dibasic)	0.5 g
KH2PO4 (monobasic)	0.3 g
0.1 g/L Bovine bile (Sigma B3883)	5 mL
0.022 g/L Ferric ammonium citrate	5 mL
Cosmic Calf Serum	50 mL
Millipore H_2O	440 mL

Supplemental components added to each 16 mL culture tube

- **320 µL of Cys/AA**
- **80 µL of ABAM**

Table A7: Components of Uppsala Encystation Media (pH 7.8).

Component	**Mass/volume used in 500 mL**
Peptone (BD ref 21186)	15 g
Glucose	5 g
NaCl (Sigma)	1 g
K_2HPO_4 (dibasic)	0.5 g
KH_2PO_4 (monobasic)	0.3 g
0.025 g/mL Bovine bile	25 mL
2.2 mg/mL Ferric ammonium citrate	5 mL
Cosmic Calf Serum	50 mL
Millipore H_2O	420 mL

Supplemental components added to each 16 mL culture tube

- **320 µL of Cys/AA**
- **80 µL of ABAM**

Appendix VI: Primers used in objective 2, GS spiking experiments

Table A8: Primers used for GS spiking experiment of counterflow centrifugation elutriation experiment. The primer names, sequence, length, Tm, %G/C and length of target

Primer Names	**Sequence (5' → 3')**	**length**	**Tm (^{o}C)**	**% G/C**	**bp**
Actin/RT-a	GTCCGTCATACCATCTGTTC	20	60.4	50.0	91
Actin/RT-b	GTTTCCTCCATACCACACG	19	60.2	52.6	
HisH4/RT-a	GTGGAGGTGTGAAGCG	16	59.3	62.5	101
HisH4/RT-b	TGTGTATGTGAGGGAGTCG	19	60.2	52.6	
GS-SPS/RT-a	GTTTGCCCTCCCAGAACTTA	20	60.4	50.0	99
GS-SPS/RT-b	GTCTTTCCAGTGAGCGTGA	19	60.2	52.6	

Table A9: Primers used for GS spiking experiment of the encystation experiment. The primer names, sequence, length, Tm, %G/C and length of target

Primer Names	**Sequence (5' → 3')**	**length**	**Tm (^{o}C)**	**% G/C**	**bp**
RiboL2/RT-a	ACAGACAAGCCCCTTCTCAA	20	60.4	50.0	103
RiboL2/RT-b	GGTCAACAGGGTTCATTGCT	20	60.4	50.0	
Cwp1/RT-1a	CGCTCTCCTTGCTCTTG	17	59.6	58.8	94
Cwp1/RT-1b	TCCGTCAGTGGCATCG	16	59.3	62.5	
Myb1/RT-1a	CGAAGGAGTCTGTAATCCAT	20	58.3	45.0	113
Myb1/RT-1b	GCAGGTGGCGACAAAAAA	18	57.6	50.0	
GS-SPS/RT-a	GTTTGCCCTCCCAGAACTTA	20	60.4	50.0	99
GS-SPS/RT-b	GTCTTTCCAGTGAGCGTGA	19	60.2	52.6	

RT-qPCR master mix and reaction conditions:

Developed and used in Dr. Yee's Laboratory, Trent University.

Table A10: RT-qPCR Master Mix components, concentration and volumes used per reaction

Component	**Concentration**	**Volume for One Sample (µL)**
RNase Free H_2O	-	8.25
PCR Buffer (BioShop)	10 X	2.5
$MgCl_2$ (BioShop)	50 mM	1
dNTP Mix (BioShop)	5 mM each	2
Glycerol	50 %	4
ROX Reference Dye (Stratagene)	2 µM	0.38
SYBR Green + DMSO (Invitrogen)	8.3 X	0.75
Forward Primer (Operon)	25 µM	0.5
Reverse Primer (Operon)	25 µM	0.5
Taq Polymerase (BioShop)	5 U/µL	0.13
Total Volume		**20**

- Rox reference dye diluted from 1mM to 2µM (1 µL into 500 µL of Rox dilution buffer) and this diluted stock stored in the -20°C freezer.

- SYBR green dye was diluted from 10,000x to 8.3x (0.5 µL into 600 µL DMSO) and this stored in the -20°C freezer.

qPCR set-up

Add 20 µL of master mix to each PCR well

Add 5 µL of specific cDNA sample (including NTC and No RT samples) to each tube/well

Add caps to tubes or seal to plate

Table A11: qPCR Reaction Conditions for the stratagene instrument

Temperature (^{o}C)	**Time (minutes)**	**Number of Cycles**
95	10	1
95	0.5	40
55-70	1	
72	0.5	
95	1	1

Appendix VII: Microscope exposure settings

Table A12: Microscope exposure settings for images taken with Leica 6000 DM Epi-fluorescent microscope for DNA quantification

Microscope setting	Measurement
Brightness	100
Gain	10
Intensity	4
Exposure time	500 ms

Appendix VIII: RNA-seq results from CCE experiments

All fractions analyzed (3, 7, 9 and 11) were compared to Fraction 5 as the calibrator fraction. Thus, genes that are downregulated in a given Fraction (3, 7, 9, 11) represent genes that are upregulated in Fraction 5 (the calibrator).

Table A13: Differentially expressed genes in Fraction 3 (G1/S) compared to Fraction 5 (G2/M). A positive fold change indicate an up-regulated gene in Fraction 3 (G1/S) and a negative fold change indicate a down-regulated gene in Fraction 3 compared to Fraction 5. A negative fold change also indicate an up-regulated gene in F5 (G2/M) compared to F3. All genes have a FDR p-value < 0.05. Cell cycle stage enrichment of these fractions is based on flow cytometry analysis. The data in this table is sorted alphabetically by Gene Description to group genes with similar names/functions.

Cell Cycle Stage	Gene Description	Gene ID	Fold Change
G1/S	3-hydroxy-3-methylglutaryl-coenzyme A reductase	GL50803_7573	1.58
G1/S	5' nucleotidase family protein	GL50803_92645	1.48
G1/S	5' nucleotidase family protein	GL50803_3983	1.34
G1/S	5-methylthioadenosine nucleosidase, S-adenosylhomocysteine nucleosidase	GL50803_20195	1.74
G1/S	Adaptin, Alpha	GL50803_17304	1.32
G1/S	Adaptin, Beta	GL50803_21423	1.28
G1/S	Adaptin, Gamma	GL50803_16364	1.30
G1/S	Adaptin, Mu	GL50803_8917	1.49
G1/S	Adaptin, Sigma	GL50803_5328	1.42
G1/S	Amino acid transporter system N2, putative	GL50803_17214	1.42
G1/S	ARF GAP	GL50803_2834	1.28
G1/S	ATP/GTP binding protein, putative	GL50803_10370	1.65
G1/S	ATPase of the PP-loop superfamily implicated in cell cycle control, putative	GL50803_11449	1.42
G1/S	ATPases of the PP-loop superfamily	GL50803_7368	1.70
G1/S	ATP-dependent RNA helicase	GL50803_16042	1.38
G1/S	ATP-dependent RNA helicase	GL50803_13791	1.36
G1/S	ATP-dependent RNA helicase HAS1, putative	GL50803_16887	1.82
G1/S	ATP-dependent RNA helicase-like protein	GL50803_15048	1.71
G1/S	Axoneme-associated protein GASP-180	GL50803_16745	1.60
G1/S	Calcineurin B subunit	GL50803_16829	1.30
G1/S	Calmodulin	GL50803_13652	1.66
G1/S	Carbamate kinase	GL50803_16453	1.39

Cell Cycle Stage	Gene Description	Gene ID	Fold Change
G1/S	CCAAT-box-binding transcription factor	GL50803_101594	1.48
G1/S	CDC19	GL50803_17413	1.34
G1/S	Chaperone protein DnaK HSP70	GL50803_14581	1.43
G1/S	Chromodomain helicase-DNA-binding protein, putative	GL50803_112978	1.61
G1/S	Clathrin heavy chain	GL50803_102108	1.52
G1/S	Coatomer beta' subunit	GL50803_9593	1.32
G1/S	Coiled-coil protein	GL50803_10167	1.66
G1/S	Coiled-coil protein	GL50803_17249	1.49
G1/S	Coiled-coil protein	GL50803_102248	1.30
G1/S	Copper-transporting P-type ATPase	GL50803_39843	1.34
G1/S	Deoxyguanosine kinase/deoxyadenosine kinase subunit, putative	GL50803_4558	2.89
G1/S	Deoxyhypusine synthase, putative	GL50803_15535	1.42
G1/S	Developmentally regulated GTP-binding protein 1	GL50803_5871	1.52
G1/S	DGTP triphosphohydrolase	GL50803_22084	1.47
G1/S	DinF protein	GL50803_16671	1.47
G1/S	DinF protein	GL50803_16841	1.36
G1/S	DinF protein	GL50803_5345	1.27
G1/S	Dipeptidyl-peptidase I precursor	GL50803_14566	1.41
G1/S	Dipeptidyl-peptidase I precursor	GL50803_8741	1.39
G1/S	DNA helicase	GL50803_11384	1.39
G1/S	DNA-dependent ATPase, putative	GL50803_8228	1.30
G1/S	DNA-directed RNA polymerase I 13.1 kDa polypeptide	GL50803_8518	1.51
G1/S	DUB-1	GL50803_5533	1.32
G1/S	ELKS	GL50803_113603	1.70
G1/S	FKBP-type peptidyl-prolyl cis-trans isomerase	GL50803_7246	1.47
G1/S	GA binding protein beta-1 chain	GL50803_6259	1.51
G1/S	Giardin, Alpha-13	GL50803_1076	1.27
G1/S	Giardin, Alpha-17	GL50803_15101	1.47
G1/S	Giardin, Alpha-8	GL50803_11649	1.67
G1/S	Giardin, Beta	GL50803_4812	1.78
G1/S	Giardin, Delta	GL50803_86676	2.03
G1/S	Giardin, Gamma	GL50803_17230	1.87
G1/S	Glucosamine 6-phosphate N-acetyltransferase	GL50803_14651	1.41
G1/S	Glutamate-rich WD-repeat protein	GL50803_14174	1.54
G1/S	Glycine-rich protein	GL50803_13616	1.47

Cell Cycle Stage	Gene Description	Gene ID	Fold Change
G1/S	Guanine phosphoribosyltransferase	GL50803_6436	1.48
G1/S	HAM1 protein	GL50803_7511	1.37
G1/S	Heat shock protein HSP 90-alpha	GL50803_13864	1.30
G1/S	High cysteine membrane protein Group 1	GL50803_103454	1.53
G1/S	Histone acetyltransferase GCN5	GL50803_10666	1.32
G1/S	H-SHIPPO 1	GL50803_103164	1.79
G1/S	H-SHIPPO 1	GL50803_9148	1.48
G1/S	Hydroxymethylglutaryl-CoA synthase	GL50803_13962	1.89
G1/S	Hypothetical protein	GL50803_15445	2.99
G1/S	Hypothetical protein	GL50803_15446	2.66
G1/S	Hypothetical protein	GL50803_12225	2.59
G1/S	Hypothetical protein	GL50803_16581	2.54
G1/S	Hypothetical protein	GL50803_17375	2.43
G1/S	Hypothetical protein	GL50803_19834	2.41
G1/S	Hypothetical protein	GL50803_6185	2.36
G1/S	Hypothetical protein	GL50803_12229	2.36
G1/S	Hypothetical protein	GL50803_16070	2.35
G1/S	Hypothetical protein	GL50803_10524	2.35
G1/S	Hypothetical protein	GL50803_29796	2.31
G1/S	Hypothetical protein	GL50803_11604	2.29
G1/S	Hypothetical protein	GL50803_4852	2.28
G1/S	Hypothetical protein	GL50803_17468	2.24
G1/S	Hypothetical protein	GL50803_10014	2.23
G1/S	Hypothetical protein	GL50803_33721	2.21
G1/S	Hypothetical protein	GL50803_16844	2.19
G1/S	Hypothetical protein	GL50803_15419	2.18
G1/S	Hypothetical protein	GL50803_14401	2.10
G1/S	Hypothetical protein	GL50803_4692	2.06
G1/S	Hypothetical protein	GL50803_28748	2.05
G1/S	Hypothetical protein	GL50803_10808	2.04
G1/S	Hypothetical protein	GL50803_4819	2.03
G1/S	Hypothetical protein	GL50803_23017	2.01
G1/S	Hypothetical protein	GL50803_3582	2.01
G1/S	Hypothetical protein	GL50803_10775	1.98
G1/S	Hypothetical protein	GL50803_7593	1.96
G1/S	Hypothetical protein	GL50803_8250	1.95
G1/S	Hypothetical protein	GL50803_2342	1.94
G1/S	Hypothetical protein	GL50803_12224	1.93
G1/S	Hypothetical protein	GL50803_15605	1.91
G1/S	Hypothetical protein	GL50803_14940	1.89
G1/S	Hypothetical protein	GL50803_21052	1.86
G1/S	Hypothetical protein	GL50803_41212	1.86

Cell Cycle Stage	Gene Description	Gene ID	Fold Change
G1/S	Hypothetical protein	GL50803_88956	1.85
G1/S	Hypothetical protein	GL50803_15499	1.78
G1/S	Hypothetical protein	GL50803_17354	1.77
G1/S	Hypothetical protein	GL50803_15094	1.77
G1/S	Hypothetical protein	GL50803_8322	1.74
G1/S	Hypothetical protein	GL50803_38209	1.73
G1/S	Hypothetical protein	GL50803_6471	1.72
G1/S	Hypothetical protein	GL50803_12218	1.71
G1/S	Hypothetical protein	GL50803_88960	1.70
G1/S	Hypothetical protein	GL50803_4540	1.70
G1/S	Hypothetical protein	GL50803_32265	1.70
G1/S	Hypothetical protein	GL50803_4554	1.67
G1/S	Hypothetical protein	GL50803_16954	1.67
G1/S	Hypothetical protein	GL50803_27235	1.66
G1/S	Hypothetical protein	GL50803_86815	1.66
G1/S	Hypothetical protein	GL50803_8446	1.66
G1/S	Hypothetical protein	GL50803_26749	1.66
G1/S	Hypothetical protein	GL50803_5648	1.66
G1/S	Hypothetical protein	GL50803_14560	1.66
G1/S	Hypothetical protein	GL50803_6558	1.65
G1/S	Hypothetical protein	GL50803_28549	1.65
G1/S	Hypothetical protein	GL50803_16648	1.64
G1/S	Hypothetical protein	GL50803_24126	1.63
G1/S	Hypothetical protein	GL50803_16602	1.62
G1/S	Hypothetical protein	GL50803_12058	1.62
G1/S	Hypothetical protein	GL50803_5615	1.61
G1/S	Hypothetical protein	GL50803_10608	1.61
G1/S	Hypothetical protein	GL50803_112557	1.61
G1/S	Hypothetical protein	GL50803_39713	1.61
G1/S	Hypothetical protein	GL50803_1643	1.60
G1/S	Hypothetical protein	GL50803_2860	1.59
G1/S	Hypothetical protein	GL50803_6751	1.59
G1/S	Hypothetical protein	GL50803_16543	1.59
G1/S	Hypothetical protein	GL50803_96570	1.59
G1/S	Hypothetical protein	GL50803_8625	1.58
G1/S	Hypothetical protein	GL50803_36613	1.58
G1/S	Hypothetical protein	GL50803_3141	1.58
G1/S	Hypothetical protein	GL50803_35157	1.58
G1/S	Hypothetical protein	GL50803_20836	1.57
G1/S	Hypothetical protein	GL50803_17507	1.56
G1/S	Hypothetical protein	GL50803_4239	1.56
G1/S	Hypothetical protein	GL50803_10341	1.56
G1/S	Hypothetical protein	GL50803_15110	1.56

Cell Cycle Stage	Gene Description	Gene ID	Fold Change
G1/S	Hypothetical protein	GL50803_32163	1.56
G1/S	Hypothetical protein	GL50803_15918	1.56
G1/S	Hypothetical protein	GL50803_21754	1.55
G1/S	Hypothetical protein	GL50803_26287	1.55
G1/S	Hypothetical protein	GL50803_6885	1.55
G1/S	Hypothetical protein	GL50803_28348	1.55
G1/S	Hypothetical protein	GL50803_6330	1.55
G1/S	Hypothetical protein	GL50803_38172	1.53
G1/S	Hypothetical protein	GL50803_25855	1.53
G1/S	Hypothetical protein	GL50803_88181	1.53
G1/S	Hypothetical protein	GL50803_16266	1.52
G1/S	Hypothetical protein	GL50803_10221	1.51
G1/S	Hypothetical protein	GL50803_24139	1.51
G1/S	Hypothetical protein	GL50803_114474	1.51
G1/S	Hypothetical protein	GL50803_17492	1.50
G1/S	Hypothetical protein	GL50803_6464	1.50
G1/S	Hypothetical protein	GL50803_15062	1.50
G1/S	Hypothetical protein	GL50803_8880	1.49
G1/S	Hypothetical protein	GL50803_15193	1.49
G1/S	Hypothetical protein	GL50803_9788	1.49
G1/S	Hypothetical protein	GL50803_10946	1.48
G1/S	Hypothetical protein	GL50803_3951	1.48
G1/S	Hypothetical protein	GL50803_16429	1.48
G1/S	Hypothetical protein	GL50803_6026	1.47
G1/S	Hypothetical protein	GL50803_19057	1.47
G1/S	Hypothetical protein	GL50803_101326	1.47
G1/S	Hypothetical protein	GL50803_27896	1.46
G1/S	Hypothetical protein	GL50803_4257	1.46
G1/S	Hypothetical protein	GL50803_16653	1.46
G1/S	Hypothetical protein	GL50803_12109	1.45
G1/S	Hypothetical protein	GL50803_10675	1.45
G1/S	Hypothetical protein	GL50803_10675	1.45
G1/S	Hypothetical protein	GL50803_113766	1.45
G1/S	Hypothetical protein	GL50803_2226	1.45
G1/S	Hypothetical protein	GL50803_31144	1.44
G1/S	Hypothetical protein	GL50803_4538	1.44
G1/S	Hypothetical protein	GL50803_16638	1.44
G1/S	Hypothetical protein	GL50803_14857	1.44
G1/S	Hypothetical protein	GL50803_2822	1.44
G1/S	Hypothetical protein	GL50803_7035	1.43
G1/S	Hypothetical protein	GL50803_17123	1.43
G1/S	Hypothetical protein	GL50803_11621	1.43
G1/S	Hypothetical protein	GL50803_8208	1.43

Cell Cycle Stage	Gene Description	Gene ID	Fold Change
G1/S	Hypothetical protein	GL50803_32309	1.43
G1/S	Hypothetical protein	GL50803_5246	1.43
G1/S	Hypothetical protein	GL50803_16615	1.43
G1/S	Hypothetical protein	GL50803_33663	1.42
G1/S	Hypothetical protein	GL50803_7825	1.42
G1/S	Hypothetical protein	GL50803_4259	1.41
G1/S	Hypothetical protein	GL50803_13790	1.41
G1/S	Hypothetical protein	GL50803_95406	1.41
G1/S	Hypothetical protein	GL50803_102022	1.41
G1/S	Hypothetical protein	GL50803_17346	1.41
G1/S	Hypothetical protein	GL50803_24695	1.41
G1/S	Hypothetical protein	GL50803_3950	1.41
G1/S	Hypothetical protein	GL50803_16414	1.41
G1/S	Hypothetical protein	GL50803_86680	1.41
G1/S	Hypothetical protein	GL50803_17624	1.40
G1/S	Hypothetical protein	GL50803_6132	1.40
G1/S	Hypothetical protein	GL50803_17330	1.40
G1/S	Hypothetical protein	GL50803_17037	1.40
G1/S	Hypothetical protein	GL50803_4705	1.39
G1/S	Hypothetical protein	GL50803_90425	1.39
G1/S	Hypothetical protein	GL50803_3720	1.39
G1/S	Hypothetical protein	GL50803_8243	1.39
G1/S	Hypothetical protein	GL50803_30474	1.39
G1/S	Hypothetical protein	GL50803_137759	1.38
G1/S	Hypothetical protein	GL50803_11720	1.38
G1/S	Hypothetical protein	GL50803_115770	1.38
G1/S	Hypothetical protein	GL50803_12889	1.38
G1/S	Hypothetical protein	GL50803_17393	1.38
G1/S	Hypothetical protein	GL50803_113133	1.37
G1/S	Hypothetical protein	GL50803_16827	1.37
G1/S	Hypothetical protein	GL50803_8423	1.37
G1/S	Hypothetical protein	GL50803_5821	1.37
G1/S	Hypothetical protein	GL50803_8075	1.37
G1/S	Hypothetical protein	GL50803_7513	1.36
G1/S	Hypothetical protein	GL50803_23694	1.36
G1/S	Hypothetical protein	GL50803_40067	1.36
G1/S	Hypothetical protein	GL50803_15186	1.36
G1/S	Hypothetical protein	GL50803_7723	1.36
G1/S	Hypothetical protein	GL50803_17584	1.35
G1/S	Hypothetical protein	GL50803_16288	1.35
G1/S	Hypothetical protein	GL50803_94762	1.35
G1/S	Hypothetical protein	GL50803_2217	1.35
G1/S	Hypothetical protein	GL50803_33023	1.35

Cell Cycle Stage	Gene Description	Gene ID	Fold Change
G1/S	Hypothetical protein	GL50803_103205	1.35
G1/S	Hypothetical protein	GL50803_13279	1.35
G1/S	Hypothetical protein	GL50803_114651	1.34
G1/S	Hypothetical protein	GL50803_101994	1.34
G1/S	Hypothetical protein	GL50803_97741	1.34
G1/S	Hypothetical protein	GL50803_16507	1.34
G1/S	Hypothetical protein	GL50803_21330	1.34
G1/S	Hypothetical protein	GL50803_38244	1.33
G1/S	Hypothetical protein	GL50803_9143	1.33
G1/S	Hypothetical protein	GL50803_9086	1.32
G1/S	Hypothetical protein	GL50803_24584	1.32
G1/S	Hypothetical protein	GL50803_34050	1.31
G1/S	Hypothetical protein	GL50803_6579	1.31
G1/S	Hypothetical protein	GL50803_27602	1.31
G1/S	Hypothetical protein	GL50803_9359	1.30
G1/S	Hypothetical protein	GL50803_5988	1.30
G1/S	Hypothetical protein	GL50803_103125	1.30
G1/S	Hypothetical protein	GL50803_16808	1.30
G1/S	Hypothetical protein	GL50803_9132	1.30
G1/S	Hypothetical protein	GL50803_27696	1.30
G1/S	Hypothetical protein	GL50803_15192	1.29
G1/S	Hypothetical protein	GL50803_21531	1.29
G1/S	Hypothetical protein	GL50803_16405	1.29
G1/S	Hypothetical protein	GL50803_8560	1.29
G1/S	Hypothetical protein	GL50803_8854	1.29
G1/S	Hypothetical protein	GL50803_17606	1.28
G1/S	Hypothetical protein	GL50803_4816	1.28
G1/S	Hypothetical protein	GL50803_96818	1.28
G1/S	Hypothetical protein	GL50803_17169	1.28
G1/S	Hypothetical protein	GL50803_17474	1.28
G1/S	Hypothetical protein	GL50803_14921	1.28
G1/S	Hypothetical protein	GL50803_90434	1.27
G1/S	Hypothetical protein	GL50803_4266	1.27
G1/S	Hypothetical protein	GL50803_42357	1.27
G1/S	Hypothetical protein	GL50803_17110	1.26
G1/S	Hypothetical protein	GL50803_3467	1.26
G1/S	Kinase, CAMK CAMKL	GL50803_16235	1.25
G1/S	Kinase, NEK	GL50803_16272	1.97
G1/S	Kinase, NEK	GL50803_11390	1.90
G1/S	Kinase, NEK	GL50803_13981	1.82
G1/S	Kinase, NEK	GL50803_15953	1.74
G1/S	Kinase, NEK	GL50803_94927	1.51
G1/S	Kinase, NEK	GL50803_14742	1.48

Cell Cycle Stage	Gene Description	Gene ID	Fold Change
G1/S	Kinase, NEK	GL50803_95717	1.44
G1/S	Kinase, NEK	GL50803_24321	1.43
G1/S	Kinase, NEK	GL50803_17231	1.43
G1/S	Kinase, NEK	GL50803_24400	1.43
G1/S	Kinase, NEK	GL50803_13964	1.35
G1/S	Kinase, NEK	GL50803_5553	1.33
G1/S	Kinase, NEK	GL50803_113553	1.27
G1/S	Kinase, NEK-frag	GL50803_5489	1.74
G1/S	Kinase, NEK-frag	GL50803_13963	1.51
G1/S	Kinase, NEK-frag	GL50803_102034	1.31
G1/S	Kinase, NEK-like	GL50803_15035	1.76
G1/S	Kinase, TTK	GL50803_4405	1.30
G1/S	La ribonucleoprotein, putative	GL50803_9803	1.69
G1/S	Lecithin-cholesterol acyl transferase, putative	GL50803_16286	1.54
G1/S	Liver stage antigen-like protein	GL50803_16595	1.79
G1/S	Lysophosphatidic acid acyltransferase, putative	GL50803_14403	1.39
G1/S	Lysyl-tRNA synthetase	GL50803_16766	1.36
G1/S	MDR protein-like protein	GL50803_40224	1.33
G1/S	Metalloprotease, insulinase family	GL50803_93551	1.61
G1/S	Metalloprotease, insulinase family	GL50803_9508	1.40
G1/S	Mitotic control protein dis3	GL50803_112718	1.47
G1/S	Nuclear LIM interactor-interacting factor 1	GL50803_9162	1.64
G1/S	P115, putative	GL50803_8855	2.00
G1/S	Periodic tryptophan protein 1, putative	GL50803_15531	1.49
G1/S	Periodic tryptophan protein 2-like protein	GL50803_94653	1.46
G1/S	Phosphatase	GL50803_14404	1.33
G1/S	Phosphatase	GL50803_15215	1.27
G1/S	Plasma membrane calcium-transporting ATPase 2	GL50803_32658	1.29
G1/S	Protein 21.1	GL50803_93011	2.32
G1/S	Protein 21.1	GL50803_17046	2.26
G1/S	Protein 21.1	GL50803_16532	2.24
G1/S	Protein 21.1	GL50803_23492	2.24
G1/S	Protein 21.1	GL50803_17585	2.13
G1/S	Protein 21.1	GL50803_15972	2.10
G1/S	Protein 21.1	GL50803_40390	2.00
G1/S	Protein 21.1	GL50803_16843	1.99
G1/S	Protein 21.1	GL50803_17551	1.96
G1/S	Protein 21.1	GL50803_12139	1.94

Cell Cycle Stage	Gene Description	Gene ID	Fold Change
G1/S	Protein 21.1	GL50803_103783	1.87
G1/S	Protein 21.1	GL50803_14434	1.85
G1/S	Protein 21.1	GL50803_24194	1.77
G1/S	Protein 21.1	GL50803_27925	1.74
G1/S	Protein 21.1	GL50803_8174	1.74
G1/S	Protein 21.1	GL50803_16326	1.73
G1/S	Protein 21.1	GL50803_14859	1.71
G1/S	Protein 21.1	GL50803_11165	1.70
G1/S	Protein 21.1	GL50803_14764	1.69
G1/S	Protein 21.1	GL50803_17097	1.69
G1/S	Protein 21.1	GL50803_13438	1.67
G1/S	Protein 21.1	GL50803_16220	1.66
G1/S	Protein 21.1	GL50803_103807	1.60
G1/S	Protein 21.1	GL50803_17096	1.58
G1/S	Protein 21.1	GL50803_16435	1.58
G1/S	Protein 21.1	GL50803_113622	1.56
G1/S	Protein 21.1	GL50803_4264	1.54
G1/S	Protein 21.1	GL50803_14254	1.54
G1/S	Protein 21.1	GL50803_10632	1.50
G1/S	Protein 21.1	GL50803_13901	1.47
G1/S	Protein 21.1	GL50803_11389	1.47
G1/S	Protein 21.1	GL50803_9030	1.45
G1/S	Protein 21.1	GL50803_17586	1.45
G1/S	Protein 21.1	GL50803_97072	1.44
G1/S	Protein 21.1	GL50803_5806	1.43
G1/S	Protein 21.1	GL50803_7375	1.43
G1/S	Protein 21.1	GL50803_15184	1.40
G1/S	Protein 21.1	GL50803_8928	1.38
G1/S	Protein 21.1	GL50803_8949	1.36
G1/S	Protein 21.1	GL50803_10219	1.34
G1/S	Protein 21.1	GL50803_5881	1.33
G1/S	Protein 21.1	GL50803_17552	1.31
G1/S	Protein 21.1	GL50803_32778	1.30
G1/S	Protein 21.1	GL50803_17023	1.27
G1/S	Protein 21.6	GL50803_17005	1.38
G1/S	RNA binding protein, putative	GL50803_92031	1.55
G1/S	RNA polymerase AI large subunit	GL50803_23496	1.62
G1/S	RNA polymerase I subunit A43	GL50803_17422	1.58
G1/S	RRNA biogenesis protein RRP5	GL50803_14702	1.39
G1/S	SALP-1	GL50803_4410	2.21
G1/S	Sec1 vATPase	GL50803_13528	1.29
G1/S	Sec13	GL50803_137698	1.35
G1/S	Serine palmitoyltransferase 1	GL50803_23015	1.42

Cell Cycle Stage	Gene Description	Gene ID	Fold Change
G1/S	Serologically defined colon cancer antigen 1	GL50803_4043	1.46
G1/S	Spindle pole protein, putative	GL50803_33660	1.85
G1/S	Spindle pole protein, putative	GL50803_24537	1.57
G1/S	Spindle pole protein, putative	GL50803_24537	1.57
G1/S	Spindle pole protein, putative	GL50803_7031	1.41
G1/S	Spindle pole protein, putative	GL50803_16729	1.40
G1/S	Spindle pole protein, putative	GL50803_14895	1.34
G1/S	Spindle pole protein, putative	GL50803_17055	1.33
G1/S	SUA5 protein	GL50803_17389	1.49
G1/S	Thymidine kinase	GL50803_8364	2.82
G1/S	Translation initiation factor	GL50803_7652	1.35
G1/S	Trichohyalin	GL50803_17571	2.07
G1/S	tRNA synthetase, Glutaminyl-tRNA synthetase	GL50803_86681	1.65
G1/S	tRNA synthetase, Isoleucyl-tRNA synthetase	GL50803_104173	1.43
G1/S	Tubulin tyrosine ligase	GL50803_9272	1.73
G1/S	U3 small nucleolar ribonucleoprotein protein IMP4, putative	GL50803_16173	1.33
G1/S	U3 small nucleolar ribonucleoprotein protein MPP10, putative	GL50803_9274	1.41
G1/S	Ubiquitin-protein ligase E3A	GL50803_17386	1.33
G1/S	Unspecified product	GL50803_4815	1.79
G1/S	Unspecified product	GL50803_27870	1.74
G1/S	Unspecified product	GL50803_32269	1.67
G1/S	Unspecified product	GL50803_31319	1.65
G1/S	Unspecified product	GL50803_20386	1.64
G1/S	Unspecified product	GL50803_117188	1.62
G1/S	Unspecified product	GL50803_117187	1.62
G1/S	Unspecified product	GL50803_31704	1.61
G1/S	Unspecified product	GL50803_93287	1.59
G1/S	Unspecified product	GL50803_36266	1.52
G1/S	Unspecified product	GL50803_39181	1.51
G1/S	Unspecified product	GL50803_38205	1.50
G1/S	Unspecified product	GL50803_31625	1.48
G1/S	Unspecified product	GL50803_32272	1.48
G1/S	Unspecified product	GL50803_39243	1.47
G1/S	Unspecified product	GL50803_6638	1.45
G1/S	Unspecified product	GL50803_99576	1.44
G1/S	Uridine kinase	GL50803_16549	1.49
G1/S	Uridine kinase	GL50803_8217	1.40
G1/S	Vacuolar protein sorting 35	GL50803_23833	1.29

Cell Cycle Stage	Gene Description	Gene ID	Fold Change
G1/S	VSP, putative	GL50803_11692	1.39
G1/S	Xaa-Pro dipeptidase	GL50803_17327	1.56
G1/S	Zinc finger domain protein	GL50803_15187	1.63
G2/M	2,3-bisphosphoglycerate-independent phosphoglycerate mutase	GL50803_8822	-2.15
G2/M	AAA family ATPase	GL50803_16867	-2.93
G2/M	ABC transporter family protein	GL50803_16575	-1.41
G2/M	Actin related protein	GL50803_8726	-2.00
G2/M	Amino acid transporter family	GL50803_7909	-1.77
G2/M	Ankyrin repeat protein	GL50803_16914	-1.90
G2/M	ARL1	GL50803_13478	-1.35
G2/M	Aspartate aminotransferase, cytoplasmic	GL50803_91056	-1.64
G2/M	ATP binding protein associated with cell differentiation, putative	GL50803_12807	-2.44
G2/M	Axoneme central apparatus protein	GL50803_16202	-1.69
G2/M	Axoneme-associated protein GASP-180	GL50803_23235	-1.50
G2/M	Caltractin	GL50803_104685	-1.85
G2/M	CDP-diacylglycerol-glycerol-3-phosphate 3-phosphatidyltransferase	GL50803_7259	-1.47
G2/M	Centrin	GL50803_6744	-1.76
G2/M	Centromere/microtubule binding protein CBF5	GL50803_16311	-1.30
G2/M	CHL1-like protein	GL50803_92673	-1.82
G2/M	Clusterin associated protein 1, putative	GL50803_16707	-1.54
G2/M	Coiled-coil protein	GL50803_115245	-1.27
G2/M	Coiled-coil protein	GL50803_11867	-1.38
G2/M	Coiled-coil protein	GL50803_16199	-1.48
G2/M	Coiled-coil protein	GL50803_7829	-1.58
G2/M	Coiled-coil protein	GL50803_21662	-1.69
G2/M	Coiled-coil protein	GL50803_9492	-1.73
G2/M	Coiled-coil protein	GL50803_3868	-1.74
G2/M	Coiled-coil protein	GL50803_15364	-1.80
G2/M	Coiled-coil protein	GL50803_40831	-1.90
G2/M	Coiled-coil protein	GL50803_95653	-1.90
G2/M	CTP synthase/UTP-ammonia lyase	GL50803_4507	-1.62
G2/M	Cyclin A	GL50803_14488	-1.69
G2/M	Cyclin B, G2/mitotic-specific	GL50803_3977	-2.28
G2/M	Cyclin B-like	GL50803_17505	-1.82
G2/M	Cyclin domain, Hypothetical protein	GL50803_17400	-2.85
G2/M	Degreening related gene dee76 protein	GL50803_17294	-1.90

Cell Cycle Stage	Gene Description	Gene ID	Fold Change
G2/M	Deoxyribonuclease, TatD family	GL50803_95789	-1.51
G2/M	Dihydrouridine synthase, putative	GL50803_3565	-1.35
G2/M	DNA topoisomerase III	GL50803_7615	-1.37
G2/M	D-tyrosyl-tRNA deacylase	GL50803_13832	-1.29
G2/M	Dynein binding protein, putative	GL50803_15549	-1.46
G2/M	Dynein heavy chain	GL50803_17243	-1.35
G2/M	Dynein heavy chain	GL50803_10538	-1.43
G2/M	Dynein light chain	GL50803_27308	-1.37
G2/M	Dynein regulatory complex	GL50803_16540	-2.60
G2/M	Dynein-like protein	GL50803_15460	-1.34
G2/M	EB1	GL50803_14048	-1.57
G2/M	Enolase	GL50803_11118	-2.21
G2/M	ERP1	GL50803_4509	-1.29
G2/M	Extracellular nuclease, putative	GL50803_8742	-1.62
G2/M	FKBP-type peptidyl-prolyl cis-trans isomerase	GL50803_10450	-1.73
G2/M	Flap structure-specific endonuclease	GL50803_16953	-2.66
G2/M	Fructose-bisphosphate aldolase	GL50803_11043	-2.42
G2/M	GiTax, an axonemal protein important for flagella function	GL50803_17116	-1.56
G2/M	Glucose-6-phosphate isomerase	GL50803_9115	-1.48
G2/M	Glyceraldehyde 3-phosphate dehydrogenase	GL50803_6687	-1.78
G2/M	Glycogen phosphorylase	GL50803_6226	-2.16
G2/M	Glycyl tRNA synthetase	GL50803_39011	-1.74
G2/M	Gmyb11	GL50803_6417	-1.78
G2/M	GTL3 aka MD0260	GL50803_104866	-1.60
G2/M	GTP-binding protein ARD-1, putative	GL50803_8140	-1.38
G2/M	Guanylate kinase	GL50803_7203	-1.75
G2/M	Heat-shock protein, putative	GL50803_16412	-1.57
G2/M	hemagglutinin protein-like protein	GL50803_8982	-1.53
G2/M	High cysteine protein	GL50803_94003	-1.57
G2/M	High cysteine protein	GL50803_14324	-1.85
G2/M	Histone methyltransferase HMT1	GL50803_9130	-1.50
G2/M	Histone methyltransferase MYST1	GL50803_17263	-1.49
G2/M	Hypothetical protein	GL50803_14252	-1.25
G2/M	Hypothetical protein	GL50803_17280	-1.26
G2/M	Hypothetical protein	GL50803_102170	-1.27
G2/M	Hypothetical protein	GL50803_16978	-1.27
G2/M	Hypothetical protein	GL50803_7230	-1.28
G2/M	Hypothetical protein	GL50803_9752	-1.28
G2/M	Hypothetical protein	GL50803_15581	-1.29
G2/M	Hypothetical protein	GL50803_16556	-1.29

Cell Cycle Stage	Gene Description	Gene ID	Fold Change
G2/M	Hypothetical protein	GL50803_16350	-1.29
G2/M	Hypothetical protein	GL50803_14994	-1.29
G2/M	Hypothetical protein	GL50803_15039	-1.30
G2/M	Hypothetical protein	GL50803_114793	-1.30
G2/M	Hypothetical protein	GL50803_11548	-1.30
G2/M	Hypothetical protein	GL50803_9098	-1.31
G2/M	Hypothetical protein	GL50803_5768	-1.32
G2/M	Hypothetical protein	GL50803_16894	-1.32
G2/M	Hypothetical protein	GL50803_9036	-1.32
G2/M	Hypothetical protein	GL50803_137705	-1.32
G2/M	Hypothetical protein	GL50803_16503	-1.32
G2/M	Hypothetical protein	GL50803_15285	-1.32
G2/M	Hypothetical protein	GL50803_7706	-1.32
G2/M	Hypothetical protein	GL50803_9697	-1.32
G2/M	Hypothetical protein	GL50803_4928	-1.32
G2/M	Hypothetical protein	GL50803_8359	-1.33
G2/M	Hypothetical protein	GL50803_36915	-1.33
G2/M	Hypothetical protein	GL50803_4155	-1.33
G2/M	Hypothetical protein	GL50803_114751	-1.33
G2/M	Hypothetical protein	GL50803_16998	-1.33
G2/M	Hypothetical protein	GL50803_4587	-1.33
G2/M	Hypothetical protein	GL50803_16951	-1.33
G2/M	Hypothetical protein	GL50803_28779	-1.33
G2/M	Hypothetical protein	GL50803_15016	-1.33
G2/M	Hypothetical protein	GL50803_15991	-1.33
G2/M	Hypothetical protein	GL50803_17367	-1.34
G2/M	Hypothetical protein	GL50803_13288	-1.34
G2/M	Hypothetical protein	GL50803_31974	-1.35
G2/M	Hypothetical protein	GL50803_137746	-1.35
G2/M	Hypothetical protein	GL50803_28477	-1.35
G2/M	Hypothetical protein	GL50803_11207	-1.35
G2/M	Hypothetical protein	GL50803_13774	-1.35
G2/M	Hypothetical protein	GL50803_27193	-1.35
G2/M	Hypothetical protein	GL50803_3746	-1.35
G2/M	Hypothetical protein	GL50803_17549	-1.35
G2/M	Hypothetical protein	GL50803_8410	-1.35
G2/M	Hypothetical protein	GL50803_10882	-1.35
G2/M	Hypothetical protein	GL50803_11932	-1.36
G2/M	Hypothetical protein	GL50803_14180	-1.36
G2/M	Hypothetical protein	GL50803_114912	-1.36
G2/M	Hypothetical protein	GL50803_8770	-1.36
G2/M	Hypothetical protein	GL50803_10773	-1.36
G2/M	Hypothetical protein	GL50803_17189	-1.36

Cell Cycle Stage	Gene Description	Gene ID	Fold Change
G2/M	Hypothetical protein	GL50803_13622	-1.36
G2/M	Hypothetical protein	GL50803_15017	-1.36
G2/M	Hypothetical protein	GL50803_5002	-1.36
G2/M	Hypothetical protein	GL50803_3146	-1.36
G2/M	Hypothetical protein	GL50803_8426	-1.36
G2/M	Hypothetical protein	GL50803_5183	-1.37
G2/M	Hypothetical protein	GL50803_37449	-1.37
G2/M	Hypothetical protein	GL50803_15939	-1.37
G2/M	Hypothetical protein	GL50803_16077	-1.37
G2/M	Hypothetical protein	GL50803_8585	-1.37
G2/M	Hypothetical protein	GL50803_3063	-1.37
G2/M	Hypothetical protein	GL50803_13700	-1.37
G2/M	Hypothetical protein	GL50803_3342	-1.37
G2/M	Hypothetical protein	GL50803_21527	-1.37
G2/M	Hypothetical protein	GL50803_16247	-1.37
G2/M	Hypothetical protein	GL50803_16297	-1.38
G2/M	Hypothetical protein	GL50803_10708	-1.38
G2/M	Hypothetical protein	GL50803_7081	-1.38
G2/M	Hypothetical protein	GL50803_7685	-1.38
G2/M	Hypothetical protein	GL50803_8738	-1.38
G2/M	Hypothetical protein	GL50803_14633	-1.39
G2/M	Hypothetical protein	GL50803_12230	-1.39
G2/M	Hypothetical protein	GL50803_16599	-1.39
G2/M	Hypothetical protein	GL50803_16430	-1.39
G2/M	Hypothetical protein	GL50803_3867	-1.39
G2/M	Hypothetical protein	GL50803_17238	-1.39
G2/M	Hypothetical protein	GL50803_6176	-1.39
G2/M	Hypothetical protein	GL50803_7639	-1.39
G2/M	Hypothetical protein	GL50803_3419	-1.40
G2/M	Hypothetical protein	GL50803_21803	-1.40
G2/M	Hypothetical protein	GL50803_8937	-1.40
G2/M	Hypothetical protein	GL50803_11714	-1.40
G2/M	Hypothetical protein	GL50803_32363	-1.40
G2/M	Hypothetical protein	GL50803_40885	-1.41
G2/M	Hypothetical protein	GL50803_112787	-1.41
G2/M	Hypothetical protein	GL50803_13342	-1.41
G2/M	Hypothetical protein	GL50803_13354	-1.41
G2/M	Hypothetical protein	GL50803_17094	-1.41
G2/M	Hypothetical protein	GL50803_17453	-1.41
G2/M	Hypothetical protein	GL50803_20413	-1.41
G2/M	Hypothetical protein	GL50803_13651	-1.42
G2/M	Hypothetical protein	GL50803_111806	-1.42
G2/M	Hypothetical protein	GL50803_15216	-1.42

Cell Cycle Stage	Gene Description	Gene ID	Fold Change
G2/M	Hypothetical protein	GL50803_13467	-1.42
G2/M	Hypothetical protein	GL50803_10881	-1.42
G2/M	Hypothetical protein	GL50803_7270	-1.42
G2/M	Hypothetical protein	GL50803_15553	-1.42
G2/M	Hypothetical protein	GL50803_36412	-1.43
G2/M	Hypothetical protein	GL50803_12093	-1.43
G2/M	Hypothetical protein	GL50803_15769	-1.43
G2/M	Hypothetical protein	GL50803_1937	-1.43
G2/M	Hypothetical protein	GL50803_8974	-1.43
G2/M	Hypothetical protein	GL50803_14318	-1.43
G2/M	Hypothetical protein	GL50803_40783	-1.43
G2/M	Hypothetical protein	GL50803_17405	-1.43
G2/M	Hypothetical protein	GL50803_93002	-1.44
G2/M	Hypothetical protein	GL50803_5784	-1.44
G2/M	Hypothetical protein	GL50803_7891	-1.44
G2/M	Hypothetical protein	GL50803_6897	-1.44
G2/M	Hypothetical protein	GL50803_24861	-1.44
G2/M	Hypothetical protein	GL50803_14400	-1.45
G2/M	Hypothetical protein	GL50803_16237	-1.45
G2/M	Hypothetical protein	GL50803_16670	-1.45
G2/M	Hypothetical protein	GL50803_27141	-1.45
G2/M	Hypothetical protein	GL50803_91476	-1.45
G2/M	Hypothetical protein	GL50803_3211	-1.45
G2/M	Hypothetical protein	GL50803_16054	-1.45
G2/M	Hypothetical protein	GL50803_8405	-1.45
G2/M	Hypothetical protein	GL50803_13787	-1.45
G2/M	Hypothetical protein	GL50803_24643	-1.46
G2/M	Hypothetical protein	GL50803_11877	-1.46
G2/M	Hypothetical protein	GL50803_10522	-1.46
G2/M	Hypothetical protein	GL50803_17313	-1.46
G2/M	Hypothetical protein	GL50803_11321	-1.46
G2/M	Hypothetical protein	GL50803_15239	-1.46
G2/M	Hypothetical protein	GL50803_16970	-1.46
G2/M	Hypothetical protein	GL50803_10423	-1.46
G2/M	Hypothetical protein	GL50803_3563	-1.47
G2/M	Hypothetical protein	GL50803_16415	-1.47
G2/M	Hypothetical protein	GL50803_86618	-1.47
G2/M	Hypothetical protein	GL50803_11696	-1.47
G2/M	Hypothetical protein	GL50803_4337	-1.47
G2/M	Hypothetical protein	GL50803_10527	-1.47
G2/M	Hypothetical protein	GL50803_22133	-1.47
G2/M	Hypothetical protein	GL50803_32730	-1.47
G2/M	Hypothetical protein	GL50803_10879	-1.47

Cell Cycle Stage	Gene Description	Gene ID	Fold Change
G2/M	Hypothetical protein	GL50803_8639	-1.47
G2/M	Hypothetical protein	GL50803_14947	-1.47
G2/M	Hypothetical protein	GL50803_112862	-1.48
G2/M	Hypothetical protein	GL50803_41834	-1.48
G2/M	Hypothetical protein	GL50803_26589	-1.48
G2/M	Hypothetical protein	GL50803_36515	-1.48
G2/M	Hypothetical protein	GL50803_14104	-1.49
G2/M	Hypothetical protein	GL50803_8942	-1.49
G2/M	Hypothetical protein	GL50803_94534	-1.49
G2/M	Hypothetical protein	GL50803_27835	-1.49
G2/M	Hypothetical protein	GL50803_2848	-1.49
G2/M	Hypothetical protein	GL50803_14906	-1.50
G2/M	Hypothetical protein	GL50803_6423	-1.50
G2/M	Hypothetical protein	GL50803_9520	-1.50
G2/M	Hypothetical protein	GL50803_17532	-1.50
G2/M	Hypothetical protein	GL50803_21048	-1.51
G2/M	Hypothetical protein	GL50803_21474	-1.51
G2/M	Hypothetical protein	GL50803_15985	-1.51
G2/M	Hypothetical protein	GL50803_17529	-1.52
G2/M	Hypothetical protein	GL50803_21138	-1.52
G2/M	Hypothetical protein	GL50803_2523	-1.52
G2/M	Hypothetical protein	GL50803_35595	-1.52
G2/M	Hypothetical protein	GL50803_8955	-1.52
G2/M	Hypothetical protein	GL50803_4150	-1.53
G2/M	Hypothetical protein	GL50803_90044	-1.53
G2/M	Hypothetical protein	GL50803_4415	-1.53
G2/M	Hypothetical protein	GL50803_102654	-1.53
G2/M	Hypothetical protein	GL50803_4622	-1.53
G2/M	Hypothetical protein	GL50803_114974	-1.53
G2/M	Hypothetical protein	GL50803_34977	-1.53
G2/M	Hypothetical protein	GL50803_94127	-1.53
G2/M	Hypothetical protein	GL50803_95787	-1.53
G2/M	Hypothetical protein	GL50803_37258	-1.53
G2/M	Hypothetical protein	GL50803_15989	-1.54
G2/M	Hypothetical protein	GL50803_17129	-1.54
G2/M	Hypothetical protein	GL50803_11700	-1.54
G2/M	Hypothetical protein	GL50803_15545	-1.54
G2/M	Hypothetical protein	GL50803_87577	-1.55
G2/M	Hypothetical protein	GL50803_16663	-1.55
G2/M	Hypothetical protein	GL50803_112112	-1.55
G2/M	Hypothetical protein	GL50803_15244	-1.55
G2/M	Hypothetical protein	GL50803_16869	-1.55
G2/M	Hypothetical protein	GL50803_11563	-1.56

Cell Cycle Stage	Gene Description	Gene ID	Fold Change
G2/M	Hypothetical protein	GL50803_31339	-1.56
G2/M	Hypothetical protein	GL50803_7566	-1.56
G2/M	Hypothetical protein	GL50803_16950	-1.56
G2/M	Hypothetical protein	GL50803_19614	-1.56
G2/M	Hypothetical protein	GL50803_41619	-1.56
G2/M	Hypothetical protein	GL50803_6927	-1.57
G2/M	Hypothetical protein	GL50803_18705	-1.57
G2/M	Hypothetical protein	GL50803_16222	-1.57
G2/M	Hypothetical protein	GL50803_7207	-1.57
G2/M	Hypothetical protein	GL50803_16126	-1.57
G2/M	Hypothetical protein	GL50803_101955	-1.58
G2/M	Hypothetical protein	GL50803_21485	-1.58
G2/M	Hypothetical protein	GL50803_113740	-1.58
G2/M	Hypothetical protein	GL50803_14003	-1.58
G2/M	Hypothetical protein	GL50803_7374	-1.58
G2/M	Hypothetical protein	GL50803_9427	-1.58
G2/M	Hypothetical protein	GL50803_8141	-1.59
G2/M	Hypothetical protein	GL50803_13874	-1.60
G2/M	Hypothetical protein	GL50803_10422	-1.60
G2/M	Hypothetical protein	GL50803_103202	-1.61
G2/M	Hypothetical protein	GL50803_92602	-1.61
G2/M	Hypothetical protein	GL50803_5274	-1.61
G2/M	Hypothetical protein	GL50803_16478	-1.61
G2/M	Hypothetical protein	GL50803_1875	-1.61
G2/M	Hypothetical protein	GL50803_7747	-1.62
G2/M	Hypothetical protein	GL50803_37809	-1.62
G2/M	Hypothetical protein	GL50803_8433	-1.62
G2/M	Hypothetical protein	GL50803_23330	-1.62
G2/M	Hypothetical protein	GL50803_14198	-1.62
G2/M	Hypothetical protein	GL50803_9414	-1.62
G2/M	Hypothetical protein	GL50803_2011	-1.63
G2/M	Hypothetical protein	GL50803_111886	-1.63
G2/M	Hypothetical protein	GL50803_12885	-1.63
G2/M	Hypothetical protein	GL50803_3705	-1.64
G2/M	Hypothetical protein	GL50803_7600	-1.64
G2/M	Hypothetical protein	GL50803_12174	-1.64
G2/M	Hypothetical protein	GL50803_32337	-1.64
G2/M	Hypothetical protein	GL50803_19078	-1.64
G2/M	Hypothetical protein	GL50803_10875	-1.64
G2/M	Hypothetical protein	GL50803_29768	-1.65
G2/M	Hypothetical protein	GL50803_9826	-1.65
G2/M	Hypothetical protein	GL50803_13945	-1.65
G2/M	Hypothetical protein	GL50803_14346	-1.65

Cell Cycle Stage	Gene Description	Gene ID	Fold Change
G2/M	Hypothetical protein	GL50803_7343	-1.66
G2/M	Hypothetical protein	GL50803_115036	-1.66
G2/M	Hypothetical protein	GL50803_31996	-1.66
G2/M	Hypothetical protein	GL50803_14027	-1.67
G2/M	Hypothetical protein	GL50803_19230	-1.68
G2/M	Hypothetical protein	GL50803_38019	-1.68
G2/M	Hypothetical protein	GL50803_4323	-1.68
G2/M	Hypothetical protein	GL50803_17454	-1.68
G2/M	Hypothetical protein	GL50803_88556	-1.69
G2/M	Hypothetical protein	GL50803_15585	-1.69
G2/M	Hypothetical protein	GL50803_27318	-1.69
G2/M	Hypothetical protein	GL50803_13699	-1.69
G2/M	Hypothetical protein	GL50803_22268	-1.69
G2/M	Hypothetical protein	GL50803_2549	-1.69
G2/M	Hypothetical protein	GL50803_6725	-1.69
G2/M	Hypothetical protein	GL50803_14850	-1.70
G2/M	Hypothetical protein	GL50803_5012	-1.70
G2/M	Hypothetical protein	GL50803_101278	-1.70
G2/M	Hypothetical protein	GL50803_16768	-1.72
G2/M	Hypothetical protein	GL50803_21897	-1.73
G2/M	Hypothetical protein	GL50803_24425	-1.73
G2/M	Hypothetical protein	GL50803_16585	-1.74
G2/M	Hypothetical protein	GL50803_15310	-1.75
G2/M	Hypothetical protein	GL50803_16445	-1.75
G2/M	Hypothetical protein	GL50803_11373	-1.75
G2/M	Hypothetical protein	GL50803_17081	-1.76
G2/M	Hypothetical protein	GL50803_17089	-1.76
G2/M	Hypothetical protein	GL50803_24043	-1.76
G2/M	Hypothetical protein	GL50803_89285	-1.76
G2/M	Hypothetical protein	GL50803_34068	-1.77
G2/M	Hypothetical protein	GL50803_8460	-1.77
G2/M	Hypothetical protein	GL50803_7552	-1.78
G2/M	Hypothetical protein	GL50803_14507	-1.78
G2/M	Hypothetical protein	GL50803_14278	-1.78
G2/M	Hypothetical protein	GL50803_3920	-1.79
G2/M	Hypothetical protein	GL50803_16731	-1.80
G2/M	Hypothetical protein	GL50803_3158	-1.80
G2/M	Hypothetical protein	GL50803_15331	-1.80
G2/M	Hypothetical protein	GL50803_8430	-1.80
G2/M	Hypothetical protein	GL50803_5657	-1.80
G2/M	Hypothetical protein	GL50803_7577	-1.80
G2/M	Hypothetical protein	GL50803_8505	-1.81
G2/M	Hypothetical protein	GL50803_16234	-1.84

Cell Cycle Stage	Gene Description	Gene ID	Fold Change
G2/M	Hypothetical protein	GL50803_10853	-1.84
G2/M	Hypothetical protein	GL50803_17312	-1.85
G2/M	Hypothetical protein	GL50803_37381	-1.85
G2/M	Hypothetical protein	GL50803_14796	-1.86
G2/M	Hypothetical protein	GL50803_4624	-1.86
G2/M	Hypothetical protein	GL50803_8979	-1.87
G2/M	Hypothetical protein	GL50803_7396	-1.88
G2/M	Hypothetical protein	GL50803_4414	-1.88
G2/M	Hypothetical protein	GL50803_34450	-1.89
G2/M	Hypothetical protein	GL50803_32489	-1.90
G2/M	Hypothetical protein	GL50803_10676	-1.90
G2/M	Hypothetical protein	GL50803_9636	-1.92
G2/M	Hypothetical protein	GL50803_16321	-1.92
G2/M	Hypothetical protein	GL50803_16050	-1.93
G2/M	Hypothetical protein	GL50803_9305	-1.94
G2/M	Hypothetical protein	GL50803_102061	-1.94
G2/M	Hypothetical protein	GL50803_100413	-1.95
G2/M	Hypothetical protein	GL50803_4711	-1.95
G2/M	Hypothetical protein	GL50803_104982	-1.95
G2/M	Hypothetical protein	GL50803_7397	-1.96
G2/M	Hypothetical protein	GL50803_5186	-1.96
G2/M	Hypothetical protein	GL50803_11955	-1.97
G2/M	Hypothetical protein	GL50803_33030	-1.98
G2/M	Hypothetical protein	GL50803_39766	-1.98
G2/M	Hypothetical protein	GL50803_36617	-1.99
G2/M	Hypothetical protein	GL50803_114546	-2.00
G2/M	Hypothetical protein	GL50803_36817	-2.00
G2/M	Hypothetical protein	GL50803_16720	-2.00
G2/M	Hypothetical protein	GL50803_36709	-2.01
G2/M	Hypothetical protein	GL50803_4149	-2.01
G2/M	Hypothetical protein	GL50803_8702	-2.03
G2/M	Hypothetical protein	GL50803_5167	-2.03
G2/M	Hypothetical protein	GL50803_17403	-2.03
G2/M	Hypothetical protein	GL50803_24423	-2.04
G2/M	Hypothetical protein	GL50803_94658	-2.05
G2/M	Hypothetical protein	GL50803_10898	-2.06
G2/M	Hypothetical protein	GL50803_23874	-2.07
G2/M	Hypothetical protein	GL50803_9633	-2.08
G2/M	Hypothetical protein	GL50803_8865	-2.09
G2/M	Hypothetical protein	GL50803_7328	-2.09
G2/M	Hypothetical protein	GL50803_13315	-2.12
G2/M	Hypothetical protein	GL50803_17011	-2.12
G2/M	Hypothetical protein	GL50803_16353	-2.15

Cell Cycle Stage	Gene Description	Gene ID	Fold Change
G2/M	Hypothetical protein	GL50803_14647	-2.15
G2/M	Hypothetical protein	GL50803_8799	-2.16
G2/M	Hypothetical protein	GL50803_22027	-2.19
G2/M	Hypothetical protein	GL50803_16267	-2.20
G2/M	Hypothetical protein	GL50803_27147	-2.22
G2/M	Hypothetical protein	GL50803_16679	-2.23
G2/M	Hypothetical protein	GL50803_5883	-2.25
G2/M	Hypothetical protein	GL50803_2012	-2.28
G2/M	Hypothetical protein	GL50803_113290	-2.29
G2/M	Hypothetical protein	GL50803_11341	-2.33
G2/M	Hypothetical protein	GL50803_32509	-2.35
G2/M	Hypothetical protein	GL50803_9523	-2.35
G2/M	Hypothetical protein	GL50803_101260	-2.35
G2/M	Hypothetical protein	GL50803_13851	-2.39
G2/M	Hypothetical protein	GL50803_16039	-2.42
G2/M	Hypothetical protein	GL50803_16411	-2.47
G2/M	Hypothetical protein	GL50803_8980	-2.47
G2/M	Hypothetical protein	GL50803_9219	-2.59
G2/M	Hypothetical protein	GL50803_39037	-2.61
G2/M	Hypothetical protein	GL50803_6542	-2.63
G2/M	Hypothetical protein	GL50803_114199	-2.63
G2/M	Hypothetical protein	GL50803_37452	-2.68
G2/M	Hypothetical protein	GL50803_7538	-2.74
G2/M	Hypothetical protein	GL50803_7242	-2.75
G2/M	Hypothetical protein	GL50803_94542	-2.82
G2/M	Hypothetical protein	GL50803_17255	-2.84
G2/M	Hypothetical protein	GL50803_11643	-2.88
G2/M	Hypothetical protein	GL50803_11342	-2.91
G2/M	Hypothetical protein	GL50803_3538	-3.18
G2/M	Hypothetical protein	GL50803_13133	-3.32
G2/M	Hypothetical protein	GL50803_12105	-3.47
G2/M	Hypothetical protein	GL50803_9598	-3.67
G2/M	Hypothetical protein with antisense transcription	GL50803_14284	-1.33
G2/M	Hypothetical protein, similar to SMC2	GL50803_23185	-1.47
G2/M	IFT complex B	GL50803_14713	-1.30
G2/M	IFT complex B	GL50803_15428	-1.31
G2/M	Intraflagellar transport particle protein IFT88	GL50803_16660	-1.40
G2/M	Katanin	GL50803_15368	-1.41
G2/M	Kinase	GL50803_17073	-1.37
G2/M	Kinase	GL50803_5643	-1.41
G2/M	Kinase, Adenylate kinase	GL50803_28234	-1.47

Cell Cycle Stage	Gene Description	Gene ID	Fold Change
G2/M	Kinase, AGC AKT	GL50803_11364	-2.52
G2/M	Kinase, CAMK CAMKL	GL50803_17566	-1.42
G2/M	Kinase, Casein kinase II beta chain	GL50803_93671	-1.53
G2/M	Kinase, CMGC CDK	GL50803_15397	-1.37
G2/M	Kinase, CMGC CDK	GL50803_8037	-2.41
G2/M	Kinase, CMGC CDK	GL50803_16802	-3.64
G2/M	Kinase, CMGC CDKL	GL50803_96616	-2.06
G2/M	Kinase, CMGC DYRK	GL50803_137695	-1.48
G2/M	Kinase, CMGC DYRK	GL50803_17558	-1.70
G2/M	Kinase, CMGC GSK	GL50803_17625	-1.78
G2/M	Kinase, CMGC MAPK	GL50803_22850	-1.80
G2/M	Kinase, CMGC RCK	GL50803_6700	-1.87
G2/M	Kinase, CMGC SRPK	GL50803_17335	-1.60
G2/M	Kinase, NEK	GL50803_9421	-1.25
G2/M	Kinase, NEK	GL50803_8152	-1.29
G2/M	Kinase, NEK	GL50803_91220	-1.32
G2/M	Kinase, NEK	GL50803_6731	-1.34
G2/M	Kinase, NEK	GL50803_7103	-1.35
G2/M	Kinase, NEK	GL50803_16792	-1.36
G2/M	Kinase, NEK	GL50803_21366	-1.39
G2/M	Kinase, NEK	GL50803_9289	-1.40
G2/M	Kinase, NEK	GL50803_40904	-1.40
G2/M	Kinase, NEK	GL50803_11554	-1.41
G2/M	Kinase, NEK	GL50803_114120	-1.43
G2/M	Kinase, NEK	GL50803_12148	-1.44
G2/M	Kinase, NEK	GL50803_7356	-1.47
G2/M	Kinase, NEK	GL50803_14934	-1.58
G2/M	Kinase, NEK	GL50803_16251	-1.61
G2/M	Kinase, NEK	GL50803_87677	-1.68
G2/M	Kinase, NEK	GL50803_17069	-1.72
G2/M	Kinase, NEK	GL50803_11311	-1.73
G2/M	Kinase, NEK	GL50803_27124	-1.73
G2/M	Kinase, NEK	GL50803_8445	-1.82
G2/M	Kinase, NEK	GL50803_5999	-2.01
G2/M	Kinase, NEK	GL50803_92498	-2.30
G2/M	Kinase, NEK	GL50803_95593	-2.59
G2/M	Kinase, NEK-frag	GL50803_13479	-1.33
G2/M	Kinase, NEK-frag	GL50803_16733	-1.55
G2/M	Kinase, NEK-frag	GL50803_17578	-1.86
G2/M	Kinase, NEK-like	GL50803_4322	-1.66
G2/M	Kinase, PLK	GL50803_104150	-1.55
G2/M	Kinase, Protein kinase gPK1	GL50803_134209	-1.44
G2/M	Kinase, Protein kinase gPK1	GL50803_134210	-1.44

Cell Cycle Stage	Gene Description	Gene ID	Fold Change
G2/M	Kinase, Ser/Thr protein kinase	GL50803_15958	-1.31
G2/M	Kinase, Ser/Thr protein kinase	GL50803_22003	-1.73
G2/M	Kinase, STE STE20	GL50803_15514	-1.36
G2/M	Kinase, STE STE20	GL50803_14436	-1.55
G2/M	Kinase, STE STE20	GL50803_16986	-1.78
G2/M	Kinesin like protein	GL50803_17264	-1.38
G2/M	Kinesin-13	GL50803_16945	-3.09
G2/M	Kinesin-14	GL50803_13797	-1.31
G2/M	Kinesin-14	GL50803_8886	-2.04
G2/M	Kinesin-5	GL50803_16425	-1.48
G2/M	Kinesin-6	GL50803_102455	-2.70
G2/M	Kinesin-like protein	GL50803_11177	-1.45
G2/M	Kinesin-related protein	GL50803_11442	-1.43
G2/M	LEK1	GL50803_86761	-1.38
G2/M	Leucine carboxyl methyltransferase	GL50803_10516	-1.82
G2/M	Leucine-rich repeat protein	GL50803_11684	-1.49
G2/M	Maebl, putative	GL50803_17391	-1.51
G2/M	Malate dehydrogenase	GL50803_3331	-3.64
G2/M	Malic enzyme	GL50803_14285	-1.96
G2/M	Median body protein	GL50803_16343	-2.23
G2/M	Mitotic spindle checkpoint protein MAD2	GL50803_100955	-2.71
G2/M	Mlh2-like protein	GL50803_33083	-1.44
G2/M	Mob1-like protein	GL50803_11044	-1.71
G2/M	Multidrug resistance protein B	GL50803_16880	-1.30
G2/M	Multidrug resistance protein B	GL50803_17305	-1.39
G2/M	Multidrug resistance-associated protein 1	GL50803_28379	-1.49
G2/M	MYG1 protein	GL50803_10858	-1.56
G2/M	Nif3-related protein	GL50803_4355	-1.52
G2/M	NOD3 protein, putative	GL50803_4165	-1.61
G2/M	Nuclear ATP/GTP-binding protein	GL50803_10976	-1.73
G2/M	Nuclear LIM interactor-interacting factor 1	GL50803_4063	-1.52
G2/M	Nucleoside diphosphate kinase	GL50803_14135	-1.86
G2/M	Nucleoside diphosphate kinase	GL50803_14135	-1.86
G2/M	NYD-SP28 protein	GL50803_23357	-1.53
G2/M	Phosphatase	GL50803_8210	-1.48
G2/M	Phosphatase 1 regulatory subunit, putative	GL50803_11885	-1.86
G2/M	Phosphatase , Dual specificity protein phosphatase CDC14A	GL50803_9270	-1.66
G2/M	Phosphatase, Protein phosphatase 2A	GL50803_9894	-1.34

Cell Cycle Stage	Gene Description	Gene ID	Fold Change
	regulatory subunit, putative		
G2/M	Phosphatase, Protein phosphatase 2C-like protein	GL50803_9293	-1.36
G2/M	Phosphatase, putative	GL50803_4357	-1.61
G2/M	Phosphatase, Ser/Thr phosphatase 2A, 65kDa reg sub A	GL50803_7439	-1.39
G2/M	Phosphatase, Ser/Thr phosphatase 2C, putative	GL50803_11740	-1.67
G2/M	Phosphatase, Ser/Thr phosphatase PP1-1	GL50803_6441	-1.34
G2/M	Phosphatase, Ser/Thr phosphatase PP1-alpha 2 catalytic subunit	GL50803_14568	-2.27
G2/M	Phosphatase, Ser/Thr phosphatase PP2A-2 catalytic subunit	GL50803_5010	-1.52
G2/M	Phosphatase, Serine/Threonine phosphatase	GL50803_10711	-1.56
G2/M	Phosphatase, Serine/threonine phosphatase PP-X isozyme 2	GL50803_14311	-1.41
G2/M	Phosphatidylinositol transfer protein alpha isoform	GL50803_4197	-1.45
G2/M	Phosphoglycerate kinase	GL50803_90872	-3.19
G2/M	Potassium-transporting ATPase alpha chain 1	GL50803_96670	-1.26
G2/M	Preimplantation protein 3	GL50803_3417	-1.54
G2/M	Protein 21.1	GL50803_17608	-1.31
G2/M	Protein 21.1	GL50803_15304	-1.31
G2/M	Protein 21.1	GL50803_101397	-1.33
G2/M	Protein 21.1	GL50803_23314	-1.33
G2/M	Protein 21.1	GL50803_3760	-1.33
G2/M	Protein 21.1	GL50803_9307	-1.34
G2/M	Protein 21.1	GL50803_8983	-1.35
G2/M	Protein 21.1	GL50803_3475	-1.35
G2/M	Protein 21.1	GL50803_111967	-1.39
G2/M	Protein 21.1	GL50803_17613	-1.39
G2/M	Protein 21.1	GL50803_88071	-1.40
G2/M	Protein 21.1	GL50803_17117	-1.40
G2/M	Protein 21.1	GL50803_17288	-1.43
G2/M	Protein 21.1	GL50803_7679	-1.46
G2/M	Protein 21.1	GL50803_6007	-1.51
G2/M	Protein 21.1	GL50803_8850	-1.51
G2/M	Protein 21.1	GL50803_17402	-1.54
G2/M	Protein 21.1	GL50803_40014	-1.55
G2/M	Protein 21.1	GL50803_12028	-1.56

Cell Cycle Stage	Gene Description	Gene ID	Fold Change
G2/M	Protein 21.1	GL50803_16227	-1.58
G2/M	Protein 21.1	GL50803_8803	-1.59
G2/M	Protein 21.1	GL50803_10374	-1.62
G2/M	Protein 21.1	GL50803_88735	-1.62
G2/M	Protein 21.1	GL50803_6284	-1.63
G2/M	Protein 21.1	GL50803_7680	-1.65
G2/M	Protein 21.1	GL50803_14872	-1.69
G2/M	Protein 21.1	GL50803_7373	-1.69
G2/M	Protein 21.1	GL50803_14158	-1.80
G2/M	Protein 21.1	GL50803_13766	-1.88
G2/M	Protein 21.1	GL50803_13055	-1.93
G2/M	Protein 21.1	GL50803_7616	-1.98
G2/M	Protein 21.1	GL50803_24590	-2.00
G2/M	Protein 21.1	GL50803_16300	-2.04
G2/M	Protein 21.1	GL50803_9720	-2.05
G2/M	Protein 21.1	GL50803_95557	-2.09
G2/M	Protein 21.1	GL50803_5188	-2.15
G2/M	Protein 21.1	GL50803_16820	-2.16
G2/M	Protein 21.1	GL50803_10911	-2.19
G2/M	Protein 21.1	GL50803_16534	-2.93
G2/M	Protein C21orf2	GL50803_16891	-2.25
G2/M	Protein disulfide isomerase PDI1	GL50803_29487	-1.64
G2/M	Pyruvate kinase	GL50803_17143	-1.99
G2/M	Pyruvate kinase	GL50803_3206	-2.40
G2/M	Rab GDI	GL50803_11495	-1.74
G2/M	RabB	GL50803_12157	-1.95
G2/M	Rho GAP, putative	GL50803_13550	-1.37
G2/M	Serine-pyruvate aminotransferase	GL50803_3313	-1.59
G2/M	Sgt1-like protein	GL50803_7850	-1.51
G2/M	Spindle pole protein, putative	GL50803_24122	-1.35
G2/M	Spindle pole protein, putative	GL50803_96018	-1.42
G2/M	Spindle pole protein, putative	GL50803_13372	-1.60
G2/M	Spindle pole protein, putative	GL50803_16013	-1.91
G2/M	Spindle pole protein, putative	GL50803_87149	-1.93
G2/M	STU2-like protein	GL50803_91480	-1.40
G2/M	Surface protein	GL50803_98861	-1.27
G2/M	Syntaxin-like protein 1	GL50803_7309	-1.62
G2/M	Telomerase catalytic subunit	GL50803_16225	-1.48
G2/M	Tem-1-like protein	GL50803_9778	-1.50
G2/M	Tenascin-37	GL50803_16477	-1.37
G2/M	Tetratricopeptide repeat protein	GL50803_16934	-1.60
G2/M	Transitional endoplasmic reticulum ATPase	GL50803_8524	-1.99

Cell Cycle Stage	Gene Description	Gene ID	Fold Change
G2/M	Trichohyalin	GL50803_16840	-1.51
G2/M	tRNA-nucleotidyltransferase, putative	GL50803_16064	-1.52
G2/M	Tubulin tyrosine ligase	GL50803_14498	-1.45
G2/M	U2 small nuclear ribonucleoprotein A, putative	GL50803_17118	-1.61
G2/M	Ubiquitin carboxyl-terminal hydrolase 4	GL50803_16090	-1.97
G2/M	Ubiquitin fusion degradation protein 1	GL50803_3994	-2.35
G2/M	Ubiquitin protein, putative	GL50803_15270	-1.30
G2/M	Ubiquitin-conjugating enzyme E2-17 kDa 3	GL50803_15252	-1.81
G2/M	Unspecified product	GL50803_99493	-1.35
G2/M	Unspecified product	GL50803_32187	-1.37
G2/M	Unspecified product	GL50803_8769	-1.37
G2/M	Unspecified product	GL50803_31645	-1.39
G2/M	Unspecified product	GL50803_38628	-1.40
G2/M	Unspecified product	GL50803_32460	-1.41
G2/M	Unspecified product	GL50803_34074	-1.42
G2/M	Unspecified product	GL50803_98853	-1.45
G2/M	Unspecified product	GL50803_38738	-1.45
G2/M	Unspecified product	GL50803_11441	-1.45
G2/M	Unspecified product	GL50803_37431	-1.45
G2/M	Unspecified product	GL50803_38853	-1.46
G2/M	Unspecified product	GL50803_9136	-1.50
G2/M	Unspecified product	GL50803_91704	-1.50
G2/M	Unspecified product	GL50803_98863	-1.51
G2/M	Unspecified product	GL50803_34978	-1.53
G2/M	Unspecified product	GL50803_33174	-1.54
G2/M	Unspecified product	GL50803_6689	-1.54
G2/M	Unspecified product	GL50803_37280	-1.56
G2/M	Unspecified product	GL50803_38050	-1.62
G2/M	Unspecified product	GL50803_94659	-1.64
G2/M	Unspecified product	GL50803_100900	-1.65
G2/M	Unspecified product	GL50803_10854	-1.66
G2/M	Unspecified product	GL50803_11954	-1.67
G2/M	Unspecified product	GL50803_87068	-1.67
G2/M	Unspecified product	GL50803_23497	-1.68
G2/M	Unspecified product	GL50803_37736	-1.69
G2/M	Unspecified product	GL50803_96421	-1.72
G2/M	Unspecified product	GL50803_20253	-1.73
G2/M	Unspecified product	GL50803_29337	-1.75
G2/M	Unspecified product	GL50803_22516	-1.77
G2/M	Unspecified product	GL50803_9637	-1.83

Cell Cycle Stage	Gene Description	Gene ID	Fold Change
G2/M	Unspecified product	GL50803_35494	-1.91
G2/M	Unspecified product	GL50803_100411	-1.92
G2/M	Unspecified product	GL50803_27146	-1.94
G2/M	Unspecified product	GL50803_18633	-1.95
G2/M	Unspecified product	GL50803_5837	-1.96
G2/M	Unspecified product	GL50803_2768	-2.00
G2/M	Unspecified product	GL50803_28904	-2.01
G2/M	Unspecified product	GL50803_11369	-2.03
G2/M	Unspecified product	GL50803_29246	-2.11
G2/M	Unspecified product	GL50803_36343	-2.66
G2/M	Vacuolar proton-ATPase subunit, putative	GL50803_18470	-1.50
G2/M	Variant-specific surface protein	GL50803_12551	-1.29
G2/M	Variant-specific surface protein	GL50803_12063	-1.30
G2/M	VSP	GL50803_41227	-1.40
G2/M	WD-40 repeat protein	GL50803_15956	-1.54
G2/M	WD-40 repeat protein	GL50803_15218	-1.77
G2/M	WD-repeat membrane protein	GL50803_16709	-1.49
G2/M	Xaa-Pro dipeptidase	GL50803_16722	-1.44
G2/M	Zinc finger domain protein	GL50803_33037	-1.37
G2/M	Zinc finger domain protein	GL50803_1935	-1.42
G2/M	Zinc transporter domain protein	GL50803_13204	-1.51

Table A14: Differentially expressed genes in Fractions 7, 9, and 11 - each compared to Fraction 5 as the reference. A positive fold change indicates an up-regulated gene in the fraction of interest (Fraction 7, 9 or 11) and a negative fold change represents a down-regulated gene in the fraction of interest compared to reference Fraction 5. Note: no down-regulated genes were identified in the F7 to F5 comparison. All genes have a FDR p-value < 0.05. The data in this table is sorted alphabetically by Gene Description to group genes with similar names/functions.

Fractions compared	Gene Description	Gene ID	Fold change
F7 vs F5	Hypothetical protein	GL50803_95451	1.81
F7 vs F5	Hypothetical protein	GL50803_9551	1.76
F7 vs F5	VSP	GL50803_137729	1.78
F9 vs F5	ABC transporter ABCA.1, putative	GL50803_137726	1.62
F9 vs F5	Cathepsin L precursor	GL50803_9548	1.97
F9 vs F5	Centromere/microtubule binding protein CBF5	GL50803_16311	1.38
F9 vs F5	Cyst wall protein 2	GL50803_5435	1.39
F9 vs F5	Cysteine protease	GL50803_114915	1.54
F9 vs F5	Flavohemoglobin	GL50803_15009	2.12
F9 vs F5	GARP-like protein 1	GL50803_7272	1.63
F9 vs F5	High cysteine membrane protein Group 4	GL50803_112828	1.63
F9 vs F5	High cysteine membrane protein Group 4	GL50803_114089	1.45
F9 vs F5	High cysteine protein	GL50803_114161	1.42
F9 vs F5	H-SHIPPO 1	GL50803_29227	1.43
F9 vs F5	Hypothetical protein	GL50803_95451	2.65
F9 vs F5	Hypothetical protein	GL50803_9551	2.30
F9 vs F5	Hypothetical protein	GL50803_9552	2.27
F9 vs F5	Hypothetical protein	GL50803_137713	2.23
F9 vs F5	Hypothetical protein	GL50803_102575	2.02
F9 vs F5	Hypothetical protein	GL50803_16523	1.82
F9 vs F5	Hypothetical protein	GL50803_37636	1.78
F9 vs F5	Hypothetical protein	GL50803_27088	1.78
F9 vs F5	Hypothetical protein	GL50803_19677	1.74
F9 vs F5	Hypothetical protein	GL50803_20165	1.73
F9 vs F5	Hypothetical protein	GL50803_3269	1.72
F9 vs F5	Hypothetical protein	GL50803_26798	1.70
F9 vs F5	Hypothetical protein	GL50803_118653	1.70
F9 vs F5	Hypothetical protein	GL50803_20276	1.68
F9 vs F5	Hypothetical protein	GL50803_105806	1.66

Fractions compared	Gene Description	Gene ID	Fold change
F9 vs F5	Hypothetical protein	GL50803_3378	1.65
F9 vs F5	Hypothetical protein	GL50803_33030	1.62
F9 vs F5	Hypothetical protein	GL50803_112059	1.61
F9 vs F5	Hypothetical protein	GL50803_99562	1.60
F9 vs F5	Hypothetical protein	GL50803_118580	1.55
F9 vs F5	Hypothetical protein	GL50803_23756	1.53
F9 vs F5	Hypothetical protein	GL50803_38584	1.51
F9 vs F5	Hypothetical protein	GL50803_90198	1.49
F9 vs F5	Hypothetical protein	GL50803_18368	1.48
F9 vs F5	Hypothetical protein	GL50803_119457	1.47
F9 vs F5	Hypothetical protein	GL50803_111806	1.46
F9 vs F5	Hypothetical protein	GL50803_91504	1.45
F9 vs F5	Hypothetical protein	GL50803_14615	1.43
F9 vs F5	Hypothetical protein	GL50803_11129	1.43
F9 vs F5	Hypothetical protein	GL50803_87826	1.40
F9 vs F5	Hypothetical protein	GL50803_114242	1.37
F9 vs F5	Leucine carboxyl methyltransferase	GL50803_10516	1.50
F9 vs F5	MCT-1 protein-like protein	GL50803_13897	1.74
F9 vs F5	Protein 21.1	GL50803_111967	1.41
F9 vs F5	Topoisomerase II	GL50803_16795	1.52
F9 vs F5	Unspecific product	GL50803_37673	2.04
F9 vs F5	Unspecific product	GL50803_118198	1.81
F9 vs F5	Unspecific product	GL50803_118199	1.79
F9 vs F5	Unspecific product	GL50803_20009	1.69
F9 vs F5	Unspecific product	GL50803_5182	1.67
F9 vs F5	Unspecific product	GL50803_20503	1.59
F9 vs F5	VSP	GL50803_41401	2.68
F9 vs F5	VSP	GL50803_137729	2.29
F9 vs F5	VSP	GL50803_113357	2.27
F9 vs F5	VSP	GL50803_137740	2.04
F9 vs F5	VSP	GL50803_137722	1.84
F9 vs F5	VSP	GL50803_137723	1.82
F9 vs F5	VSP	GL50803_89315	1.75
F9 vs F5	VSP	GL50803_4313	1.72
F9 vs F5	VSP	GL50803_26894	1.71
F9 vs F5	VSP	GL50803_102662	1.69
F9 vs F5	VSP	GL50803_14331	1.67
F9 vs F5	VSP	GL50803_136003	1.66
F9 vs F5	VSP	GL50803_136004	1.66
F9 vs F5	VSP	GL50803_137681	1.65
F9 vs F5	VSP	GL50803_10562	1.65

Fractions compared	Gene Description	Gene ID	Fold change
F9 vs F5	VSP	GL50803_137606	1.64
F9 vs F5	VSP	GL50803_103001	1.60
F9 vs F5	VSP	GL50803_111732	1.60
F9 vs F5	VSP presumed INR	GL50803_137714	1.60
F9 vs F5	VSP with INR	GL50803_137605	1.80
F9 vs F5	VSP with INR	GL50803_11470	1.60
F9 vs F5	5-methylthioadenosine nucleosidase, S-adenosylhomocysteine nucleosidase	GL50803_20195	-1.42
F9 vs F5	Alpha-13 giardin	GL50803_1076	-1.38
F9 vs F5	ATP/GTP binding protein, putative	GL50803_10370	-1.53
F9 vs F5	C4 group specific protein	GL50803_13747	-1.94
F9 vs F5	Cyclin domain, Hypothetical protein	GL50803_17400	-1.38
F9 vs F5	Deoxyguanosine kinase/deoxyadenosine kinase subunit, putative	GL50803_4558	-2.07
F9 vs F5	Giardin, Gamma	GL50803_17230	-1.84
F9 vs F5	High cysteine membrane protein Group 1	GL50803_11309	-1.63
F9 vs F5	High cysteine membrane protein Group 2	GL50803_16721	-1.47
F9 vs F5	Hypothetical protein	GL50803_13651	-1.34
F9 vs F5	Hypothetical protein	GL50803_8446	-1.39
F9 vs F5	Hypothetical protein	GL50803_12224	-1.39
F9 vs F5	Hypothetical protein	GL50803_10522	-1.41
F9 vs F5	Hypothetical protein	GL50803_113133	-1.42
F9 vs F5	Hypothetical protein	GL50803_96818	-1.42
F9 vs F5	Hypothetical protein	GL50803_4415	-1.42
F9 vs F5	Hypothetical protein	GL50803_4590	-1.42
F9 vs F5	Hypothetical protein	GL50803_87577	-1.43
F9 vs F5	Hypothetical protein	GL50803_23017	-1.44
F9 vs F5	Hypothetical protein	GL50803_9219	-1.45
F9 vs F5	Hypothetical protein	GL50803_10014	-1.46
F9 vs F5	Hypothetical protein	GL50803_24423	-1.47
F9 vs F5	Hypothetical protein	GL50803_2342	-1.48
F9 vs F5	Hypothetical protein	GL50803_12229	-1.48
F9 vs F5	Hypothetical protein	GL50803_4819	-1.49

Fractions compared	Gene Description	Gene ID	Fold change
F9 vs F5	Hypothetical protein	GL50803_17484	-1.49
F9 vs F5	Hypothetical protein	GL50803_12230	-1.50
F9 vs F5	Hypothetical protein	GL50803_14647	-1.51
F9 vs F5	Hypothetical protein	GL50803_16367	-1.52
F9 vs F5	Hypothetical protein	GL50803_38019	-1.52
F9 vs F5	Hypothetical protein	GL50803_15446	-1.53
F9 vs F5	Hypothetical protein	GL50803_10524	-1.58
F9 vs F5	Hypothetical protein	GL50803_3549	-1.60
F9 vs F5	Hypothetical protein	GL50803_9636	-1.62
F9 vs F5	Hypothetical protein	GL50803_12225	-1.62
F9 vs F5	Hypothetical protein	GL50803_14921	-1.64
F9 vs F5	Hypothetical protein	GL50803_16581	-1.64
F9 vs F5	Hypothetical protein	GL50803_4852	-1.65
F9 vs F5	Hypothetical protein	GL50803_29796	-1.66
F9 vs F5	Hypothetical protein	GL50803_8770	-1.68
F9 vs F5	Hypothetical protein	GL50803_6185	-1.70
F9 vs F5	Hypothetical protein	GL50803_17375	-1.94
F9 vs F5	Kinase, NEK	GL50803_92498	-1.40
F9 vs F5	Kinase, NEK-frag	GL50803_17578	-1.36
F9 vs F5	Kinase, NEK-frag	GL50803_5489	-1.45
F9 vs F5	Leucine-rich repeat protein	GL50803_17198	-1.45
F9 vs F5	Manganese-dependent inorganic pyrophosphatase, putative	GL50803_8163	-1.37
F9 vs F5	MDR protein-like protein	GL50803_40224	-1.51
F9 vs F5	Neurogenic locus Notch protein precursor	GL50803_16322	-1.55
F9 vs F5	P115, putative	GL50803_8855	-1.49
F9 vs F5	Programmed cell death protein-like protein	GL50803_2933	-1.46
F9 vs F5	Protein 21.1	GL50803_27925	-1.44
F9 vs F5	Protein 21.1	GL50803_17046	-1.52
F9 vs F5	Protein 21.1	GL50803_11165	-1.53
F9 vs F5	Protein 21.1	GL50803_17585	-1.56
F9 vs F5	Protein 21.1	GL50803_16532	-1.66
F9 vs F5	putative 5-3 deoxyribonucleotidase	GL50803_678	-1.48
F9 vs F5	SALP-1	GL50803_4410	-1.59
F9 vs F5	Spindle pole protein, putative	GL50803_16729	-1.37

Fractions compared	Gene Description	Gene ID	Fold change
F9 vs F5	Tenascin precursor	GL50803_8687	-1.36
F9 vs F5	Thymidine kinase	GL50803_8364	-1.82
F9 vs F5	Transitional endoplasmic reticulum ATPase	GL50803_8524	-1.37
F9 vs F5	Trichohyalin	GL50803_17571	-1.51
F9 vs F5	UBC3	GL50803_24068	-1.38
F9 vs F5	Unspecific product	GL50803_8769	-1.54
F9 vs F5	Unspecific product	GL50803_9637	-1.71
F11 vs F5	18S rRNA	GL50803_r0019	3.03
F11 vs F5	18S rRNA	GL50803_r0025	3.02
F11 vs F5	Cathepsin L precursor	GL50803_9548	2.68
F11 vs F5	Eukaryotic translation initiation factor 5A	GL50803_14614	2.42
F11 vs F5	High cysteine protein	GL50803_101589	2.27
F11 vs F5	Hypothetical protein	GL50803_95451	4.88
F11 vs F5	Hypothetical protein	GL50803_9551	3.70
F11 vs F5	Hypothetical protein	GL50803_9552	3.19
F11 vs F5	Hypothetical protein	GL50803_102575	2.96
F11 vs F5	Hypothetical protein	GL50803_137713	2.52
F11 vs F5	Hypothetical protein	GL50803_19677	2.51
F11 vs F5	Hypothetical protein	GL50803_16522	2.46
F11 vs F5	Hypothetical protein	GL50803_13268	2.44
F11 vs F5	Hypothetical protein	GL50803_3269	2.42
F11 vs F5	Hypothetical protein	GL50803_119191	2.40
F11 vs F5	Hypothetical protein	GL50803_8394	2.38
F11 vs F5	Hypothetical protein	GL50803_33030	2.31
F11 vs F5	Hypothetical protein	GL50803_27056	2.21
F11 vs F5	Hypothetical protein	GL50803_34093	2.20
F11 vs F5	Hypothetical protein	GL50803_37636	2.17
F11 vs F5	Hypothetical protein	GL50803_15472	2.15
F11 vs F5	Hypothetical protein	GL50803_15045	2.08
F11 vs F5	Hypothetical protein	GL50803_99562	2.07
F11 vs F5	Hypothetical protein	GL50803_16424	1.96
F11 vs F5	Kinase, NEK	GL50803_11040	2.35
F11 vs F5	Leucine carboxyl methyltransferase	GL50803_10516	2.04
F11 vs F5	MCT-1 protein-like protein	GL50803_13897	2.57
F11 vs F5	Ribosomal protein L13	GL50803_14622	2.07
F11 vs F5	Ribosomal protein L13a	GL50803_11247	2.16
F11 vs F5	Ribosomal protein L19	GL50803_16431	2.27
F11 vs F5	Ribosomal protein L21	GL50803_15520	2.44

Fractions compared	Gene Description	Gene ID	Fold change
F11 vs F5	Ribosomal protein L23A	GL50803_7870	2.49
F11 vs F5	Ribosomal protein L26	GL50803_15046	2.21
F11 vs F5	Ribosomal protein L27	GL50803_8462	2.33
F11 vs F5	Ribosomal protein L31B	GL50803_16368	2.39
F11 vs F5	Ribosomal protein L34	GL50803_36069	2.40
F11 vs F5	Ribosomal protein L35	GL50803_6133	2.47
F11 vs F5	Ribosomal protein L36-1	GL50803_16114	2.29
F11 vs F5	Ribosomal protein L37	GL50803_14171	2.86
F11 vs F5	Ribosomal protein L37a	GL50803_5517	2.97
F11 vs F5	Ribosomal protein L44	GL50803_9810	2.28
F11 vs F5	Ribosomal protein S13	GL50803_16652	2.48
F11 vs F5	Ribosomal protein S15	GL50803_15260	2.61
F11 vs F5	Ribosomal protein S2	GL50803_8118	2.35
F11 vs F5	Ribosomal protein S21	GL50803_7082	2.47
F11 vs F5	Ribosomal protein S23	GL50803_14699	2.41
F11 vs F5	RNA polymerase II subunit Rpb12	GL50803_9509	2.32
F11 vs F5	VSP	GL50803_41401	3.18
F11 vs F5	VSP	GL50803_137722	2.99
F11 vs F5	VSP	GL50803_137723	2.95
F11 vs F5	VSP	GL50803_137729	2.90
F11 vs F5	VSP	GL50803_4313	2.56
F11 vs F5	VSP	GL50803_26894	2.46
F11 vs F5	VSP	GL50803_14331	2.45
F11 vs F5	VSP	GL50803_136004	2.41
F11 vs F5	VSP	GL50803_136003	2.40
F11 vs F5	VSP	GL50803_137681	2.40
F11 vs F5	VSP	GL50803_112647	2.24
F11 vs F5	VSP	GL50803_103001	2.13
F11 vs F5	VSP	GL50803_11521	2.00
F11 vs F5	VSP presumed INR	GL50803_137714	2.15
F11 vs F5	VSP with INR	GL50803_40592	2.37
F11 vs F5	VSP with INR	GL50803_137605	2.37
F11 vs F5	VSP with INR	GL50803_11470	2.04
F11 vs F5	Hypothetical protein	GL50803_90659	-2.01
F11 vs F5	Hypothetical protein	GL50803_19324	-2.67

Appendix IX: Gene clusters for DAVID analysis for G1/S phase genes identified from RNA-seq analysis of elutriations E2 and E3.

Table A15: G1/S genes in Ankyrin cluster from DAVID. These genes are upregulated in F3 compared to F5 in the RNA-seq analysis. All genes have a FDR p-value < 0.05. The data in this table is sorted alphabetically by Gene Description to group genes with similar names/functions.

Gene Description	Gene ID	Fold Change
Axoneme-associated protein GASP-180	GL50803_16745	1.60
ELKS	GL50803_113603	1.70
GA binding protein beta-1 chain	GL50803_6259	1.51
Hypothetical protein	GL50803_112557	1.61
Hypothetical protein	GL50803_30474	1.39
Hypothetical protein	GL50803_11720	1.38
Kinase, NEK	GL50803_16272	1.97
Kinase, NEK	GL50803_11390	1.90
Kinase, NEK	GL50803_13981	1.82
Kinase, NEK	GL50803_15953	1.74
Kinase, NEK	GL50803_94927	1.51
Kinase, NEK	GL50803_95717	1.44
Kinase, NEK	GL50803_17231	1.43
Kinase, NEK	GL50803_24400	1.43
Kinase, NEK	GL50803_113553	1.27
Kinase, NEK-frag	GL50803_5489	1.74
Kinase, NEK-frag	GL50803_102034	1.31
Kinase, NEK-like	GL50803_15035	1.76
Protein 21.1	GL50803_93011	2.32
Protein 21.1	GL50803_17046	2.26
Protein 21.1	GL50803_16532	2.24
Protein 21.1	GL50803_23492	2.24
Protein 21.1	GL50803_17585	2.13
Protein 21.1	GL50803_15972	2.10
Protein 21.1	GL50803_40390	2.00
Protein 21.1	GL50803_16843	1.99
Protein 21.1	GL50803_17551	1.96
Protein 21.1	GL50803_12139	1.94
Protein 21.1	GL50803_103783	1.87
Protein 21.1	GL50803_14434	1.85
Protein 21.1	GL50803_24194	1.77
Protein 21.1	GL50803_27925	1.74
Protein 21.1	GL50803_8174	1.74
Protein 21.1	GL50803_16326	1.73
Protein 21.1	GL50803_14859	1.71
Protein 21.1	GL50803_11165	1.70

Gene Description	Gene ID	Fold Change
Protein 21.1	GL50803_14764	1.69
Protein 21.1	GL50803_17097	1.69
Protein 21.1	GL50803_13438	1.67
Protein 21.1	GL50803_16220	1.66
Protein 21.1	GL50803_103807	1.60
Protein 21.1	GL50803_17096	1.58
Protein 21.1	GL50803_16435	1.58
Protein 21.1	GL50803_113622	1.56
Protein 21.1	GL50803_4264	1.54
Protein 21.1	GL50803_14254	1.54
Protein 21.1	GL50803_10632	1.50
Protein 21.1	GL50803_11389	1.47
Protein 21.1	GL50803_13901	1.47
Protein 21.1	GL50803_9030	1.45
Protein 21.1	GL50803_17586	1.45
Protein 21.1	GL50803_97072	1.44
Protein 21.1	GL50803_5806	1.43
Protein 21.1	GL50803_7375	1.43
Protein 21.1	GL50803_15184	1.40
Protein 21.1	GL50803_8928	1.38
Protein 21.1	GL50803_8949	1.36
Protein 21.1	GL50803_10219	1.34
Protein 21.1	GL50803_5881	1.33
Protein 21.1	GL50803_17552	1.31
Protein 21.1	GL50803_32778	1.30
Protein 21.1	GL50803_17023	1.27
Spindle pole protein, putative	GL50803_33660	1.85

Table A16: G1/S genes in cellular protein localization/transport cluster from DAVID. These genes are upregulated in F3 compared to F5 in the RNA-seq analysis. All genes have a FDR p-value < 0.05. The data in this table is sorted alphabetically by Gene Description to group genes with similar names/functions.

Gene Description	Gene ID	Fold Change
Adaptin, Alpha	GL50803_17304	1.32
Adaptin, Beta	GL50803_21423	1.28
Adaptin, Gamma	GL50803_16364	1.30
Adaptin, Mu	GL50803_8917	1.49
Adaptin, Sigma	GL50803_5328	1.42
Clathrin heavy chain	GL50803_102108	1.52
Hypothetical protein	GL50803_17110	1.26

Table A17: G1/S genes in phosphoinositide binding cluster from DAVID. These genes are upregulated in F3 compared to F5 in the RNA-seq analysis. All genes have a FDR p-value < 0.05. The data in this table is sorted alphabetically by Gene Description to group genes with similar names/functions.

Gene Description	Gene ID	Fold Change
Hypothetical protein	GL50803_7723	1.36
Hypothetical protein	GL50803_42357	1.27
Liver stage antigen-like protein	GL50803_16595	1.79

Appendix X: Gene clusters for DAVID analysis for G2/M genes identified from RNA-seq analysis of Fraction 5 from elutriations E2 and E3.

Table A18: G2/M genes in Serine/threonine kinase cluster from DAVID. These genes are upregulated in F5 compared to F3 in the RNA-seq analysis. All genes have a FDR p-value < 0.05. The data in this table is sorted alphabetically by Gene Description to group genes with similar names/functions.

Gene Description	Gene ID	Fold Change
Kinase, AGC AKT	GL50803_11364	2.52
Kinase, CAMK CAMKL	GL50803_17566	1.42
Kinase, CMGC CDK	GL50803_16802	3.64
Kinase, CMGC CDK	GL50803_8037	2.41
Kinase, CMGC CDK	GL50803_15397	1.37
Kinase, CMGC DYRK	GL50803_137695	1.48
Kinase, CMGC GSK	GL50803_17625	1.78
Kinase, CMGC MAPK	GL50803_22850	1.80
Kinase, CMGC RCK	GL50803_6700	1.87
Kinase, CMGC SRPK	GL50803_17335	1.60
Kinase, NEK	GL50803_95593	2.59
Kinase, NEK	GL50803_92498	2.30
Kinase, NEK	GL50803_8445	1.82
Kinase, NEK	GL50803_11311	1.73
Kinase, NEK	GL50803_17069	1.72
Kinase, NEK	GL50803_9289	1.40
Kinase, NEK	GL50803_40904	1.40
Kinase, NEK	GL50803_21366	1.39
Kinase, NEK	GL50803_16792	1.36
Kinase, NEK	GL50803_6731	1.34
Kinase, NEK	GL50803_91220	1.32
Kinase, NEK	GL50803_8152	1.29
Kinase, NEK	GL50803_9421	1.25
Kinase, PLK	GL50803_104150	1.55
Kinase, STE STE20	GL50803_14436	1.55
Kinase, STE STE20	GL50803_15514	1.36

Table A19: G2/M genes in the phosphorus metabolic process or protein phosphorylation cluster from DAVID. These genes are upregulated in F5 compared to F3 in the RNA-seq analysis. All genes have a FDR p-value < 0.05. The data in this table is sorted alphabetically by Gene Description to group genes with similar names/functions.

Gene Description	Gene ID	Fold Change
Kinase	GL50803_5643	1.41
Kinase	GL50803_17073	1.37
Kinase, AGC AKT	GL50803_11364	2.52
Kinase, CAMK CAMKL	GL50803_17566	1.42
Kinase, CMGC CDK	GL50803_16802	3.64
Kinase, CMGC CDK	GL50803_8037	2.41
Kinase, CMGC CDK	GL50803_15397	1.37
Kinase, CMGC CDKL	GL50803_96616	2.06
Kinase, CMGC DYRK	GL50803_17558	1.70
Kinase, CMGC DYRK	GL50803_137695	1.48
Kinase, CMGC GSK	GL50803_17625	1.78
Kinase, CMGC MAPK	GL50803_22850	1.80
Kinase, CMGC RCK	GL50803_6700	1.87
Kinase, CMGC SRPK	GL50803_17335	1.60
Kinase, NEK	GL50803_95593	2.59
Kinase, NEK	GL50803_92498	2.30
Kinase, NEK	GL50803_5999	2.01
Kinase, NEK	GL50803_8445	1.82
Kinase, NEK	GL50803_11311	1.73
Kinase, NEK	GL50803_27124	1.73
Kinase, NEK	GL50803_17069	1.72
Kinase, NEK	GL50803_87677	1.68
Kinase, NEK	GL50803_16251	1.61
Kinase, NEK	GL50803_14934	1.58
Kinase, NEK	GL50803_7356	1.47
Kinase, NEK	GL50803_12148	1.44
Kinase, NEK	GL50803_114120	1.43
Kinase, NEK	GL50803_11554	1.41
Kinase, NEK	GL50803_9289	1.40
Kinase, NEK	GL50803_40904	1.40
Kinase, NEK	GL50803_21366	1.39
Kinase, NEK	GL50803_16792	1.36
Kinase, NEK	GL50803_7103	1.35
Kinase, NEK	GL50803_6731	1.34
Kinase, NEK	GL50803_91220	1.32
Kinase, NEK	GL50803_8152	1.29
Kinase, NEK	GL50803_9421	1.25
Kinase, NEK-frag	GL50803_17578	1.86
Kinase, NEK-frag	GL50803_16733	1.55

Gene Description	Gene ID	Fold Change
Kinase, NEK-frag	GL50803_13479	1.33
Kinase, NEK-like	GL50803_4322	1.66
Kinase, PLK	GL50803_104150	1.55
Kinase, STE STE20	GL50803_16986	1.78
Kinase, STE STE20	GL50803_14436	1.55
Kinase, STE STE20	GL50803_15514	1.36
Phosphatase	GL50803_8210	1.48
Phosphatase 2C, Ser/Thr	GL50803_11740	1.67
Phosphatase 2C-like protein	GL50803_9293	1.36
Phosphatase, Dual specificity, CDC14A	GL50803_9270	1.66
Phosphatase, putative	GL50803_4357	1.61
Protein 21.1	GL50803_95557	2.09
Vacuolar proton-ATPase subunit, putative	GL50803_18470	1.50

Table A20: G2/M genes in Ankyrin cluster from DAVID. These genes are upregulated in F5 compared to F3 in the RNA-seq analysis. All genes have a FDR p-value < 0.05. The data in this table is sorted alphabetically by Gene Description to group genes with similar names/functions.

Gene Description	Gene ID	Fold Change
Ankyrin repeat protein	GL50803_16914	1.90
Axoneme-associated protein GASP-180	GL50803_23235	1.50
Coiled-coil protein	GL50803_40831	1.90
Hypothetical protein	GL50803_114199	2.63
Hypothetical protein	GL50803_6542	2.63
Hypothetical protein	GL50803_9523	2.35
Hypothetical protein	GL50803_11714	1.40
Hypothetical protein	GL50803_11207	1.35
Hypothetical protein	GL50803_3746	1.35
Kinase	GL50803_5643	1.41
Kinase, NEK	GL50803_5999	2.01
Kinase, NEK	GL50803_8445	1.82
Kinase, NEK	GL50803_87677	1.68
Kinase, NEK	GL50803_14934	1.58
Kinase, NEK	GL50803_114120	1.43
Kinase, NEK	GL50803_9289	1.40
Kinase, NEK	GL50803_21366	1.39
Kinase, NEK	GL50803_7103	1.35
Kinase, NEK	GL50803_6731	1.34
Kinase, NEK	GL50803_91220	1.32
Kinase, NEK	GL50803_8152	1.29
Kinase, NEK	GL50803_9421	1.25
Kinase, NEK-frag	GL50803_17578	1.86
Kinase, NEK-frag	GL50803_13479	1.33
Kinase, NEK-like	GL50803_4322	1.66
Kinase, STE STE20	GL50803_16986	1.78
Protein 21.1	GL50803_16534	2.93
Protein 21.1	GL50803_10911	2.19
Protein 21.1	GL50803_16820	2.16
Protein 21.1	GL50803_5188	2.15
Protein 21.1	GL50803_95557	2.09
Protein 21.1	GL50803_9720	2.05
Protein 21.1	GL50803_16300	2.04
Protein 21.1	GL50803_24590	2.00
Protein 21.1	GL50803_7616	1.98
Protein 21.1	GL50803_13055	1.93
Protein 21.1	GL50803_13766	1.88
Protein 21.1	GL50803_14158	1.80

Gene Description	Gene ID	Fold Change
Protein 21.1	GL50803_14872	1.69
Protein 21.1	GL50803_7373	1.69
Protein 21.1	GL50803_7680	1.65
Protein 21.1	GL50803_6284	1.63
Protein 21.1	GL50803_10374	1.62
Protein 21.1	GL50803_88735	1.62
Protein 21.1	GL50803_8803	1.59
Protein 21.1	GL50803_16227	1.58
Protein 21.1	GL50803_12028	1.56
Protein 21.1	GL50803_40014	1.55
Protein 21.1	GL50803_17402	1.54
Protein 21.1	GL50803_6007	1.51
Protein 21.1	GL50803_8850	1.51
Protein 21.1	GL50803_7679	1.46
Protein 21.1	GL50803_17288	1.43
Protein 21.1	GL50803_88071	1.40
Protein 21.1	GL50803_17117	1.40
Protein 21.1	GL50803_111967	1.39
Protein 21.1	GL50803_17613	1.39
Protein 21.1	GL50803_8983	1.35
Protein 21.1	GL50803_3475	1.35
Protein 21.1	GL50803_9307	1.34
Protein 21.1	GL50803_101397	1.33
Protein 21.1	GL50803_23314	1.33
Protein 21.1	GL50803_3760	1.33
Protein 21.1	GL50803_17608	1.31
Protein 21.1	GL50803_15304	1.31
Kinase, Ser/Thr protein kinase	GL50803_22003	1.73
Kinase, Ser/Thr protein kinase	GL50803_15958	1.31

Table A21: G2/M genes in the glucose catabolic process cluster from DAVID. These genes are upregulated in F5 compared to F3 in the RNA-seq analysis. All genes have a FDR p-value < 0.05. The data in this table is sorted alphabetically by Gene Description to group genes with similar names/functions.

Gene Description	Gene ID	Fold Change
2,3-bisphosphoglycerate-independent phosphoglycerate mutase	GL50803_8822	2.15
Enolase	GL50803_11118	2.21
Fructose-bisphosphate aldolase	GL50803_11043	2.42
Glucose-6-phosphate isomerase	GL50803_9115	1.48
Glyceraldehyde 3-phosphate dehydrogenase	GL50803_6687	1.78
Malate dehydrogenase	GL50803_3331	3.64
Phosphoglycerate kinase	GL50803_90872	3.19
Pyruvate kinase	GL50803_3206	2.40
Pyruvate kinase	GL50803_17143	1.99

Table A22: G2/M genes in the adenylate nucleotide binding/ATP binding cluster from DAVID. These genes are upregulated in F5 compared to F3 in the RNA-seq analysis. All genes have a FDR p-value < 0.05. The data in this table is sorted alphabetically by Gene Description to group genes with similar names/functions.

Gene Description	Gene ID	Fold Change
AAA family ATPase	GL50803_16867	2.93
ABC transporter family protein	GL50803_16575	1.41
Adenylate kinase	GL50803_28234	1.47
Centrin	GL50803_6744	1.76
CHL1-like protein	GL50803_92673	1.82
Dihydrouridine synthase, putative	GL50803_3565	1.35
Dynein heavy chain	GL50803_17243	1.35
Heat-shock protein, putative	GL50803_16412	1.57
Hypothetical protein	GL50803_17089	1.76
Hypothetical protein	GL50803_17454	1.68
Hypothetical protein, similar to SMC2	GL50803_23185	1.47
Katanin	GL50803_15368	1.41
Kinase	GL50803_5643	1.41
Kinase	GL50803_17073	1.37
Kinase, AGC AKT	GL50803_11364	2.52
Kinase, CAMK CAMKL	GL50803_17566	1.42
Kinase, CMGC CDK	GL50803_16802	3.64
Kinase, CMGC CDK	GL50803_8037	2.41
Kinase, CMGC CDK	GL50803_15397	1.37
Kinase, CMGC CDKL	GL50803_96616	2.06
Kinase, CMGC DYRK	GL50803_17558	1.70
Kinase, CMGC DYRK	GL50803_137695	1.48
Kinase, CMGC GSK	GL50803_17625	1.78
Kinase, CMGC MAPK	GL50803_22850	1.80
Kinase, CMGC RCK	GL50803_6700	1.87
Kinase, CMGC SRPK	GL50803_17335	1.60
Kinase, NEK	GL50803_95593	2.59
Kinase, NEK	GL50803_92498	2.30
Kinase, NEK	GL50803_5999	2.01
Kinase, NEK	GL50803_8445	1.82
Kinase, NEK	GL50803_11311	1.73
Kinase, NEK	GL50803_27124	1.73
Kinase, NEK	GL50803_17069	1.72
Kinase, NEK	GL50803_87677	1.68
Kinase, NEK	GL50803_16251	1.61
Kinase, NEK	GL50803_14934	1.58
Kinase, NEK	GL50803_7356	1.47
Kinase, NEK	GL50803_12148	1.44
Kinase, NEK	GL50803_114120	1.43

Gene Description	Gene ID	Fold Change
Kinase, NEK	GL50803_11554	1.41
Kinase, NEK	GL50803_9289	1.40
Kinase, NEK	GL50803_40904	1.40
Kinase, NEK	GL50803_21366	1.39
Kinase, NEK	GL50803_16792	1.36
Kinase, NEK	GL50803_7103	1.35
Kinase, NEK	GL50803_6731	1.34
Kinase, NEK	GL50803_91220	1.32
Kinase, NEK	GL50803_8152	1.29
Kinase, NEK	GL50803_9421	1.25
Kinase, NEK-frag	GL50803_17578	1.86
Kinase, NEK-frag	GL50803_16733	1.55
Kinase, NEK-frag	GL50803_13479	1.33
Kinase, NEK-like	GL50803_4322	1.66
Kinase, PLK	GL50803_104150	1.55
Kinase, STE STE20	GL50803_16986	1.78
Kinase, STE STE20	GL50803_14436	1.55
Kinase, STE STE20	GL50803_15514	1.36
Kinesin like protein	GL50803_17264	1.38
Kinesin-5	GL50803_16425	1.48
Kinesin-6	GL50803_102455	2.70
Kinesin-13	GL50803_16945	3.09
Kinesin-14	GL50803_8886	2.04
Kinesin-14	GL50803_13797	1.31
Kinesin-related protein	GL50803_11442	1.43
Mlh2-like protein	GL50803_33083	1.44
Multidrug resistance-associated protein 1	GL50803_28379	1.49
Nucleoside diphosphate kinase	GL50803_14135	1.86
Nucleoside diphosphate kinase	GL50803_14135	1.86
Potassium-transporting ATPase alpha chain 1	GL50803_96670	1.26
Protein 21.1	GL50803_95557	2.09
Transitional endoplasmic reticulum ATPase	GL50803_8524	1.99

Table A23: G2/M genes in the motor activity/microtubule cytoskeleton cluster from DAVID. These genes are upregulated in F5 compared to F3 in the RNA-seq analysis. All genes have a FDR p-value < 0.05. The data in this table is sorted alphabetically by Gene Description to group genes with similar names/functions.

Gene Description	Gene ID	Fold Change
Dynein heavy chain	GL50803_10538	1.43
Dynein light chain	GL50803_27308	1.37
Hypothetical protein	GL50803_17089	1.76
Hypothetical protein	GL50803_17454	1.68
Kinesin like protein	GL50803_17264	1.38
Kinesin-5	GL50803_16425	1.48
Kinesin-6	GL50803_102455	2.70
Kinesin-13	GL50803_16945	3.09
Kinesin-14	GL50803_8886	2.04
Kinesin-14	GL50803_13797	1.31
Kinesin-related protein	GL50803_11442	1.43

Table A24: G2/M genes in the calcium/EF hand cluster from DAVID. These genes are upregulated in F5 compared to F3 in the RNA-seq analysis. All genes have a FDR p-value < 0.05. The data in this table is sorted alphabetically by Gene Description to group genes with similar names/functions.

Gene description	Gene ID	Fold Change
Caltractin	GL50803_104685	1.85
Centrin	GL50803_6744	1.76
Hypothetical protein	GL50803_16411	2.47
Hypothetical protein	GL50803_101260	2.35
Hypothetical protein	GL50803_14947	1.47
Phosphatase, 2A regulatory subunit, putative	GL50803_9894	1.34

Table A25: 3 G2/M genes in the metal ion binding cluster from DAVID. These genes are upregulated in F5 compared to F3 in the RNA-seq analysis. All genes have a FDR p-value < 0.05. The data in this table is sorted alphabetically by Gene Description to group genes with similar names/functions.

Gene Description	Gene ID	Fold Change
2,3-bisphosphoglycerate-independent phosphoglycerate mutase	GL50803_8822	2.15
Actin related protein	GL50803_8726	2.00
Caltractin	GL50803_104685	1.85
Centrin	GL50803_6744	1.76
Enolase	GL50803_11118	2.21
Fructose-bisphosphate aldolase	GL50803_11043	2.42
GiTax, an axonemal protein that is important for flagella function	GL50803_17116	1.56
GTP-binding protein ARD-1, putative	GL50803_8140	1.38
Hypothetical protein	GL50803_16411	2.47
Hypothetical protein	GL50803_101260	2.35
Hypothetical protein	GL50803_14796	1.86
Hypothetical protein	GL50803_7207	1.57
Hypothetical protein	GL50803_14947	1.47
Hypothetical protein	GL50803_10708	1.38
Hypothetical protein	GL50803_7081	1.38
Hypothetical protein	GL50803_4928	1.32
Kinase, NEK	GL50803_14934	1.58
Kinase, NEK	GL50803_7356	1.47
Malic enzyme	GL50803_14285	1.96
Nuclear ATP/GTP-binding protein	GL50803_10976	1.73
Phosphatase, 2A regulatory subunit, putative	GL50803_9894	1.34
Phosphatase, 2C-like protein	GL50803_9293	1.36
Phosphatase, Ser/Thr phosphatase 2C, putative	GL50803_11740	1.67
Phosphatase, Ser/Thr phosphatase PP1-1	GL50803_6441	1.34
Phosphatase, Ser/Thr phosphatase PP1-alpha 2 catalytic subunit	GL50803_14568	2.27
Phosphatase, Ser/Thr phosphatase PP2A-2 catalytic subunit	GL50803_5010	1.52
Phosphatase, Serine/Threonine phosphatase	GL50803_10711	1.56
Phosphatase, Serine/threonine phosphatase PP-X isozyme 2	GL50803_14311	1.41
Protein 21.1	GL50803_6284	1.63
Protein 21.1	GL50803_16227	1.58

Gene Description	Gene ID	Fold Change
Protein 21.1	GL50803_101397	1.33
Pyruvate kinase	GL50803_3206	2.40
Pyruvate kinase	GL50803_17143	1.99
Xaa-Pro dipeptidase	GL50803_16722	1.44
Zinc finger domain protein	GL50803_1935	1.42

Appendix XI: Microarray results from Dr. Svard's laboratory

Microarray conditions:

Culture tubes containing Giardia trophozoites (WB clone 6 strain) were incubated with aphidicolin for 6 hours. The media was removed and fresh supplemented media was added and the allowed to continue to grow till they were harvested. Cells were collected at 0, 1, 2, 3, 4, 5, 6, 6.5 and 8 hours post release from the drug. Two biological replicates were used in the data analysis.

Total RNA was isolated from the time points based on the manufacture's protocol (Trizol, Invitrogen, USA). The isolated samples were treated with DNase I and the integrity was verified by agarose gel electrophoresis. 2 μg of the total RNA from each time point sample was converted to labelled cDNA by using random hexamer primers, Superscript III and aminoallyl-dUTP. The aminoallyl groups were coupled to the fluorescent molecules Cyanine-3 or Cyanine-5 which were used to detect the presence of genes in the microarray experiment.

Each microarray slide is composed of aminosilane surface coated glass that is spotted with 70 nucleotide-long oligonucleotides representing 9115 genes and Open Reading Frames (ORFs) within the Giardia WB genome. Genes identified only in the RNA-seq results were represented as probes on the microarray, but their changes in expression were not above the 1.4 cut off in both microarray replicates.

Table A26: Genes identified in the microarray experiment from aphidicolin synchronized Giardia WB trophozoite cultures. Results are from the analysis of 2 - 3 independent experiments. Cell cycle stage identified for each gene is based on its peak expression at the indicated stage.

Cell Cycle Stage	Gene Description	Gene ID
G1	AP complex subunit beta	GL50803_21423
G1	Arginine deiminase (EC 3.5.3.6)	GL50803_112103
G1	Axoneme-associated protein GASP-180	GL50803_16745
G1	Carbamate kinase	GL50803_16453
G1	Cyst wall protein 1	GL50803_5638
G1	Cyst wall protein 2	GL50803_5435
G1	Cyst wall protein 3	GL50803_2421
G1	Giardin, Beta	GL50803_4812
G1	Giardin, Delta	GL50803_86676
G1	H-SHIPPO 1	GL50803_9148
G1	Hypothetical protein	GL50803_10524
G1	Hypothetical protein	GL50803_10808
G1	Hypothetical protein	GL50803_23017
G1	Hypothetical protein	GL50803_6185
G1	Hypothetical protein	GL50803_6928
G1	Intraflagellar transport particle protein IFT88	GL50803_16660
G1	Kinase, Deoxyguanosine kinase/deoxyadenosine kinase subunit, putative	GL50803_4558
G1	Kinase, Deoxynucleoside kinase	GL50803_17451
G1	Kinase, NEK	GL50803_11390
G1	Kinase, NEK	GL50803_17231
G1	Kinase, NEK	GL50803_24321
G1	Kinase, Nucleoside diphosphate	GL50803_14135
G1	Kinase, Thymidine	GL50803_8364
G1	Ornithine carbamoyltransferase	GL50803_10311
G1	P115, putative	GL50803_8855
G1	Protein 21.1	GL50803_101168
G1	Protein 21.1	GL50803_11165
G1	Protein 21.1	GL50803_13766
G1	Protein 21.1	GL50803_16532
G1	Protein 21.1	GL50803_17053
G1	Protein 21.1	GL50803_23492
G1	Protein 21.1	GL50803_27925
G1	Protein 21.1	GL50803_40390
G1	Protein 21.1	GL50803_6081

Cell Cycle Stage	Gene Description	Gene ID
G1	Protein 21.1	GL50803_8174
G1	SALP-1	GL50803_4410
G1	Spindle pole protein, putative	GL50803_24537
G1	Tubulin beta chain	GL50803_101291
G1	Unspecified product	GL50803_31095
G1	ZipA	GL50803_16811
S	ARL protein, putative	GL50803_13523
S	Bip	GL50803_17121
S	Cathepsin B	GL50803_16779
S	Chaperone protein dnaJ	GL50803_15398
S	CTP synthase (UTP--ammonia ligase)	GL50803_17587
S	FKBP-type peptidyl-prolyl cis-trans isomerase	GL50803_10570
S	High cysteine membrane protein Group 1	GL50803_11309
S	Histone H2A	GL50803_14256
S	Histone H2B	GL50803_121045
S	Histone H3	GL50803_3367
S	Histone H4	GL50803_135001
S	Hypothetical protein	GL50803_10196
S	Hypothetical protein	GL50803_10675
S	Hypothetical protein	GL50803_11305
S	Hypothetical protein	GL50803_13272
S	Hypothetical protein	GL50803_16602
S	Hypothetical protein	GL50803_22855
S	Hypothetical protein	GL50803_5800
S	Hypothetical protein	GL50803_90434
S	Isoleucyl-tRNA synthetase	GL50803_104173
S	Kinase, NEK	GL50803_137733
S	Nucleolar GTP-binding protein 1, putative	GL50803_16371
S	Polyadenylate-binding protein, putative	GL50803_5942
S	Protein disulfide isomerase PDI3	GL50803_14670
S	Ribosomal protein S16	GL50803_4652
S	Ribosomal protein S16	GL50803_4652
S	Ribosomal protein S20	GL50803_6022
S	Ribosomal protein S8, 40S	GL50803_5845
S	RNA helicase-like protein, ATP-dependent	GL50803_15048
S	S-adenosylmethionine synthetase	GL50803_5659
S	Translation elongation factor 1-gamma	GL50803_12102

Cell Cycle Stage	Gene Description	Gene ID
S	Translation initiation factor 2 gamma subunit	GL50803_2970
S	Translation initiation factor 6 (eIF-6), eukaryotic	GL50803_14606
S	VSP	GL50803_122564
G2/M - early	AAA family ATPase	GL50803_16867
G2/M - early	Aldose reductase (EC 1.1.1.21)	GL50803_7260
G2/M - early	ATP-dependent RNA helicase HAS1, putative	GL50803_16887
G2/M - early	Coiled-coil protein	GL50803_11867
G2/M - early	FEN-1 nuclease	GL50803_5488
G2/M - early	Glutamate-rich WD-repeat protein	GL50803_14174
G2/M - early	Hypothetical protein	GL50803_10423
G2/M - early	Hypothetical protein	GL50803_10675
G2/M - early	Hypothetical protein	GL50803_11955
G2/M - early	Hypothetical protein	GL50803_13268
G2/M - early	Hypothetical protein	GL50803_14850
G2/M - early	Hypothetical protein	GL50803_15062
G2/M - early	Hypothetical protein	GL50803_15089
G2/M - early	Hypothetical protein	GL50803_16424
G2/M - early	Hypothetical protein	GL50803_16658
G2/M - early	Hypothetical protein	GL50803_34093
G2/M - early	Kinesin-like protein	GL50803_13825
G2/M - early	Phosphatase, Serine/threonine-protein phosphatase	GL50803_15215
G2/M - early	Ribosomal protein L37	GL50803_14171
G2/M - early	Spindle pole protein, putative	GL50803_13372
G2/M - early	Spindle pole protein, putative	GL50803_16013
G2/M - early	Spindle pole protein, putative	GL50803_17055
G2/M - early	Syntaxin-like protein 1	GL50803_7309
G2/M - early	TCP-1 chaperonin subunit eta	GL50803_16124
G2/M - early	Ubiquitin-conjugating enzyme E2-17 kDa 3	GL50803_15252
G2/M - early	Unspecified product	GL50803_29042
G2/M - early	Unspecified product	GL50803_11954
G2/M - early/mid	5-3 deoxyribonucleotidase, putative	GL50803_678
G2/M - early/mid	Calmodulin	GL50803_5333
G2/M - early/mid	Caltractin	GL50803_104685
G2/M - early/mid	Centrin	GL50803_6744
G2/M - early/mid	GTL3 aka MD0260	GL50803_104866
G2/M - early/mid	Heat shock protein HSP 90-alpha	GL50803_13864
G2/M - early/mid	Hypothetical protein	GL50803_114546
G2/M - early/mid	Hypothetical protein	GL50803_114623
G2/M - early/mid	Hypothetical protein	GL50803_13851

Cell Cycle Stage	Gene Description	Gene ID
G2/M - early/mid	Hypothetical protein	GL50803_15039
G2/M - early/mid	Hypothetical protein	GL50803_16267
G2/M - early/mid	Hypothetical protein	GL50803_16812
G2/M - early/mid	Hypothetical protein	GL50803_30645
G2/M - early/mid	Hypothetical protein	GL50803_41834
G2/M - early/mid	Hypothetical protein	GL50803_7328
G2/M - early/mid	Hypothetical protein	GL50803_7352
G2/M - early/mid	Hypothetical protein	GL50803_7444
G2/M - early/mid	Hypothetical protein	GL50803_8394
G2/M - early/mid	Hypothetical protein	GL50803_9636
G2/M - early/mid	Kinase	GL50803_5643
G2/M - early/mid	Kinase, CAMK CAMKL	GL50803_16034
G2/M - early/mid	Kinase, CAMK CAMKL	GL50803_17566
G2/M - early/mid	Kinase, CMGC GSK	GL50803_17625
G2/M - early/mid	Kinase, CMGC SRPK	GL50803_17335
G2/M - early/mid	Kinase, NEK	GL50803_3957
G2/M - early/mid	Kinase, NEK	GL50803_5375
G2/M - early/mid	Kinase, NEK-frag	GL50803_14648
G2/M - early/mid	Kinase, Pyruvate	GL50803_3206
G2/M - early/mid	Kinesin-6	GL50803_102455
G2/M - early/mid	Pescadillo homolog	GL50803_16313
G2/M - early/mid	Phosphatase, Dual specificity protein phosphatase CDC14A	GL50803_9270
G2/M - early/mid	Protein 21.1	GL50803_5188
G2/M - early/mid	Protein 21.1	GL50803_7268
G2/M - early/mid	Protein 21.1	GL50803_9720
G2/M - early/mid	Ribosomal protein L12	GL50803_14938
G2/M - early/mid	Ribosomal protein S21, 40S	GL50803_7082
G2/M - early/mid	Tubulin alpha chain	GL50803_103676
G2/M - early/mid	Unspecified product	GL50803_20253
G2/M - early/mid	Unspecified product	GL50803_23126
G2/M - early/mid	Unspecified product	GL50803_27257
G2/M - early/mid	Zinc transporter domain protein	GL50803_6664
G2/M - mid/late	Actin related protein	GL50803_8726
G2/M - mid/late	ATP/GTP binding protein, putative	GL50803_10370
G2/M - mid/late	Axonemal p66.0	GL50803_114462
G2/M - mid/late	Axoneme central apparatus protein	GL50803_16202
G2/M - mid/late	Coiled-coil protein	GL50803_95653
G2/M - mid/late	Cyclin B, G2/mitotic-specific	GL50803_3977
G2/M - mid/late	Cyclin domain, hypothetical protein	GL50803_17400
G2/M - mid/late	Cyclin-dependent kinases regulatory subunit	GL50803_2661
G2/M - mid/late	Dynein intermediate chain	GL50803_33218
G2/M - mid/late	Dynein regulatory complex	GL50803_16540

Cell Cycle Stage	Gene Description	Gene ID
G2/M - mid/late	E04F6.2 like protein	GL50803_15455
G2/M - mid/late	Fructose-bisphosphate aldolase	GL50803_11043
G2/M - mid/late	Giardia trophozoite antigen GTA-1	GL50803_17090
G2/M - mid/late	GTP-binding protein ARD-1, putative	GL50803_8140
G2/M - mid/late	High cysteine protein	GL50803_94003
G2/M - mid/late	H-SHIPPO 1	GL50803_91354
G2/M - mid/late	Hypothetical protein	GL50803_10299
G2/M - mid/late	Hypothetical protein	GL50803_103202
G2/M - mid/late	Hypothetical protein	GL50803_10422
G2/M - mid/late	Hypothetical protein	GL50803_10527
G2/M - mid/late	Hypothetical protein	GL50803_10881
G2/M - mid/late	Hypothetical protein	GL50803_112112
G2/M - mid/late	Hypothetical protein	GL50803_11342
G2/M - mid/late	Hypothetical protein	GL50803_12105
G2/M - mid/late	Hypothetical protein	GL50803_12230
G2/M - mid/late	Hypothetical protein	GL50803_13288
G2/M - mid/late	Hypothetical protein	GL50803_13467
G2/M - mid/late	Hypothetical protein	GL50803_13584
G2/M - mid/late	Hypothetical protein	GL50803_14198
G2/M - mid/late	Hypothetical protein	GL50803_14317
G2/M - mid/late	Hypothetical protein	GL50803_14492
G2/M - mid/late	Hypothetical protein	GL50803_14583
G2/M - mid/late	Hypothetical protein	GL50803_14796
G2/M - mid/late	Hypothetical protein	GL50803_14921
G2/M - mid/late	Hypothetical protein	GL50803_14947
G2/M - mid/late	Hypothetical protein	GL50803_16543
G2/M - mid/late	Hypothetical protein	GL50803_16581
G2/M - mid/late	Hypothetical protein	GL50803_16648
G2/M - mid/late	Hypothetical protein	GL50803_16663
G2/M - mid/late	Hypothetical protein	GL50803_16720
G2/M - mid/late	Hypothetical protein	GL50803_16935
G2/M - mid/late	Hypothetical protein	GL50803_16996
G2/M - mid/late	Hypothetical protein	GL50803_17116
G2/M - mid/late	Hypothetical protein	GL50803_17255
G2/M - mid/late	Hypothetical protein	GL50803_17312
G2/M - mid/late	Hypothetical protein	GL50803_21527
G2/M - mid/late	Hypothetical protein	GL50803_21943
G2/M - mid/late	Hypothetical protein	GL50803_23874
G2/M - mid/late	Hypothetical protein	GL50803_24451
G2/M - mid/late	Hypothetical protein	GL50803_24453
G2/M - mid/late	Hypothetical protein	GL50803_27141
G2/M - mid/late	Hypothetical protein	GL50803_28015
G2/M - mid/late	Hypothetical protein	GL50803_29147

Cell Cycle Stage	Gene Description	Gene ID
G2/M - mid/late	Hypothetical protein	GL50803_29796
G2/M - mid/late	Hypothetical protein	GL50803_30851
G2/M - mid/late	Hypothetical protein	GL50803_31031
G2/M - mid/late	Hypothetical protein	GL50803_31870
G2/M - mid/late	Hypothetical protein	GL50803_31998
G2/M - mid/late	Hypothetical protein	GL50803_32489
G2/M - mid/late	Hypothetical protein	GL50803_3538
G2/M - mid/late	Hypothetical protein	GL50803_37381
G2/M - mid/late	Hypothetical protein	GL50803_3934
G2/M - mid/late	Hypothetical protein	GL50803_4018
G2/M - mid/late	Hypothetical protein	GL50803_4149
G2/M - mid/late	Hypothetical protein	GL50803_4590
G2/M - mid/late	Hypothetical protein	GL50803_4597
G2/M - mid/late	Hypothetical protein	GL50803_4624
G2/M - mid/late	Hypothetical protein	GL50803_5167
G2/M - mid/late	Hypothetical protein	GL50803_5883
G2/M - mid/late	Hypothetical protein	GL50803_6171
G2/M - mid/late	Hypothetical protein	GL50803_6542
G2/M - mid/late	Hypothetical protein	GL50803_6725
G2/M - mid/late	Hypothetical protein	GL50803_7207
G2/M - mid/late	Hypothetical protein	GL50803_7242
G2/M - mid/late	Hypothetical protein	GL50803_8038
G2/M - mid/late	Hypothetical protein	GL50803_8201
G2/M - mid/late	Hypothetical protein	GL50803_8426
G2/M - mid/late	Hypothetical protein	GL50803_8460
G2/M - mid/late	Hypothetical protein	GL50803_8727
G2/M - mid/late	Hypothetical protein	GL50803_8770
G2/M - mid/late	Hypothetical protein	GL50803_88556
G2/M - mid/late	Hypothetical protein	GL50803_8865
G2/M - mid/late	Hypothetical protein	GL50803_8979
G2/M - mid/late	Hypothetical protein	GL50803_9121
G2/M - mid/late	Hypothetical protein	GL50803_9219
G2/M - mid/late	Hypothetical protein	GL50803_9305
G2/M - mid/late	Hypothetical protein	GL50803_9505
G2/M - mid/late	Kinase, Adenylate	GL50803_28234
G2/M - mid/late	Kinase, AGC AKT	GL50803_11364
G2/M - mid/late	Kinase, AGC PKA	GL50803_86444
G2/M - mid/late	Kinase, CMGC CDK	GL50803_16802
G2/M - mid/late	Kinase, CMGC CDK	GL50803_8037
G2/M - mid/late	Kinase, CMGC RCK	GL50803_6700
G2/M - mid/late	Kinase, Guanylate	GL50803_7203
G2/M - mid/late	Kinase, NEK	GL50803_11311
G2/M - mid/late	Kinase, NEK	GL50803_12148
G2/M - mid/late	Kinase, NEK	GL50803_17069

Cell Cycle Stage	Gene Description	Gene ID
G2/M - mid/late	Kinase, NEK	GL50803_8445
G2/M - mid/late	Kinase, NEK	GL50803_95593
G2/M - mid/late	Kinase, STE STE20	GL50803_10609
G2/M - mid/late	Kinesin-like protein	GL50803_16945
G2/M - mid/late	Kinesin-like protein	GL50803_17264
G2/M - mid/late	Malate dehydrogenase	GL50803_3331
G2/M - mid/late	Median body protein	GL50803_16343
G2/M - mid/late	Mitogen-activated protein kinase	GL50803_22850
G2/M - mid/late	Mitotic spindle checkpoint protein MAD2	GL50803_100955
G2/M - mid/late	NOD3 protein, putative	GL50803_4165
G2/M - mid/late	Nuclear LIM interactor-interacting factor 1	GL50803_4063
G2/M - mid/late	Nucleoside diphosphate kinase	GL50803_14135
G2/M - mid/late	Peptidyl-prolyl cis-trans isomerase (PPIase)	GL50803_17163
G2/M - mid/late	Phosphatase, Serine/threonine-protein	GL50803_14568
G2/M - mid/late	Phosphatidylinositol transfer protein alpha isoform	GL50803_4197
G2/M - mid/late	Phosphatidylinositol-4-phosphate 5-kinase, putative	GL50803_2622
G2/M - mid/late	Protein 21.1	GL50803_10911
G2/M - mid/late	Protein 21.1	GL50803_13437
G2/M - mid/late	Protein 21.1	GL50803_14158
G2/M - mid/late	Protein 21.1	GL50803_4383
G2/M - mid/late	Protein 21.1	GL50803_6007
G2/M - mid/late	Protein 21.1	GL50803_7679
G2/M - mid/late	Protein 21.1	GL50803_8850
G2/M - mid/late	Protein F17L21.10	GL50803_6724
G2/M - mid/late	Protein LRP16	GL50803_14730
G2/M - mid/late	Serine-pyruvate aminotransferase	GL50803_3313
G2/M - mid/late	SnRNP Sm-like protein, putative	GL50803_6408
G2/M - mid/late	Spindle pole protein, putative	GL50803_21444
G2/M - mid/late	Spindle pole protein, putative	GL50803_24537
G2/M - mid/late	Synaptobrevin-like protein	GL50803_14469
G2/M - mid/late	Triosephosphate isomerase	GL50803_93938
G2/M - mid/late	Tubulin specific chaperone E	GL50803_16535
G2/M - mid/late	Tubulin tyrosine ligase	GL50803_14498
G2/M - mid/late	Unspecified product	GL50803_23497
G2/M - mid/late	Unspecified product	GL50803_37431
G2/M - mid/late	Unspecified product	GL50803_4557
G2/M - mid/late	Unspecified product	GL50803_8769
G2/M - mid/late	Unspecified product	GL50803_9637

Cell Cycle Stage	Gene Description	Gene ID
G2/M - mid/late	WD-40 repeat protein	GL50803_15218
G2/M - mid/late	WD-40 repeat protein	GL50803_15956
G2/M - mid/late	Zinc transporter domain protein	GL50803_13204